2010-02-08

Cross-Talk Between Factors Involved in mRNA Translation and Decay: A Dissertation

Shubhendu Ghosh
University of Massachusetts Medical School Worcester

CROSS-TALK BETWEEN FACTORS INVOLVED IN mRNA TRANSLATION AND DECAY

A Dissertation Presented

By

Shubhendu Ghosh

Submitted to the Faculty of the
University of Massachusetts Graduate School of Biomedical Sciences, Worcester
In partial fulfillment of the requirements for the degree of

DOCTOR OF PHILOSOPHY

February 8, 2010

Biomedical Science

CROSS-TALK BETWEEN FACTORS INVOLVED IN mRNA TRANSLATION AND DECAY

A Dissertation Presented
By

Shubhendu Ghosh

The signatures of the Dissertation Committee signifies
completion and approval as to style and content of the Dissertation

_____
Allan Jacobson, Ph.D., Thesis Advisor

_____
Paul Dobner, Ph.D., Member of Committee

_____
Duane Jenness, Ph.D., Member of Committee

_____
Craig Peterson, Ph.D., Member of Committee

_____
Robert H. Singer, Ph.D., Member of Committee

The signature of the Chair of the Committee signifies that the written dissertation
Meets the requirements of the Dissertation Committee

_____
Richard Baker, Ph.D, Chair of Committee

The signature of the Dean of the Graduate School of Biomedical Sciences signifies
that the student has met all graduation requirements of the school

_____
Anthony Carruthers, Ph.D.,
Dean of the Graduate School of Biomedical Sciences

Department of Molecular Genetics and Microbiology
February 8, 2010

Abstract

The proper workings of an organism rely on the accurate expression of genes throughout its lifetime. An important determinant for protein production is the availability of template mRNA molecules, the net effect of which is governed by their rates of synthesis *vs.* their rates of degradation. Normal mRNAs are proposed to be relatively stable in the cytoplasm while present in a protective, circularized conformation – the closed loop – through eIF4G-bridged interactions with 3'-bound poly(A) binding protein (Pab1p) and 5'-bound eIF4E. Introduction of a premature nonsense codon into an otherwise normal mRNA results in its rapid destabilization in cells, suggesting that not all stop codons behave the same, and events at premature termination events that lead to accelerated degradation of nonsense-containing mRNAs likely differ from those at normal termination, in which normal decay rates are maintained. The enhanced degradation observed for nonsense-containing mRNAs occurs through an evolutionarily conserved pathway involving the products of the *UPF1*, *UPF2/NMD2*, and *UPF3* genes, the precise biochemical roles of which have remained elusive. We have developed a yeast cell-free translation system that allows us to assay biochemical events occurring at premature termination codons, compare them to those occurring at normal terminators, and study the role of Upf1p in these events. We find that premature termination is an inefficient process compared to normal termination and that one outcome of termination at a premature termination codon (PTC) is reinitiation at a nearby start codon. This *in vitro* post-termination reinitiation phenotype is dependent on the presence of Upf1p, a finding we have recapitulated *in vivo*. We also developed

biochemical assays to define a role for Upf1p in translation following premature termination *in vitro* and find that Upf1p is involved in post-termination ribosome dissociation and reutilization. Supporting this idea are our findings that Upf1p predominantly cosediments with purified 40S ribosomal subunits. Finally, using our *in vitro* translation/toeprinting system, we have further characterized events leading to the formation of the mRNA closed loop structure and find that two states of the closed loop exist. The first requires the preinitiation 48S complex and includes Pab1p, eIF4G, eIF4E, and eIF3, whereas the second is formed after 60S joining and additionally requires the translation termination factors eRF1 and eRF3.

Table of Contents

Title……..i

Signature Page……..ii

Abstract……..iii

List of Figures……viii

Chapter I - Introduction……1

Overview……..2

Translation, mRNA stability determinants, and the closed loop model…....3

General cytoplasmic mRNA turnover……..6

Conditional mRNA decay through protein binding……....10

Conditional mRNA decay through RNA interference……....13

Cytoplasmic RNA quality control……...15

Work done in this thesis……....30

Chapter II - A faux 3'-UTR promotes aberrant termination and triggers nonsense-mediated mRNA decay……....33

Summary……..…34

Toeprint analyses of initiation and premature termination in cell extracts……..35

Aberrant toeprints are dependent on the presence of NMD factors……..37

Aberrant toeprints derived from PTCs in wild-type extracts in the presence of CHX are dependent on upstream AUGs……...37

Reinitiation at upstream AUGs is favored over downstream reinitiation….40

eRF1 activity is required prior to any reinitiation event……41

An extended 3'-UTR leads to aberrant termination events……42

Tethered Pab1p stabilizes nonsense-containing mRNAs……43

Chapter III - Translational competence of ribosomes released from a premature termination codon is modulated by NMD factors……59

Summary……60

Mutations in a *PGK1/LUC* reporter attenuate its reinitiation activity……62

Reinitiation on nonsense-containing *PGK1/LUC* mRNA is sensitive to mutations in the NMD pathway……63

A small percentage of ribosomes reinitiate downstream of the premature stop codon……65

NMD is independent of translation reinitiation……65

NMD-deficient extracts manifest a translation defect *in vitro*……66

Upf1p affects translation *in vitro*……68

Translation initiation is compromised in *upf1*Δ extracts……68

Initiation efficiency depends on prior termination events……70

Addition of WT ribosomal subunits enhances translation in *upf1*Δ extracts……73

Chapter IV - Translation factors promote formation of two states of the closed loop mRNP……85

Summary……86

Responsiveness of the yeast cell-free translation system to the presence or absence of a 5' cap and/or a 3' poly(A) tail on *LUC* mRNA……87

AUG toeprints and cap analog resistance are specific and independent of the polynucleotide concentration……87

Resistance to cap analog is mRNA size dependent but is not mRNA sequence dependent……..89

Cap analog resistance is not due to cap-independent translation……...89

Translation of poly(A)-deficient mRNA is sensitive to cap analog……...90

Pab1p is required for cap analog resistance of the *miniUAA1* mRNA……91

Cell-free extracts derived from mutants defective in Pab1p activity, or the activity of Pab1p-interacting proteins, are markedly sensitive to cap analog……..92

Cap analog resistance is independent of translation termination……...94

Cap analog resistance or sensitivity of *miniUAA1* mRNA appears at the onset of translation……95

Polysome profiling of ribosome:mRNA association in wild-type and mutant extracts……95

Two states of the closed loop structure of mRNA can be distinguished...97

Chapter V – Discussion……117

Elaborating the "closed loop" model……...118

Normal and premature termination are biochemically distinct events.....121

A role for Upf1p in translation……125

Future directions……129

Appendices……133

Appendix A – Methods used in Chapter II……..134

Appendix B – Methods used in Chapter III……138

Appendix C – Methods used in Chapter IV……152

Appendix D – Toeprinting overview……156

References……..160

List of Figures

Chapter II

Fig. 2.1 : General schematic and sequences of selected regions of the *UAA*, *UGA*, *Fusion*, and *AAA CAN1/LUC* RNAs……46

Fig. 2.2 : Toeprint analyses of termination in cell extracts in the absence of CHX……47

Fig. 2.3 : Toeprint analyses of initiation and termination in cell extracts in the presence of CHX……48

Fig. 2.4 : Aberrant toeprints derived from PTCs in wild-type extracts in the presence of CHX are dependent on upstream AUGs……49

Fig. 2.5 : Ribosomes can reinitiate translation at AUG codons upstream or downstream of the stop codon……50

Fig. 2.6 : Ribosomes can migrate to AUG codons 21 or 32 nt upstream of premature stop codons……51

Fig. 2.7 : Reinitiation at upstream AUGs is favored over downstream reinitiation……52

Fig. 2.8 : RNAs translated in *sup45-2* extracts in the presence of CHX yield only +12 toeprints……53

Fig. 2.9 : General schematic and sequences of the *mini* RNAs……54

Fig. 2.10 : Aberrant toeprint signals are eliminated when PTCs are flanked by a normal 3'-UTR……55

Fig. 2.11 : Stabilization of nonsense-containing mRNAs by tethered Pab1p…….56

Fig. 2.12 : Tethered Pab1p interacts with Sup35p……57

Fig. 2.13 : PTC-containing mRNA is stabilized by tethered Sup35p, but not by tethered Sup45p……58

Chapter III

Fig. 3.1 : Reinitiation activity is reduced in strains bearing mutations in the NMD pathway……75

Fig. 3.2 : Determination of ribosomal initiation efficiency and proportion of ribosomes that reinitiate downstream of the *PGK1* stop codon……77

Fig. 3.3 : A strong stem loop structure does not eliminate nonsense-mediated mRNA decay……78

Fig. 3.4 : Translation of *CAN1/LUC* mRNA is decreased in *upf1Δ* extracts……79

Fig. 3.5 : Purified FLAG-Upf1p can complement translation defects *in vitro*……80

Fig. 3.6 : Formation of 80S toeprints is diminished in *upf1Δ* extracts……81

Fig. 3.7 : Initiation efficiency depends on prior termination events……82

Fig. 3.8 : Purified FLAG-Upf1p restores efficient translational activity to *upf1Δ* extracts……83

Fig. 3.9 : 40S and 60S ribosomal subunits enhance translation in *upf1Δ* extracts……84

Chapter IV

Fig. 4.1 : Yeast cell extracts recapitulate the synergy between the cap structure and the poly(A) tail *in vitro*……99

Fig. 4.2 : General schematic of the *miniUAA1*, *UAA*, and *AAA* mRNAs……100

Fig. 4.3 : Toeprint analyses of initiation on long and short mRNAs in the presence of CHX in wild-type extracts……101

Fig. 4.4 : AUG toeprints and cap analog resistance are specific and independent of polynucleotide concentration……102

Fig. 4.5 : Cap analog sensitivity in the presence of CHX in wild-type extracts is mRNA size dependent……103

Fig. 4.6 : Cap analog resistance of the *miniUAA1* mRNA is cap and poly(A) dependent in wild-type extracts and suggests formation of a stable closed loop structure……104

Fig. 4.7 : Formation of a stable closed-loop structure on a capped and polyadenylated mRNA in the presence of an 80S complex requires Pab1p interactions with eIF4G, mRNA, and Sup35p……105

Fig. 4.8 : Formation of a stable closed-loop structure on a capped and polyadenylated mRNA in the presence of an 80S complex requires Pab1p interactions with eIF4G……...106

Fig. 4.9 : Formation of a stable closed-loop structure on a capped and polyadenylated mRNA in the presence of an 80S complex requires Sup35p……107

Fig. 4.10 : Cap analog resistance depends on the presence of a poly(A) tail.....108

Fig. 4.11 : Increased Mg^{2+} concentration does not affect sensitivity or resistance to cap analog in different extracts……109

Fig. 4.12 : Toeprinting analyses of *miniUAA1* mRNA in initiation-defective extracts……110

Fig. 4.13 : Sensitivity to cap analog is independent of the termination event.....111

Fig. 4.14 : Cap analog resistance or sensitivity of the *miniUAA1* mRNA appears at the onset of translation……112

Fig. 4.15 : Typical polysome profile of an extract after micrococcal nuclease treatment and translation of the *miniUAA1* mRNA……..…113

Fig. 4.16 : Translation of the *miniUAA1* mRNA as assayed by sucrose density centrifugation and northern blot analysis……...114

Fig. 4.17 : Stabilization of the closed-loop structure on a capped and polyadenylated mRNA in the presence of a 48S complex requires Pab1p interactions with eIF4G and *miniUAA1* mRNA……...115

Fig. 4.18 : Termination-defective extracts manifest normal rates of ribosome recruitment……116

Chapter V

Fig. 5.1 : Two states model of the closed loop……..131

Fig. 5.2 : Upf1p enhances ribosome reutilization post-termination from a PTC..132

Chapter I

Introduction

Chapter I - Introduction

Overview

The respective levels of individual cellular mRNAs are an important determinant of gene expression. The advent of accurate multiplexed quantitative methodologies, such as microarray analyses, have allowed genome-wide views of changes in mRNA levels under different conditions (He *et al.* 2003; Mata *et al.* 2005), leading to the use of transcript abundance as a hallmark with which to predict changes in pathway activities (Johansson *et al.* 2007). Although transcriptional activation has been a predominant focus of studies seeking to elucidate the mechanisms by which steady-state levels of all RNAs are controlled, it is critical to recognize that these levels are reflective of the sum of both transcript synthesis as well as degradation. In addition, many RNA degradation pathways are affected by translation (Doma and Parker 2007). There is growing appreciation of the interplay between translation and RNA decay factors and the work described in this thesis provides biochemical evidence for a translational role for factors involved in nonsense-mediated mRNA decay, a pathway in cells that eliminates mRNA transcripts that prematurely terminate translation. This chapter will introduce our current understanding of mRNA stability and its relationship to translation, the pathways involved in cytoplasmic mRNA degradation, and mechanisms that mediate RNA quality control, including a detailed description of the nonsense-mediated mRNA decay pathway. I will conclude by providing the rationale for the work described in the remaining chapters of the thesis.

Translation, mRNA stability determinants, and the closed loop model

The generation of most mRNAs involves nuclear processing events that result in the modification of the 5' end with a 7-methyl guanosine cap structure and, with the exception of histone mRNAs, a 3' poly(A) tail. Work conducted in a variety of model systems has shown that these features are important for the translatability of an mRNA, in terms of both translational efficiency as well as mRNA stability. Both have been found to be required for the translation and stabilities of mRNAs in different systems (Peltz *et al.* 1987; Munroe and Jacobson 1990; Gallie 1991). Introduction of synthetic RNAs differing in cap and/or poly(A) status have demonstrated that these structures act synergistically to stimulate translation *in vivo* (Gallie 1991). Experiments conducted in reticulocyte cell-free extracts using mRNAs that differ only in the length of their poly(A) tails demonstrated that both modifications were necessary for optimal translation of the *in vitro*-synthesized VSV.N and rabbit β-globin transcripts. Poly(A)$^-$ or uncapped RNAs were translated two-fold less and uncapped,poly(A)$^-$ transcripts were translated four-fold less than the capped, polyadenylated mRNAs, suggesting that each modification was important for the translatability of the message (Munroe and Jacobson 1990). Cytoplasmic poly(A)-binding protein [PABP; Pab1p in yeast; (Sachs *et al.* 1986)] has been shown to play a role in determining translational efficiency and that suppressors of *pab1* mutants (*spb* mutants) in yeast include those affecting 60S ribosomal subunits (Sachs and Davis 1990).

A relationship between poly(A) metabolism and mRNA stability has also been noted. It has been observed that decay of individual mRNAs is preceded by shortening of the poly(A) tail (Muhlrad and Parker 1992; Hsu and Stevens 1993) and mRNAs lacking poly(A) tails are preferentially degraded in *Xenopus* oocytes or crude extracts (Huez *et al.* 1978; Peltz and Ross 1987). Decay intermediates that accumulate when the 5' to 3' Xrn1p exoribonuclease is inhibited show shortened poly(A) tails (Shyu *et al.* 1991; Hsu and Stevens 1993; Muhlrad *et al.* 1994). The relationship between deadenylation and decay has been demonstrated to be present for mRNAs with a range of decay rates and has been found to be dependent on specific sequence elements (see below). Unstable mRNAs harboring such sequence elements promote rapid deadenylation and decay of the message, such that a block in one process usually leads to a block in the other (Shyu *et al.* 1991; Muhlrad and Parker 1992).

The "closed loop" model has been proposed to account for the requirement of structures found at either end of the mRNA (the 5' cap and 3' poly(A) tail and associated PABP) to stimulate translation and prevent degradation of an mRNA. This model postulates that the poly(A) tail and its associated PABP acts as a translational enhancer, a function achieved by the interaction of factors located at the 5' and 3' ends of an mRNA to form a closed loop structure thereby allowing the Pab1p located at the 3' end of the message to stimulate the formation of 80S ribosomal complexes (Munroe and Jacobson 1990). Such a model is supported by electron micrographs of circular polysomes (Bloemendal *et al.* 1967; Hsu and Coca-Prados 1979) and structural maps of rabbit α-globin and murine β-globin mRNAs which suggested that the 5' and 3' ends of the mRNAs were in close proximity (Heindell *et al.* 1978; Lockard *et al.* 1986). The

closed loop model further predicts that as a consequence of the ability of Pab1p to stimulate 80S formation, the 5' cap remains protected from decapping enzymes and the RNA is protected from degradation (Jacobson 1996). Further support for this model comes from experiments showing that yeast Pab1p can physically interact with the eIF4G component of the eIF4F complex (Tarun and Sachs 1996). Moreover, atomic force microscopy has shown that purified eIF4e, eIF4G, and Pab1p can circularize a capped, polyadenylated RNA (Wells *et al.* 1998). Electron microscopy studies in various systems have visualized polyribosomes as circular structures (Yazaki *et al.* 2000; Madin *et al.* 2004) and polyribsomes formed by a wheat-germ continuous cell-free translation system have been found to form a double-row structure in which small subunits of non-adjacent ribosomes are in close proximity (Kopeina *et al.* 2008).

In addition to mRNA 5' and 3'-associated factors, other studies looking at determinants of mRNA stability in various systems have also suggested that the processes of translation and mRNA turnover are linked [reviewed in (Peltz *et al.* 1991; Jacobson and Peltz 1996; Jacobson and Peltz 2000)]. It has been observed using chimeric constructs in yeast that the *MATα1* coding region contains an instability element and that translation of this region is required for rapid decay of the transcript (Parker and Jacobson 1990). Similar observations have been made for the unstable *HIS3* and *STE3* mRNAs (Heaton *et al.* 1992; Herrick and Jacobson 1992). The presence of an early stop codon in an ORF has also been found to destabilize an mRNA implying that impaired translation of an mRNA can hasten its degradation in a process termed nonsense-mediated mRNA decay [NMD; (Losson and Lacroute 1979)]. This inverse correlation is strengthened by the observation that coexpression of a

nonsense-suppressing tRNA leads to restoration of a normal decay rate for the PTC-containing mRNA (Losson and Lacroute 1979; Gozalbo and Hohmann 1990) or that altered translation termination factors that suppress termination can antagonize NMD (Keeling *et al.* 2004).

General cytoplasmic mRNA turnover

RNA decay mechanisms have been most extensively studied to understand the fate of mRNAs in the cytoplasm. Proper mRNP packaging allows the export of the mRNA to the cytoplasm where it likely is maintained in a “circularized” state, interacts with the protein synthesis machinery, and undergoes translation. During the life of an mRNA molecule in the cytoplasm, progressive deadenylation of the 3’-poly(A) tail [by the Ccr4-NOT deadenylase complex in yeast (Tucker *et al.* 2001); or PARN in human cells (Korner and Wahle 1997)] can lead to the gradual loss of bound Pab1p and presumably disruption of the closed-loop structure of the mRNP. This leads to the association of additional factors with the mRNA, accessibility of the 5’ cap to the Dcp1p/Dcp2p decapping complex and subsequent 5’→3’ exonucleolytic digestion of the decapped mRNA by the Xrn1p exoribonuclease (Garneau *et al.* 2007). Alternatively, 3’→5’ decay of the mRNA can occur via the the multisubunit exosome complex (Beelman and Parker 1995). Thus, one mechanism for turnover of many cytoplasmic mRNAs is a deadenylation-dependent, 5’→3’ process that is regulated by the rate of decapping. Given its importance to the decay pathway, it is not surprising that efficient decapping requires the activity of several accessory factors [reviewed in (Coller and Parker 2004)]. Following deadenylation, the activities of the heptameric Lsm1p-7p

complex, the Dhh1p RNA helicase (also known as RCK/p54 or Me31B in higher eukaryotes), and Pat1p are proposed to enable recruitment of the decapping complex (Fischer and Weis 2002), since loss of any of these factors leads to the accumulation of capped, deadenylated mRNAs. In addition to their roles as stimulators of Dcp1p/Dcp2p activity, Dhh1p and Pat1p also behave as translational repressors (Coller and Parker 2005). Other factors that act as enhancers of mRNA decapping (EDC) activity are the Edc1, Edc2, and Edc3 (Lsm16) proteins. Edc1p and Edc2p have been shown to be RNA-binding proteins that interact with the Dcp1p/Dcp2p complex (Dunckley *et al.* 2001; Schwartz *et al.* 2003). Edc3p is unique in seemingly being rate-limiting for the regulated degradation of only two transcripts in yeast – the *YRA1* pre-mRNA (Dong *et al.* 2007) and *RPS28B* mRNA (Badis *et al.* 2004).

Following deadenylation, an alternative pathway can degrade mRNA. The exosome, a large multisubunit complex that acts in the nucleus and the cytoplasm can mediate 3'→5' mRNA decay (Mitchell *et al.* 1997; Allmang *et al.* 1999). A nine subunit exosome core comprised of catalytically inactive 3'→5' prokaryotic exonuclease homologues is present in both the nucleus and the cytoplasm, with the complex in each compartment possessing at least one additional defining catalytic factor (Allmang *et al.* 1999). Structural and functional studies [reviewed in (Schmid and Jensen 2008)] have determined that the yeast exosome is composed of 11 subunits, nine of which (Rrp4p, Rrp40p, Csl4p, Ski6p/Rrp41p, Rrp42p, Rrp43p, Rrp45p, Rrp46p, Mtr3p) comprise a nuclease-free scaffold. The tenth subunit, Dis3p/Rrp44p, is a nuclease component, and the eleventh subunit is either the 3'→5' exonuclease Rrp6p (found in the nuclear exosome) or Ski7p (in the cytoplasmic exosome). The exosome structure appears to be

conserved in humans, except that: i) the association of Dis3p/Rrp44p is not as stable with the 9-subunit scaffold as in yeast (Chen *et al.* 2001); ii) Rrp6p in humans may be present in both the nucleus and cytoplasm (van Dijk *et al.* 2007); and iii) humans may have an additional nuclear subunit, MPP6, not present in yeast (Schilders *et al.* 2005). Modeling of the exosome suggests a channel-containing ring-like structure formed by the 9-subunit scaffold, with the location of Dis3p/Rrp44p remaining ill-defined (Liu *et al.* 2006). Until recently, it was thought that the exosome possessed only 3'→5' exonuclease activity. However, recent work has demonstrated that Dis3p/Rrp44p has an endoribonuclease activity mediated through a highly conserved PIN domain at its N-terminus (Lebreton *et al.* 2008). Exosome activity in the cytoplasm requires the Ski2p/Ski3p/Ski8p complex which is thought to be recruited to the exosome via interaction with Ski7p (Wang *et al.* 2005).

In the yeast *Schizosaccharomyces pombe*, an additional pathway has been identified in which some mRNAs do not undergo deadenylation prior to decapping. Instead, Lsm1p-dependent decapping is preceded by the addition of one to two uridyl residues to the 3' end of the polyadenylated mRNA by Cid1p, a putative poly(U) polymerase (PUP) and/or terminal uridyl transferase (TUTase) (Rissland and Norbury 2009). Additional transcripts that undergo poly(U)-dependent degradation are the metazoan histone RNAs, which are unique in not possessing a poly(A) tail (Marzluff *et al.* 2008). Instead, the 3'-end of the transcript ends in a conserved stem-loop that is the binding site for a stem-loop binding protein, SLBP1. Bridging of histone mRNA 5' and 3' ends is effected by SLBP-interacting protein 1 (SLIP1), which interacts with both SLBP and eIF4G. Accelerated degradation of histone mRNAs occurs upon termination of DNA

synthesis at the end of S-phase in cells. SLBP, in the presence of the ATR kinase and the NMD factor Upf1p (see below), acts to recruit factors involved in poly(U) addition, followed by binding of the heptameric Lsm1p-7p complex, and the triggering of exosome-mediated 3'→5' decay. This pathway is not the exclusive mode of histone mRNA decay since these RNAs can also serve as substrates for decapping by the Dcp1p/2p complex and 5'→3' decay by Xrn1p (Mullen and Marzluff 2008).

It has been proposed that degradation of mRNAs in the cytoplasm may take place in P bodies, discrete foci highly enriched in components of the decay machinery (Dcp1p/Dcp2p, Pat1p, Dhh1p, Lsm1-7p, and Xrn1p, among others) into which translationally repressed mRNAs are thought to localize to undergo degradation (Parker and Sheth 2007). However, the significance of P bodies remains unclear since recent evidence suggests that assembly of these structures is not essential for mRNA decay (Hu *et al.* 2009; Stalder and Muhlemann 2009). P bodies have been detected in all eukaryotes in which they have been sought, although their composition varies depending on the organism (Parker and Sheth 2007). P body assembly and size appear to depend on the pool of nontranslating, ribosome-free mRNAs (Teixeira *et al.* 2005). Overexpression of a nontranslating mRNA fragment leads to larger P bodies, as does inhibition of translation initiation under conditions of stress, or through the use of conditional alleles of initiation factors (Kedersha *et al.* 2005; Teixeira *et al.* 2005). However, inhibition of translation elongation by treatment of cells with cycloheximide, which traps mRNAs associated with ribosomes, leads to a loss of P bodies suggesting an inverse relationship between ribosome-associated mRNAs and P bodies (Sheth and Parker 2003; Teixeira *et al.* 2005). Translational repression is thought to be an

upstream step in the compartmentalization of mRNPs to P bodies, since loss of Pat1p and/or Dhh1p, which can act as translational repressors, leads to a loss in observable P bodies and increased accumulation of the mRNAs in polysomes (Sheth and Parker 2003). Conversely, overexpression of Dhh1p or Pat1p leads to increased translation repression and increased P body formation (Coller and Parker 2005).

Conditional mRNA decay through protein binding

The presence of a cap and poly(A) tail at either end of an mRNA and the factors that associate with them to confer stability from cellular nucleases highlight the importance of both *cis*-acting sequence elements and sequence-specific *trans*-acting factors in regulating mRNA decay. mRNA stability determinants are usually present in the 3'-untranslated regions (UTRs) of the mRNAs they regulate, although coding region and 5'-UTR elements have also been described (Tucker and Parker 2000).

One of the most well-characterized 3'-UTR sequence determinants is the mammalian adenylate-uridylate rich element (ARE) present in many metazoan transcripts that exhibit rapid response to cellular cues such as those encoding cytokines, proto-oncogenes, and interferons [reviewed in (Khabar 2005)]. AREs were originally defined as having the pentameric sequence AUUUA, but have since been further subclassified according to the number and context of the AUUUA pentamers (Chen and Shyu 1995). These sequences can be bound by ARE-binding proteins (ARE-BPs) to stabilize or destabilize ARE-containing transcripts (Khabar 2005). The Hu family of ARE-BPs is comprised of four members - HuR (HuA), HuB (Hel-N1), HuC, and HuD – and these proteins are mammalian homologs of *Drosophila* ELAV proteins that

possess mRNA stabilizing effects. HuR, the best studied member, is ubiquitous, contains three RNA recognition motifs (RRMs), and targets transcripts such as those derived from the *TNF*, *IL-3*, and *VEGF* genes. Other classes of ARE-BPs target mRNAs for degradation. These include the RRM-containing AU-rich binding factor 1 (AUF1) and the KH splicing regulatory protein, KSRP. Originally identified as a promoter of *c-myc* degradation *in vitro*, AUF1 has four functionally distinct isoforms (p37, p40, p42, and p45). A different structural class of destabilizing ARE-BPs, typified by CCCH-type zinc fingers, includes tristetraprolin (TTP), BRF1, and BRF2. TTP has been found to bind and destabilize the *TNF-α*, *IL-3*, *GM-CSF*, and *COX-2* transcripts. T-cell internal antigen 1 (TIA-1) and TIA-related protein (TIAR) constitute a set of ARE-BPs that do not lead to mRNA decay upon binding, but instead induce translational silencing and aggregation of *TNF-α* mRNA into stress granules. RHAU is an RNA helicase that was isolated as an ARE-BP of the urokinase plasminogen activator mRNA (Meister and Tuschl 2004). Destabilizing AREs appear to function by enhancing the recruitment of decay factors to target mRNAs. The ARE itself has been seen to interact directly with the exosome (Gitlin and Andino 2003) and ARE-BPs can directly/indirectly interact with mRNA decay factors [reviewed in (Garneau *et al.* 2007)]. AUF1(p37), KSRP, RHAU, and TTP have also all been found to interact with the exosome. KSRP and RHAU also bind to the PARN deadenylase, while TTP has been shown to interact with the decapping enzyme and the CCR4 deadenylase to modulate PARN activity *in vitro*. The mechanism by which the Hu proteins stabilize their targets is not fully understood. It is thought that they might either compete with destabilizing factors for binding to AREs or somehow enhance PABP:poly(A) interaction to prevent deadenylation. This is thought to be the

mechanism for other mRNA stabilizing elements such as the U-rich ARE sequence recognized by Pub1p in yeast or poly(C)-rich elements recognized by KH-domain RNA binding proteins.

Another 3'-UTR sequence-specific modulator of mRNA stability is the evolutionarily conserved PUF family of proteins that have been proposed to support the mitotic proliferation of stem cells [reviewed in (Wickens *et al.* 2002)]. PUF proteins usually have eight consecutive Puf repeats, each about 40 amino acids long, that form a three-helix domain that stacks into a crescent-shaped structure thought to bind RNA targets on one surface and interacting proteins on the other. PUF target sequences are sometimes referred to as Nanos Response Elements (NREs), and have a "UGUR" core recognition sequence (Wickens *et al.* 2002). Individual PUFs can target multiple mRNAs, and PUF target specificity is mediated in part by interactions with other 3'-UTR-binding proteins such as Nanos and cytoplasmic polyadenylation element-binding proteins [CPEBs; (Wickens *et al.* 2002)]. PUFs function to enhance degradation of target mRNAs by accelerating deadenylation (Olivas and Parker 2000). Puf3p in yeast can also promote decapping after deadenylation (Olivas and Parker 2000), while Pumilio may effect deadenylation-independent repression of *hunchback* mRNAs in *Drosophila* (Chagnovich and Lehmann 2001).

The iron-response element (IRE), a *cis*-acting stem-loop sequence that is present in the 5' or 3' UTRs of certain mammalian mRNAs involved in iron metabolism, is modulated through the binding of the iron response proteins, IRP1 and IRP2. Whereas 5'-UTR localized IREs act to repress translation of mRNA [e.g., ferritin mRNA; (Aziz and Munro 1987; Hentze *et al.* 1987)], those in the 3'-UTR appear to modulate

mRNA stability (Leipuviene and Theil 2007). Transferrin receptor 1 (TfR1) mRNA contains five IRE stem-loops that constitute a 3'-UTR instability element (Casey *et al.* 1988). The TfR1 mRNA also contains an ARE, which confers a short half-life to the mRNA through a deadenylation-independent endonucleolytic cleavage event in the absence of IRPs (Mullner *et al.* 1989). IRP binding to the IREs in iron-deficient cells blocks this cleavage event and increases the half-life of the TfR1 mRNA, leading to production of the receptor and to increased iron uptake into cells (Mullner *et al.* 1989).

As previously mentioned, metazoan histone RNA decay is regulated through the binding of SLBP to the stem-loop at the 3' end of the histone RNAs (Marzluff *et al.* 2008). This degradation pathway also requires Upf1p, a putative RNA helicase involved in the elimination of mRNAs containing premature translation termination codons (see below), which is thought to bind SLBP and stimulate poly(U) addition (Mullen and Marzluff 2008). Another mammalian pathway that utilizes Upf1p in the absence of an abnormally positioned stop codon is the Staufen 1-mediated decay (SMD) pathway, in which Staufen 1 (STAU1) recruits Upf1p to the 3'-UTR of the *ARF1* mRNA to stimulate its degradation (Kim *et al.* 2005).

Conditional mRNA decay through RNA interference

Small non-coding RNAs (ncRNAs) – which include antisense transcripts, small interfering RNAs (siRNAs), and microRNAs (miRNAs) – play critical roles in maintaining gene expression in eukaryotes by binding to complementary/near-complementary sites on target RNAs and affecting their degradation or translation. Although originally thought to be restricted to multicellular organisms, recent evidence suggests that similar

mechanisms may operate in some yeasts (Drinnenberg *et al.* 2009). RNA interference (RNAi) has mainly been characterized through the effects of siRNAs and miRNAs, each of which follows a distinct pathway for biogenesis (Meister and Tuschl 2004). siRNAs are 21-23 nucleotide RNA molecules that are usually perfectly complementary to their target sequences. They constitute a part of the Argonaute (AGO) RNA-induced silencing complex (RISC), a multiprotein complex that uses the siRNA strand to recognize the complementary target sites on mRNAs and induce their degradation. miRNAs are 20-25 nucleotides long, may have mismatches to their target sequences and are also present in multiprotein miRNP/RISC complexes containing an AGO family member. mRNA degradation by RISCs/miRNPs is thought to occur by inducing cleavages at sites of the RNA duplexes, although recent evidence suggests that miRNAs can trigger deadenylation by the CAF1-CCR4 deadenylase (Chen *et al.* 2009; Fabian *et al.* 2009). These mechanisms are thought to function in innate immune responses against viruses and transposable elements (Gitlin *et al.* 2002). Many endogenous genes also contain miRNA binding sites in their 3' UTRs, which serve to regulate target mRNA expression during different cellular processes (Taft *et al.* 2009).

Antisense transcripts to specific mRNAs can also act to stabilize their target transcripts (Faghihi and Wahlestedt 2009), e.g., an antisense transcript to the induced nitric oxide synthase (*iNOS*) mRNA stabilizes the mRNA by binding to the HuR ARE-binding protein and the target, presumably inhibiting deadenylation and decay (Matsui *et al.* 2008).

Cytoplasmic RNA quality control

Quality control checkpoints at different stages of gene expression maximize the fidelity of gene output, and the fidelity of protein synthesis is dependent not only on a functional translational apparatus, but on the integrity of mRNA coding sequences as well.

Studies from yeast have shown that rRNAs in mature ribosomes with deleterious point mutations in the peptidyl transferase center (25S rRNA) or the decoding site (18S rRNA) undergo more rapid decay than their wild-type counterparts (LaRiviere *et al.* 2006; Cole *et al.* 2009). This process, termed nonfunctional rRNA decay (NRD), is a late stage ribosome quality control pathway that takes place in the cytoplasm. Degradation of the mutant 18S rRNA, but not 25S rRNA, is dependent on translation elongation, since addition of elongation inhibitors such as cycloheximide or hygromycin B stabilized these transcripts. Whereas both mutant transcripts are partly subject to exosome-mediated decay, only the aberrant 18S transcript is sensitive to Ski7p and Xrn1p and appears to localize in P bodies. Further analysis has provided evidence that 18S NRD is also dependent on Dom34p and Hbs1p, factors that participate in the “no-go decay” (NGD) pathway (discussed below) used to eliminate transcripts containing stalled ribosomes (Cole *et al.* 2009).

mRNAs that exhibit translational defects are also subject to accelerated degradation. Transcripts lacking in-frame stop codons undergo non-stop decay (NSD), which serves to not only downregulate the production of extended polypeptides, but also to release ribosomes that are stalled at the 3’ end of an mRNA with no codon at the A-site (Frischmeyer *et al.* 2002; van Hoof *et al.* 2002). NSD requires eRF3 (Sup35p in

yeast) and the exosome co-factor, Ski7p (van Hoof *et al.* 2002). The latter protein shows similarity to translation elongation factor eEF1A and may serve to recruit the exosome to the mRNA. In addition, translation through the poly(A) tail likely displaces Pab1p, leading to the promotion of decapping and Xrn1p-mediated decay (Ito-Harashima *et al.* 2007).

Transcripts in yeast on which translation elongation is blocked, e.g. by the introduction of a stem-loop structure, are recognized and degraded by the “no-go” mRNA decay (NGD) pathway (Doma and Parker 2006). Unlike NMD (see below) or NSD which initiate exonucleolytic digestion of their transcripts, NGD initiates an endonucleolytic cleavage event close to the stalled ribosome by an as yet unidentified factor. The cleaved fragments are further degraded by the combined actions of the 3’→5’ exosome and the 5’→3’ Xrn1 proteins. NGD involves the activity of the eRF1-related factor, Dom34p, and Hbs1p, a GTPase family member related to eEF1A, and may mimic the roles of eRF1 (Sup45p in yeast) and eRF3 (also a GTPase) in ribosome dissociation from the mRNA (Doma and Parker 2006).

The most well studied pathway in this category is the evolutionarily conserved nonsense-mediated mRNA decay (NMD) (Jacobson and Izaurralde 2007; Brogna and Wen 2009) pathway that targets mRNAs containing premature translation termination codons (PTCs), thus minimizing the accumulation of potentially toxic truncated polypeptides (Pulak and Anderson 1993). Observations in yeast made in the late 1970’s suggested that transcripts bearing PTCs were rendered unstable through the NMD pathway (Losson and Lacroute 1979), a finding later extended to mammalian cells (Kinniburgh *et al.* 1982; Daar and Maquat 1988), flies (Schneuwly *et al.* 1989), worms

(Pulak and Anderson 1993), and zebrafish (Wittkopp *et al.* 2009). It has also been observed that there is a polarizing effect to this instability, such that nonsense mutations positioned 5'-proximal to the beginning of the ORF are more destabilizing than more distally located PTCs (Losson and Lacroute 1979; Peltz *et al.* 1993) and detailed studies of the *PGK1* transcript have shown that only PTCs located in the first two-thirds of the *PGK1* protein coding sequence render the mRNA unstable (Peltz *et al.* 1993).

However, the presence of a premature nonsense codon alone in the mRNA is insufficient to lead to NMD. A series of observations have suggested that ribosome recognition of the early stop is necessary to invoke NMD. Mutations or drugs that impair translation initiation (Ruiz-Echevarria *et al.* 1998; Zuk and Jacobson 1998; Welch and Jacobson 1999) or elongation (Herrick *et al.* 1990; Zhang *et al.* 1997; Zuk *et al.* 1999) have been found to stabilize nonsense-containing mRNAs. Nonsense mRNAs that have been stabilized in cells treated with cycloheximide (CHX) can be rendered unstable again upon the removal of CHX (Cui *et al.* 1995). Both nonsense mRNAs and NMD factors have been found to be polysome associated (He *et al.* 1993; Peltz *et al.* 1993; Mangus and Jacobson 1999); and NMD factors have been biochemically shown to be capable of interacting with the translation termination release factors eRF1 and eRF3 (Czaplinski *et al.* 1998).

All eukaryotes have a conserved set of core NMD factors encoded by the *UPF1*, *UPF2/NMD2*, and *UPF3* genes and higher eukaryotes additionally require the products encoded by the *SMG1* and *SMG5-9* genes (Jacobson and Izaurralde 2007; Yamashita *et al.* 2009). The central component of the NMD pathway is the ATPase/helicase Upf1p, with the other factors serving to regulate its function.

UPF1 - A major breakthrough in the understanding of the nonsense-mediated decay pathway came from the discovery that *UPF1* encodes a trans-acting factor that regulates this process in yeast (Leeds *et al.* 1991). Loss of function alleles of *UPF1* were isolated in a screen aimed at selecting high temperature up frameshift suppressors of *his4-38*, a +1 frameshift mutation near the 5' end of the *HIS4* gene that causes translation termination at a nearby downstream stop codon (Culbertson *et al.* 1980). *upf1* mutants were found to stabilize the *his4-38* mRNA by reducing its decay rate. Moreover, loss of *UPF1* function was found to increase stabilities and steady state levels of transcripts from nonsense-containing alleles of *HIS4* and *LEU2*, but had no effect on their WT counterparts. Further characterization of *UPF1* has revealed that it is nonessential for vegetative growth and produces a 3.1kb transcript with an ORF that encodes a 109-KDa polypeptide (Leeds *et al.* 1992). Analysis of the protein sequence has revealed that the N-terminus contains a cysteine/histidine-rich (CH) zinc-finger-like domain, whereas the C-terminus possesses a nucleotide (ATP) binding site and RNA helicase (superfamily I) motifs (Leeds *et al.* 1991; Altamura *et al.* 1992). Western blot analyses have shown that Upf1p in yeast is present at very low levels, approximately 1600 molecules/cell (Jacobson and Peltz 1996). The subcellular localization of Upf1p has been investigated using either an N-terminal FLAG epitope tag (Peltz *et al.* 1993) or a C-terminal triple HA epitope tag (Atkin *et al.* 1995), neither of which affect activity of the protein. Sucrose gradient fractionation studies have revealed that most Upf1p co-sediments with polysomes, although some is seen with monosomes and mRNP fractions (Peltz *et al.* 1993; Atkin *et al.* 1995). Confocal microscopy has also indicated a predominantly cytoplasmic localization for Upf1p (Peltz *et al.* 1994; Atkin *et al.* 1995).

The FLAG-tagged allele of Upf1p has been purified from yeast and further characterized for biochemical activity (Czaplinski *et al.* 1995). The *UPF1* sequence had predicted an NTP-binding and possible NTPase domain for Upf1p, a prediction confirmed using the purified protein. It has been shown that FLAG-Upf1p possesses nucleic acid-dependent ATPase activity *in vitro* and that purified variants containing a mutation in a conserved lysine in the NTP binding and hydrolysis motif (K436Q) lose this function, which correlates with the observation that introduction of this allele *in vivo* inactivates NMD (Czaplinski *et al.* 1995). Furthermore, it has been found that in the absence of ATP, FLAG-Upf1p is able to bind to single-stranded DNA or RNA, and that hydrolysis of ATP results in its release from the single-stranded nucleic acid (Czaplinski *et al.* 1995). Characterization of Upf1p's helicase activity has revealed that it possesses ATP-dependent 5' to 3' DNA and RNA helicase activity (Czaplinski *et al.* 1995). Comparisons of structural analyses of the Upf1p helicase core in three states (phosphate-, AMPPNP-, and ADP-bound forms) in combination with mutational analyses suggest the presence of a single-stranded RNA binding channel able to undergo conformational changes upon ATP binding and hydrolysis (Cheng *et al.* 2007). It has been demonstrated that Upf1p can interact biochemically with the translation termination factors eRF1 and eRF3 (Sup45p and Sup35p, resp., in yeast) in yeast and human cells (Czaplinski *et al.* 1998; Wang *et al.* 2001) and further analysis has shown that the Upf1p N-terminal CH domain interacts with eRF3 (Ivanov *et al.* 2008) and Upf2p/Nmd2p (He *et al.* 1997; Kadlec *et al.* 2006). Moreover, studies using purified factors and synthetic poly(U) RNA have shown that eRF3 and RNA compete for binding to Upf1p and that eRF1 and eRF3 can inhibit Upf1p ATPase activity (Czaplinski *et al.* 1998). Genetic data also suggests Upf1p can

affect nonsense codon readthrough (Maderazo *et al.* 2000; Keeling *et al.* 2004). It has recently been proposed that the CH domain may play a RING-related role for Upf1p to mediate E3 ubiquitin ligase activity in yeast (Takahashi *et al.* 2008).

NMD has been found in all eukaryotes studied to date and homology searches have identified *UPF1* (as well as *UPF2* and *UPF3*) orthologs in all eukaryotic model organisms: *SMG2* in *C.elegans* (Page *et al.* 1999); *hUPF1/Rent1* in humans and mice (Perlick *et al.* 1996; Applequist *et al.* 1997); *Drosophila* Dm*UPF1* (Gatfield *et al.* 2003); and *Upf1* in zebrafish (Wittkopp *et al.* 2009). Whereas *UPF1* is not essential for viability in yeast or worms (Leeds *et al.* 1991; Page *et al.* 1999), loss of Upf1 function in higher organisms leads to developmental arrest (Medghalchi *et al.* 2001; Metzstein and Krasnow 2006; Wittkopp *et al.* 2009). It is now well established that Upf1p is a phosphoprotein in non-yeast eukaryotes (Page *et al.* 1999; Yamashita *et al.* 2001) and that cycles of Upf1p phosphorylation and dephosphorylation are critical for NMD function (Ohnishi *et al.* 2003; Grimson *et al.* 2004), with factors (*SMGs1,3-7;* discussed below) regulating the phosphorylation status being conserved in all metazoans. There is some evidence to suggest that Upf1p may be phosphorylated in yeast as well (Wang *et al.* 2006), although what role this may play in NMD is not known since no yeast homologs of the *SMG* factors have been found.

***UPF2/NMD2* -** The second core NMD factor (so-called because it is required for NMD in all organisms tested) was identified in yeast by two strategies (Cui *et al.* 1995; He and Jacobson 1995) and has orthologs in mammals (Mendell *et al.* 2000; Serin *et al.* 2001), flies (Gatfield *et al.* 2003), worms (Pulak and Anderson 1993), and zebrafish (Wittkopp

et al. 2009). The Peltz lab utilized a genetic screen (Cui *et al.* 1995) to complement a *upf2* allele that had been previously isolated as an allosuppressor of the *his4-38* allele (Culbertson *et al.* 1980), whereas the Jacobson lab utilized the yeast two-hybrid system to detect Upf1p-interacting proteins *in vivo* (He and Jacobson 1995). Among the six genes identified by two-hybrid analysis (*NMD1-4*, *DBP2*, and *SNP1*), *NMD2* was found to be allelic to *UPF2*. Cloning and characterization of yeast *UPF2/NMD2* has indicated an ORF 3267 nt in length consisting of 2 exons and a 5'-proximal intron, with a protein product predicted to have a mass of 126-kDa that is not essential for viability. Structural determination from sequence analysis has inferred a highly acidic region near the C-terminus, a putative bipartite nuclear localization sequence near the N-terminus, and a putative helical transmembrane domain in the middle of the protein all of which have been found to be essential for function (He and Jacobson 1995). Further analysis of the sequence has revealed that NMD2 possesses 3 MIF4G (middle portion of eIF4G) or 4GH (eIF4G homology) domains (Aravind and Koonin 2000; Ponting 2000). In eIF4G, this domain has been found to bind eIF4A and eIF3 (Lamphear *et al.* 1995; Imataka and Sonenberg 1997), as well as to RNA (Pestova *et al.* 1996). Mutations in *S.pombe* Upf2p 4GH domains are sufficient to abrogate its function (Mendell *et al.* 2000). Two-hybrid analysis has shown that the hUpf2 can interact with eIF4AI and Sui1 (Mendell *et al.* 2000) and recent structural studies have shown that the third MIF4G domain of hUpf2 is capable of binding RNA (Kadlec *et al.* 2004). The C-terminal 157 amino acids of Upf2p/Nmd2p constitutes the Upf1p-interacting domain with the last 56 amino acids being critical for decay function *in vivo* (He *et al.* 1996) and biophysical studies have demonstrated that two distinct structural elements in this region bind in a bipartite

fashion on opposite surfaces of Upf1p (Clerici *et al.* 2009). Coimmunoprecipitation studies have confirmed that hUpf1p and hUpf2p interact with each other as well. Genetic and biochemical data have also shown that Upf2p/Nmd2p can interact with Upf3p and eRF3 (He *et al.* 1997; Wang *et al.* 2001; Chamieh *et al.* 2008) and that hUpf2 is capable of binding to RNA (Kadlec *et al.* 2004). Upf2p/Nmd2p has been shown to act as a bridge between Upf1p and Upf3p to form a trimeric complex (He *et al.* 1997; Chamieh *et al.* 2008). Upf2p/Nmd2p is polysome-associated in yeast (Atkin *et al.* 1995) and present at very low levels (Jacobson and Peltz 1996). Yeast and human Upf2p have been proposed to be phosphorylated (Chiu *et al.* 2003; Wang *et al.* 2006), although the precise role of this phosphorylation remains to be elucidated.

UPF3 – The least abundant of the Upf factors (Jacobson and Peltz 1996) and initially isolated as an allosuppressor of *his4-38* (Culbertson *et al.* 1980), the third core NMD factor, encoded by *UPF3*, was subsequently shown to be specifically involved in the degradation of PTC-containing mRNAs (Leeds *et al.* 1992). Cloning and characterization of the yeast gene have revealed that *UPF3* is not essential for cell viability and consists of an 1161 nt ORF with a 44.9-KDa predicted protein product that is cytoplasmic and polysome-associated (Lee and Culbertson 1995; Shirley *et al.* 1998). The protein contains three putative nuclear localization sequences (NLSs), each of which is functional on a heterologous reporter; and two putative nuclear export sequences (NESs), only one of which appears to be functional (Lee and Culbertson 1995; Shirley *et al.* 1998; Shirley *et al.* 2002). Early studies in yeast showed that disruption of *UPF3*, *UPF1*, or both yielded the same degree of *his4-38* mRNA

stabilization, suggesting that both genes function in the same pathway (Lee and Culbertson 1995). Yeast two-hybrid studies have demonstrated that a fragment of Upf3p spanning residues 78-278 interacts with a domain of Upf2p/Nmd2p encompassing residues 564-771 (He *et al.* 1997). This region of Upf2p/Nmd2p is distinct from its Upf1p-binding domain (He *et al.* 1996). Two-hybrid analysis has also shown that Upf1p can interact with Upf3p when bridged by Upf2p/Nmd2p, suggesting that all three Upf proteins form a complex and function in the same pathway. In support of this conclusion, deletion of all three genes in a single strain give a similar decay phenotype to the single or double deletion strains (He *et al.* 1997) and genetic studies have shown that Upf1p is the central effector of this pathway, and is regulated by Upf2p/Nmd2p and Upf3p (Maderazo *et al.* 2000). Upf3p has also been shown to interact with eRF3 (Wang *et al.* 2001) and can affect readthrough of nonsense codons (Maderazo *et al.* 2000).

Human orthologs to yeast Upf3p derive from 2 genes, one of which is X-linked, and are known as *hUPF3* and *hUPF3-X* or *hUPF3a* and *hUPF3b* (Serin *et al.* 2001). Whereas hUpf1p and hUpf2p are found in the cytoplasm, hUpf3p-X is detected primarily in the nuclei of HeLa cells. Coimmunoprecipitation studies using tagged alleles have also shown that hUpf3p and hUpf2p interact (Serin *et al.* 2001) and structural studies have elucidated the interaction domains involved (Kadlec *et al.* 2004). In mammalian cells, it has been shown that hUpf3p can bind to the exon-junction complex (EJC) factor Magoh-Y14 to act as a bridge between the EJC and hUpf2p (Chamieh *et al.* 2008).

Additional regulators of Upf1p function - In yeast, only *UPF1*, *UPF2/NMD2*, and *UPF3* are specifically required for NMD, whereas additional genes are required for NMD function in higher eukaryotes. Upf1p has been demonstrated to be the key effector, whereas Upf2p and Upf3p regulate Upf1p function (Page *et al.* 1999; Maderazo *et al.* 2000). Initially identified in a genetic screen in worms (Pulak and Anderson 1993), *SMG1* and *SMGs5-7* have been found to be regulators of Upf1p phosphorylation in all metazoan cells, except flies which lack *SMG7* (Muhlemann *et al.* 2008). *SMG1* encodes a serine/threonine kinase that functions to phosphorylate Upf1p (Page *et al.* 1999; Denning *et al.* 2001; Yamashita *et al.* 2001). *SMG3* (*UPF2*) and *SMG4* (*UPF3*) enhance phosphorylation of Upf1p, whereas *SMG5*, *SMG6*, and *SMG7* function to promote dephosphorylation of Upf1p (Page *et al.* 1999; Wilkinson 2003), though not directly. None of these proteins are phosphatases themselves, but are thought to recruit protein phosphatase 2A (PP2A) (Anders *et al.* 2003; Chiu *et al.* 2003; Ohnishi *et al.* 2003). It has recently been shown that *SMG6* encodes an endonuclease that functions in NMD (Huntzinger *et al.* 2008; Eberle *et al.* 2009). Recently, two novel NMD factors, SMG-8 and SMG-9, were isolated in metazoan cells (Yamashita *et al.* 2009). They have been proposed to regulate the kinase activity of SMG-1 in addition to bridging the SURF (SMG-1, UPF1, eRF1, eRF3) complex on ribosomes to the EJC on PTC-containing mRNAs.

Nonsense Substrate Spectrum - mRNAs containing premature stop codons can arise at the DNA level through mutations, frameshifting events, or programmed DNA gene rearrangements in the genome of an organism or at the RNA level through errors in

transcription, RNA processing, or alternative RNA splicing events that generate in-frame nonsense codons. Identification and characterization of the Upf factors required for NMD have enabled the screening in various organisms for NMD substrates (He *et al.* 1993; Pulak and Anderson 1993; Muhlrad and Parker 1999; Johns *et al.* 2007). The use of DNA microarray technology has led to the realization that a significant portion of the yeast transcriptome is subject to NMD regulation, approximately 750 genes (He *et al.* 2003). In addition to the predicted classes of NMD substrates in yeast – mRNAs from genes containing PTCs, inefficiently spliced pre-mRNAs, mRNAs undergoing leaky scanning, and mRNAs containing upstream ORFs (u-ORFs) – a number of other classes of substrates have been recognized. These include pseudogene mRNAs, mRNAs derived from transposable elements or their LTRs, bicistronic mRNAs, and mRNAs that use +1 frameshifting in their translation (He *et al.* 2003). This study also confirmed, at the genome-wide level, prior observations that Upf1p, Upf2p/Nmd2p, and Upf3p function in the same pathway since inactivation of either of these genes resulted in similar expression profiles. Although these early studies could not distinguish direct from indirect effects of loss of NMD function in cells (Rehwinkel *et al.* 2006), later studies directed towards RNAs that were specifically associated with Nmd factors have shown good correlation with the previous data (Johansson *et al.* 2007).

Nonsense Recognition - Translation termination involves the translating ribosome encountering a nonsense codon in its A-site, subsequent binding of release factors, polypeptide hydrolysis, and ribosome subunit dissociation. In normal termination, the terminating ribosome dissociates efficiently from the mRNA without accelerating the

mRNA's decay rate. Termination is carried out by two classes of release factors: class I factors (eRF1 in eukaryotes; Sup45p in yeast) recognize stop codons and trigger hydrolysis of the ester bond connecting the polypeptide chain and the tRNAs in the ribosomal P site while class II release factors (eRF3 in eukaryotes; Sup35p in yeast) are GTPases that stimulate class I factor activity (Zhouravleva *et al.* 1995). The essential eRF1 and eRF3 proteins interact and are thought to function as a complex. It has been found that eRF3's GTPase activity is dependent on ribosome-bound eRF1 and is necessary for eRF1 recognition of the stop codon and subsequent polypeptide chain release (Alkalaeva *et al.* 2006). Normal termination is also stimulated by PABP (Pab1p in yeast) (Cosson *et al.* 2002). This is thought to occur through PABP's interaction with eRF3, leading to termination, ribosome dissociation, and possibly *in cis* recycling of ribosomal subunits (Cosson *et al.* 2002; Hosoda *et al.* 2003).

When a stop codon occurs sufficiently upstream of its normal position, however, accelerated degradation of the mRNA (NMD) ensues. Recognition of the PTC in most eukaryotes, which occurs in a *UPF*-dependent manner, triggers decapping of the substrate mRNA, usually without prior deadenylation, and the decapped transcript is then degraded primarily by the 5'→3' Xrn1p exonuclease, with some degradation occurring 3'→5' by the cytoplasmic exosome [reviewed in (Jacobson and Izaurralde 2007)]. Decay activity in *Drosophila* NMD is instituted by endonucleolytic cleavage of the nonsense mRNA by the PIN-containing SMG6 protein followed by exosome-mediated digestion of the 5' cleavage fragment and Xrn1-mediated degradation of the unprotected 3' cleavage fragment (Gatfield and Izaurralde 2004).

Despite conservation of the NMD pathway, the detailed mechanism by which PTCs are recognized has yet to be resolved. Based on the complexity of the organism, there are two predominant models for NMD induction:

Pioneer Round Model – hypothesized to function in mammalian cells, this model is predicated on the recognition of splicing-dependent “marks”- the exon junction complex (EJC) - present on the mRNAs post-termination by the surveillance machinery. In mammalian cells, NMD is activated when a PTC is 50-55 nucleotides upstream of an exon-exon junction (Zhang *et al.* 1998), the site of deposition of the exon junction complex (EJC). The latter contains the Upf2 and Upf3X proteins in addition to factors involved in pre-mRNA splicing (RNPS1, UAP56, and SRm160), factors involved in mRNA export (REF/Aly, Y14, and Magoh), and factors with incompletely characterized functions (eIF4AIII and Barentz/MLN51)(Le Hir *et al.* 2001). The “pioneer round model” proposes that translation by the first, or pioneer, ribosome is able to displace EJCs from each spliced junction (Ishigaki *et al.* 2001). Hence, the presence of a PTC upstream of an EJC allows Upf1 that is part of the SURF (Smg1, Upf1, eRF1, and eRF3) complex on the terminating ribosome to interact with the EJC through Upf2, leading to Upf1 phosphorylation by the Smg1 kinase, recruitment of Smgs5-7 (which serve to dephosphorylate phospho-Upf1) to form the decay-inducing complex (DECID), and subsequent decapping and decay (Behm-Ansmant and Izaurralde 2006; Kashima *et al.* 2006). Cycles of phosphorylation/dephosphorylation of Upf1 are required for Upf1 to mediate its function, although the significance of this cycle remains to be elucidated. Amongst other observations, tethering EJC factors downstream of a normal termination codon leads to mRNA destabilization, providing support for this model (Ivanov *et al.*

2008). Other observations suggest that excessive distance between the premature termination codon and the poly(A) tail of metazoan mRNAs may also trigger NMD (Eberle *et al.* 2008).

NMD of some transcripts in mammalian cells has been observed to be nucleus-associated and cytoplasmic nonsense-containing mRNAs appear to be immune to the NMD pathway. This has prompted the idea that only newly synthesized mRNAs that are bound by the nuclear cap binding complex CBP80/CBP20, and not the cytoplasmic cap binding factor eIF4E, are subject to decay (Ishigaki *et al.* 2001; Lejeune *et al.* 2002), and recent studies have provided evidence to show that Upf1 is associated with CBP80-containing mRNAs (Yamashita *et al.* 2009). This is in contrast to findings in yeast that show that NMD is not limited to newly synthesized transcripts (Maderazo *et al.* 2003; Gaba *et al.* 2005). The discovery of Smg-8 and Smg-9 has provided additional mechanistic insight into the events following recognition of the PTC (Yamashita *et al.* 2009). It is hypothesized that Smgs-1, 8, and 9 (the SMG1 complex – SMG1C) binds to Upf1p prior to its incorporation into the SURF complex. This SMG1C:SURF complex assembles onto the terminating ribosome of a CBP80/20-bound nonsense substrate mRNA. Smg-8 is thought to maintain Upf1 hypophosphorylated by suppressing Smg-1 kinase activity in the SURF complex. Association of the EJC with the ribosome:SURF complex through Upf1:Upf2 interaction leads to Smg-1-mediated phosphorylation of Upf1, recruitment of Smgs 5-7, followed by decapping and decay of the mRNA.

***Faux* 3'-UTR Model** - in lower eukaryotes, NMD is predicated on the idea that PTC recognition occurs due to an absence of factors 3' to the nonsense codon that are associated with a normal 3'-UTR. According to this "faux 3'-UTR" model (Jacobson

1996), normal termination codons are located in the vicinity of bound Pab1p. Interaction between 3'-bound Pab1p, or a factor whose UTR-association is enhanced by Pab1p, and the terminating ribosome precludes the stable interaction of the Upf complex to the ribosome and mediates efficient peptide hydrolysis and ribosome release. At a PTC, the absence of proximal Pab1p leads to stable binding of the Upf proteins, a prerequisite for decapping and subsequent Xrn1p-mediated degradation. The polarity effect observed by nonsense codon position supports this model (Losson and Lacroute 1979; Peltz *et al.* 1993) as do mutations that lead to extended 3'-UTRs resulting in mRNAs with shortened half-lives (Muhlrad and Parker 1999). Moreover, this model also accounts for observed interactions between the eRFs and the Upf proteins (Czaplinski *et al.* 1998) as well as Pab1p (Cosson *et al.* 2002; Hosoda *et al.* 2003). Although initially thought to be limited to lower eukaryotes, this model may be operational in higher eukaryotic cells, since localizing Pab1p downstream of a PTC suppresses the NMD of those reporter mRNAs (Behm-Ansmant *et al.* 2007; Eberle *et al.* 2008; Ivanov *et al.* 2008; Silva *et al.* 2008; Singh *et al.* 2008).

Deletion of *UPF1*, *NMD2/UPF2*, and/or *UPF3* in yeast leads to similar decay phenotypes (He *et al.* 1997), Nmd2p can bridge Upf1p and Upf3p (He *et al.* 1997), and Upf1p activity is regulated by Nmd2p and Upf3p (Maderazo *et al.* 2000). These observations suggest that all three factors may be recruited and function as a complex. However, polysome distribution analyses indicate that ribosome association of these factors is not necessarily codependent (Atkin *et al.* 1997) and recent evidence from studies on P bodies suggests that these three factors may not be recruited as a complex to a PTC-containing mRNA (Sheth and Parker 2006). Upf1p may be recruited

to the termination complex at the PTC, where it is proposed to induce translational repression (Muhlrad and Parker 1999) and targets the mRNA to P bodies (Sheth and Parker 2006). Nmd2p/Upf2p and Upf3p are present in P bodies and interact with the Upf1p-bound mRNA to induce decapping by the Dcp1p/Dcp2p complex and subsequent Xrn1p-mediated decay (Sheth and Parker 2006).

Work done in this thesis

The mechanistic details regarding NMD in yeast still remain a mystery. Why does the presence of a premature nonsense codon cause an mRNA to become unstable? Shouldn't a stop codon be just that…a signal to terminate translation? Why does the presence of a PTC lead to such aggressive destruction of the mRNA? Moreover, why should the position of the PTC in the ORF affect NMD-sensitivity? What is the role of the NMD factors? Despite a wealth of data, satisfactory answers to these fundamental questions remain inadequate. The "*faux* 3'-UTR" model offers a comprehensive blueprint for the mechanistic aspects determining recognition of a premature nonsense codon This model predicts that recognition of nonsense codon as being premature stems from the lack of interaction between the terminating ribosome and poly(A) tail-associated Pab1p, but this hypothesis has never been tested directly. In Chapter II of this thesis, we have sought to address this question by artificially tethering Pab1p in the vicinity of an otherwise NMD-sensitive PTC. We show that NMD of a PTC can be suppressed in the presence of proximal Pab1p. Furthermore, implicit in the "*faux* 3'-UTR" model is the notion that there exist mechanistic differences in translation termination at normal *vs.* premature stop codons and that the NMD factors facilitate

events at premature termination. In this chapter, I also elaborate the development and use of an *in vitro* assay system that allows us to take advantage of the translation of synthetic mRNAs by yeast cell-free extracts from different genetic backgrounds to address these issues. We demonstrate that premature termination is an inefficient process and biochemically distinct from normal termination.

In yeast, Upf1p, Nmd2p/Upf2p, and Upf3p are required for NMD to occur. However, we have yet to understand what functions these factors perform. Despite extensive characterization of its biochemical properties, Upf1p's function at premature termination and mode of action are relatively unknown. Prior observations and some results from our work presented in Chapter II indicate a role for Upf1p in translation initiation. However, there is very little understanding of what Upf1p is doing. In Chapter III of this dissertation, I detail our investigations dissecting a role for Upf1p in translation initiation and provide evidence as to its function at premature termination. Using a series of constructs *in vivo*, we show that the Upf proteins mediate translation reinitiation subsequent to a premature termination event in *cis*. To further understand this phenotype and reconcile them with previous observations, we developed a series of novel *in vitro* translation assays and used our cell-free translation system to show that Upf1p-dependent initiation/reinitiation phenotypes are a consequence of its role at premature termination.

mRNA translatability and stability have been shown to require the 5' cap structure and 3' poly(A) tail. The "*faux* 3'-UTR" model also suggests that the structure of an mRNP is important in determining whether an mRNA is viewed as normal or aberrant by the cell. The "closed loop" model for mRNP structure was proposed over 20

years ago (Jacobson and Favreau 1983). Except for electron micrographic evidence which allows us to directly visualize these structures, an assay system to readily monitor this structure and understand the requirements for its maintenance have been lacking. We have once again taken advantage of our cell-free translation/toeprinting system to biochemically assay, monitor the strength of, and factors required to maintain a circularized mRNA structure. In Chapter IV of this dissertation, I detail our findings showing that, consistent with previous observations, factors that interact with both ends of the mRNA and those that are involved in translation initiation are required to form and maintain a stable closed loop. Surprisingly, we find that translation termination factors also play a role in this process. Using drugs that allow us to detect early *vs.* late steps in translation initiation, we show that we are able to detect two distinct forms of the closed loop structure. In Chapter V, I discuss the implications of our findings.

Chapter II

A faux 3'-UTR promotes aberrant termination and triggers nonsense-mediated mRNA decay

The work presented in this chapter has been published as:

Amrani N., Ganesan R., Kervestin S., Mangus D.A., **Ghosh S.**, and Jacobson A. (2004). A faux 3'-UTR promotes aberrant termination and triggers nonsense-mediated mRNA decay. Nature **432**(7013):112-8.

SG's contributions to this work include extract preparation and optimization, handling and processing of toeprint gels, all luciferase assays, and northern blotting of non-MS2 constructs.

Chapter II - A faux 3’-UTR promotes aberrant termination and triggers nonsense-mediated mRNA decay

Summary

Nonsense-mediated mRNA decay (NMD) is triggered by premature translation termination (Pulak and Anderson 1993; Maquat 1995; Jacobson and Peltz 1996), but the features distinguishing that event from normal termination are unknown. One model for NMD suggests that decay-inducing factors bound to mRNA during early processing events are routinely removed by elongating ribosomes, but maintain an mRNA association when termination is premature, thereby triggering rapid turnover (Gonzalez *et al.* 2001). Recent experiments (Gatfield *et al.* 2003; Maderazo *et al.* 2003; LeBlanc and Beemon 2004) challenge this notion and point to a model which posits that mRNA decay is activated by the intrinsically aberrant nature of premature termination (Hilleren and Parker 1999; Jacobson and Peltz 2000). Here we use a primer extension inhibition (toeprinting) assay (Sachs *et al.* 2002) to delineate ribosome positioning and find that premature translation termination in yeast extracts is indeed aberrant. Ribosomes encountering premature UAA or UGA codons in the *CAN1* mRNA fail to release and, instead, migrate to upstream AUGs. This anomaly depends on prior nonsense codon recognition and is eliminated in extracts derived from cells lacking the principal NMD factor, Upf1p, or by flanking the nonsense codon with a normal 3'-UTR. Tethered poly(A)-binding protein (Pab1p), used as a mimic of a normal 3'-UTR, recruits the termination factor Sup35p (eRF3) and stabilizes nonsense-containing mRNAs. These findings indicate that efficient termination and mRNA stability are dependent on a properly configured 3'-UTR.

Results

Toeprint analyses of initiation and premature termination in cell extracts

The results presented in this chapter are largely based on data obtained by the studying ribosomal positioning on various synthetic mRNAs using the toeprinting technique (see Appendix D). The yeast *can1-100* allele contains a premature UAA codon at position 47 of the *CAN1* coding region that effectively terminates translation and destabilizes the *CAN1* mRNA (Maderazo *et al.* 2000). We constructed a gene fusion encompassing the UAA-containing segment of this allele and the firefly *LUC* coding region, and used this construct to generate synthetic mRNA (*UAA* RNA). Mutagenesis techniques were used to create a variant with a weak terminator (Bonetti *et al.* 1995) (CAA UGA CAA) at codon 47 (*UGA* RNA) and two control RNAs with no early stop codon (*Fusion* and *AAA* RNAs; Fig. 2.1). *In vivo* expression experiments demonstrated that the *UAA* and *UGA* RNAs were substrates for NMD, but the *Fusion* RNA was not (data not shown). Translation reactions in wild-type extracts were incubated with these mRNAs and subjected to toeprinting analyses (see Appendix D), using sensitivity to the cap analog ^{7}mGpppG, an inhibitor of translation initiation, as a means to distinguish *bona fide* toeprints from background bands (Sachs *et al.* 2002). Toeprints corresponding to ribosomes stalled with a stop codon in their A sites were obtained with the *UAA* and *UGA* RNAs at the expected position, 12-14 nucleotides (nt) downstream of the premature nonsense codons (Sachs *et al.* 2002) (Fig. 2.2(a), lanes 1 and 3). The toeprints were dependent on mRNA translation, because they were sensitive to cap analog (lanes 2 and 4) and dependent on the presence of the stop

codon, because they were absent in the *Fusion* RNA (lanes 5 and 6). Whereas toeprints were readily detectable from premature termination codons in the absence of CHX in wild-type extracts [e.g., Fig. 2.2(a)], no toeprints were obtained under the same conditions when the normal termination codons of the *Fusion* and *ADE2* RNAs were analyzed even after long periods of translation [Fig. 2.2(b)] or upon incubation in extracts with temperature-sensitive eRF1 (data not shown). These results suggest that ribosomes terminating prematurely are released much less efficiently than those encountering normal terminators.

Addition of the elongation inhibitor cycloheximide (CHX) to the translation reactions also failed to reveal toeprints from normal terminators (data not shown), but did allow detection of additional toeprints (Kozak 1998; Dmitriev *et al.* 2003). CHX-dependent initiator AUG toeprints on the *UAA, UGA*, *Fusion,* and *AAA* RNAs were sensitive to cap analog (Fig. 2.3(a), +16 arrow, lanes 1-6 and Fig. 2.3(b), top panel) and reflect 80S ribosomes, centered on AUG codons, protecting 16-18 nt 3' of those codons. Other CHX-dependent toeprints were present in close proximity to the locations of the early stop codons. These unanticipated bands mapped to a position 6-7 nt downstream of the U of the terminator in both the *UAA* and *UGA* RNAs (Fig. 2.3(a), lanes 1 and 3, +6 arrow), as well as to a position 17 nt downstream of the terminator U in the *UGA* RNA (lane 3, +17 arrow). The appearance of these toeprints was dependent on concurrent mRNA translation (lanes 2 and 4), the presence of yeast extract (lanes 7-9), and termination codon recognition (lanes 5 and 6 and Fig. 2.3(b), bottom panel). The dependence of these toeprints on prior termination codon recognition was underscored by experiments showing that, after CHX addition, the +6 toeprint of the *UAA* RNA

accumulated subsequent to the disappearance of the +12 toeprint [Fig. 2.3(c)], and by the observation that extracts of *sup45-2* cells with defective eRF1 (Stansfield *et al.* 1997) only yielded the +12 toeprint, regardless of the presence or absence of CHX (Fig. 2.2(a), lanes 7-12 and Fig. 2.8, lanes 7, 8, 17, and 18).

Aberrant toeprints are dependent on the presence of NMD factors

Most importantly, the aberrant toeprints of the *UAA* and *UGA* RNAs were linked to NMD because they failed to accumulate in extracts lacking Upf1p or Upf2p/Nmd2p (Fig. 2.3(d) and data not shown). The lack of aberrant toeprints in *upf1Δ* or *upf2Δ/nmd2Δ* extracts cannot be due to inefficient translation since these extracts display premature terminator +12 toeprints in the absence of CHX (Fig. 2.2(a), lanes 13-18 and data not shown) and normal initiator AUG toeprints in the presence of CHX (data not shown).

Aberrant toeprints derived from PTCs in wild-type extracts in the presence of CHX are dependent on upstream AUGs

The *UAA* and *UGA* RNAs both contained AUG codons just upstream of their premature terminators [Fig. 2.1]. To determine whether these AUGs were relevant to the toeprints of Figs. 2.3(a) and (b), we analyzed two RNAs in which the upstream AUGs were mutated. Toeprint analyses of the *UAA-M* and *UGA-M* RNAs in wild-type extracts supplemented with CHX, in the presence or absence of cap analog, showed that: a) mutation of the –11 AUG of the *UAA* RNA eliminated the +6 band (Fig. 2.4, compare lanes 1 and 3) and b) mutation of the –11 and –1 AUGs in the *UGA* RNA led

to the disappearance of the +6 and +17 bands (compare lanes 7 and 9) and to the appearance of a +12 toeprint characteristic of weak terminators (Bonetti *et al.* 1995) (lane 9 and data not shown). These results indicate that the +6 toeprints obtained with the *UAA* and *UGA* RNAs correspond to the P site of the ribosome stalled at the –11 AUG and that the +17 toeprint derived from the *UGA* RNA corresponds to ribosomes stalled at the –1 AUG (Kozak 1998). One explanation for these results is that post-termination ribosomes fail to be released at premature terminators and are able to scan backwards and reinitiate at the –11 AUG in the *UAA* RNA or at the –11 or –1 AUG in the *UGA* RNA. Such retroreinitiation has been previously suggested by studies in mammalian cells (Peabody and Berg 1986; Thomas and Capecchi 1986). The propensity for backwards scanning was independently confirmed by analyses of luciferase activity obtained *in vitro* from RNAs harboring in-frame *LUC* fusions to upstream or downstream AUGs (Fig. 2.5). Six constructs were made in which the *LUC* ORF was in frame with AUGs at either -11 in the *Fusion, UAA, UAA-W,* and *UAA-DS* RNAs or at +5 in the *UAA-M-DS* and *UAA-DS* constructs (designated *Inf-Fusion, Inf-UAA, Inf-UAA-W, Inf-UAA-DS, Inf-UAA-M+5D* and *Inf-UAA+5DS,* respectively). A seventh construct, used as a control, contained the UAA stop codon, but lacked the –11 and +5 AUGs (*Inf-UAA-M*). Constructs containing the -11 AUG in frame with the *LUC* ORF were made by insertion of an A at position 4 downstream of the stop codon, or its equivalent position in the case of the control *Inf-Fusion* RNA. Constructs containing the +5 AUG in frame with the *LUC* ORF were made by insertion of an A at position 10 downstream of the stop codon, plus a deletion of the G at position 4 in the case of the *Inf-UAA+5DS*. Translation of these RNAs *in vitro* showed that ribosomes effectively

reinitiate at the upstream -11 AUG, or at the downstream +5 AUG, and are able to produce luciferase activity that is dependent on the presence of both the termination codon and flanking AUG codons (Fig. 2.5). Consistent with the toeprint data of Fig. 2.7 (see below), ribosomes exiting the premature stop codon prefer retroreinitiation to downstream reinitiation (compare *Inf-UAA-DS* to *Inf-UAA+5DS*). Moreover, as expected from the toeprinting results of Fig. 2.3(d), the *in vitro* translational yield of all RNAs is markedly reduced in *upf1Δ* extracts (Fig. 2.5). These data showing that the luciferase activity obtained from an in-frame fusion of the –11 AUG to the *LUC* ORF was 4-5-fold greater in the presence of the codon 47 UAA and the –11 AUG than in their absence (Fig. 2.5) support the notion that ribosomes can reinitiate translation at AUG codons upstream or downstream of the stop codon in an NMD-dependent manner. While retroreinitiation is alternatively explainable as leaky scanning (Kozak 1998), the absence of a toeprint signal at the –11 AUG in the *Fusion* or *AAA* RNAs or in *upf1Δ* extracts [Fig.2.3(d)], as well as the chase experiments of Fig. 2.3(c), reduce the likelihood of that explanation. Collectively, these experiments indicate that access to internal AUG codons of the *UAA* and *UGA* mRNAs depends on prior recognition of a downstream premature stop codon.

The distance limits of retroreinitiation were assessed by constructing nonsense-containing RNAs that harbor AUG codons 21 or 32 nt upstream of the premature terminator (Fig. 2.6). Control RNAs (*Fusion-21* and *Fusion-32*), containing the -21 and -32 AUGs, respectively, but not the premature stop codon, were also constructed. Toeprint analyses revealed strong bands, sensitive to cap analog, in the *UAA-M-21* and *UGA-M-21* RNAs at positions 16-18 nt downstream of the –21 AUG (lanes 3-6, see

asterisks) and other bands at comparable positions in the *UAA-M-32* and *UGA-M-32* RNAs (lanes 9-12, see asterisks). Additional bands ~19 nt downstream of the –32 AUGs (lanes 9 and 11), bands upstream of the -21 toeprints (lanes 3 and 5, arrow a), and bands downstream (lanes 3, 5, 9, and 11, arrow b) may arise from translocating ribosomes, ribosomes scanning backwards that collide with those already engaged at the initiation codon, or the binding of non-ribosomal factors to the RNA. The nonspecific band indicated by arrow c in the *UGA-M-21* and *UGA-M-32* samples may reflect the binding of factors specific to AUGs at least 21 nt upstream of the UGA since this band is absent in the *UGA, UGA-M, UGA-DS* and *UGA-M-DS* RNAs (data not shown). It is important to note that none of the aforementioned toeprint bands are detected with the *Fusion-21* and *Fusion-32* control RNA (lanes 1, 2, 7, and 8). These experiments thus demonstrate that yeast ribosomes can reinitiate *in vitro* at least 32 nt 5' to a premature terminator.

Reinitiation at upstream AUGs is favored over downstream reinitiation

To test the relative efficiencies of upstream and downstream reinitiation, we constructed mRNAs that presented both options (Fig. 2.7). Analysis of the *UAA-DS* RNA (containing the –11 AUG and another AUG 5 nt downstream of the stop codon) showed only the cap analog-sensitive +6 toeprint (lanes 3 and 4). A derivative of this RNA lacking the –11 AUG (*UAA-M-DS* RNA) exhibited a new translation-dependent toeprint signal 24-25 nt downstream of the stop codon (lanes 1 and 2) that corresponds to ribosomes stalled with their P site on the +5 AUG. Similar results were obtained with derivatives of the *UGA* RNA. Mutation of only the –11 AUG in the *No-11-UGA* RNA led

to elimination of the +6 toeprint and maintenance of the +17 toeprint (lanes 5 and 6). Analysis of an RNA containing the +5 AUG as well as the upstream -11 and -1 AUGs (*UGA-DS* RNA) showed only the +6 and +17 toeprints (lanes 7 and 8). However, mutation of both upstream AUGs accompanied by inclusion of a +5 AUG (*UGA-M-DS* RNA) eliminated the retroreinitiation toeprints but generated a translation-dependent signal 24-25 nt downstream of the UGA stop codon (lanes 9 and 10). Since toeprints are only detected at downstream AUGs when proximal upstream AUGs are eliminated, post-termination ribosomes exiting premature termination codons must have a propensity for backwards scanning.

eRF1 activity is required prior to any reinitiation event

Regardless of the site of post-termination reinitiation, all nonsense-containing RNAs yielded toeprints corresponding to ribosomes stalled with the stop codon in their A sites when translated in *sup45-2* extracts (Fig. 2.8). RNAs having weak terminators yield strong translation-dependent toeprints 12-14 nt downstream of the premature stop codon (lanes 5, 6, 13-22, and 25-28) and RNAs with strong terminators yield faint bands at the same position (lanes 3, 4, 7-12). No comparable toeprints are obtained with the *Fusion* RNAs (lanes 1, 2 and 23, 24). Unlike wild-type extracts, those from *sup45-2* cells show no differences with RNAs that do or do not contain upstream or downstream AUGs (Figs. 2.4, 2.6, and 2.7 *vs.* Fig. 2.8) and are thus incapable of scanning either backward or forward after premature termination. The epistasis of the toeprints obtained in *sup45-2* extracts to those obtained in wild-type extracts provides additional evidence that the aberrant toeprints do not arise from leaky scanning and suggests that, prior to

any reinitiation event, a premature stop codon in the ribosomal A site must be recognized by eRF1 and trigger peptide hydrolysis in the adjoining P site (Stansfield *et al.* 1997; Song *et al.* 2000). Interestingly, translation of the WT-like *mini* RNAs (Fig. 2.9 and see below) in *sup45-2* extracts in the presence of CHX did not yield detectable cap analog-sensitive toeprints, reinforcing the notion that normal termination is different from premature termination [Fig. 2.10(c)].

An extended 3'-UTR leads to aberrant termination events

To determine whether aberrant termination and its consequences resulted from the relative positioning of a nonsense codon within an mRNA, four constructs were made in which the *PGK1* 3'-UTR (Peltz *et al.* 1993; Muhlrad and Parker 1999) was inserted immediately downstream of early stop codons in *can1* alleles. These "*mini*" wild-type mRNA mimics included the *miniUAA, miniUAA-M,* and *miniUGA* RNAs, as well the *miniUAA-M-W* RNA (which has the UAA in weak context (Bonetti *et al.* 1995) but lacks the upstream AUG) (Fig. 2.9). All *mini* RNAs yielded normal levels of initiator AUG toeprints in CHX-supplemented wild-type extracts (data not shown), but lacked the aberrant +6 toeprint [Fig. 2.10(a)]. Unlike the normal terminators of the *Fusion* and *ADE2* RNAs, translation programmed by the *mini* RNAs in *sup45-2* extracts yielded cap analog-sensitive +14 toeprint signals in the absence of CHX [Fig. 2.10(b)], but not in its presence [Fig. 2.10(c)]. The lack of aberrant toeprints at +6 and/or +17 with these mimics of wild-type mRNA indicates that backwards scanning, or at least its apparent end-product, is eliminated when termination codons are flanked by normal 3'-UTR sequences. These results indicate that aberrant termination promotes the novel

initiation events and raise the question of why a 3'-UTR created by a premature termination codon should differ from that of a wild-type mRNA.

Tethered Pab1p stabilizes nonsense-containing mRNAs

The “faux UTR” model suggests that the downstream element (DSE) thought to be a key *cis*-acting regulator of NMD (Peltz *et al.* 1993) promotes mRNA decay because it lacks a termination regulatory factor (or factors) normally present on a legitimate 3'-UTR, a hypothesis that may also explain why deletions that eliminate most coding sequences downstream of premature terminators stabilize mRNAs that would otherwise be substrates for NMD (Peltz *et al.* 1993; Muhlrad and Parker 1999). This inadequacy could occur because translation to the normal end of a coding region remodels an mRNP (Hilleren and Parker 1999) or because proximity to the poly(A) tail (and bound Pab1p) has a qualitative and/or quantitative influence on the nature of proteins bound to the UTR (Jacobson and Peltz 2000). To test whether proximity of a termination codon to Pab1p is germane to NMD, the *in vivo* stability of mRNAs bearing an MS2 coat protein binding-site 3' to premature terminators in the *CAN1* and *PGK1* mRNAs was assessed in cells expressing an MS2-Pab1p fusion. Pab1p tethered 37-73 nt 3' to premature UAA, UGA, or UAG codons promoted 5- to 11-fold increases in mRNA stability and abundance [Fig. 2.11(a) and (b)]. MS2 dimer or MS2-Sxl tethered at the same position, or MS2-Pab1p tethered 164 nt downstream (3' to the DSE) had no effect on mRNA stability or abundance [Fig. 2.11(a)]. MS2-Pab1p-mediated stabilization was: a) specific for mRNA containing the MS2-binding site since the *CYH2* pre-mRNA, an NMD substrate, was not detectable on these blots [Fig. 2.11(a)] , b) not attributable to non-specific effects on translation since the average number of ribosomes associated with

the *PGK1-MS2* mRNA does not change in the presence or absence of tethered Pab1p [Fig. 2.11(c)], and c) partially manifested by tethered fragments of Pab1p [Fig. 2.11(d)]. The ability of the latter fusion proteins, including those containing only RRMs1-4 or just the C-terminus of Pab1p, to partially stabilize the *PGK1-MS2* mRNA suggests that Pab1p-mediated mRNA stabilization might be attributable to protein:protein interactions characteristic of its respective domains (Mangus *et al.* 2003). To test this possibility, we utilized anti-MS2 coat protein antibodies to immunoprecipitate mRNPs and assayed for the presence of co-immunoprecipitated regulatory factors. Fig. 2.12(a) shows that, in the presence of MS2-Pab1p or MS2-Sxl, this method selectively precipitates *PGK1* nonsense mRNAs containing the MS2 binding site (lanes 4 and 7). Western blotting demonstrated that immunoprecipitation of these mRNPs from extracts containing MS2-Pab1p led to the recovery of MS2-Pab1p and Sup35p (Fig. 2.12(b), left panel), but did not lead to the recovery of eIF4G or eIF4E (data not shown). We attribute co-immunoprecipitation (co-IP) of Sup35p to a specific interaction with MS2-Pab1p because the reciprocal co-IP was also productive (Fig. 2.12(b), right panel) and because no comparable recovery of Sup35p was obtained from immunoprecipitates of MS2-Pab1p lacking the Sup35p-interaction domain [Fig. 2.12(c)]. As an additional test for the specificity of Sup35p recruitment, inactivation of Upf1p was utilized to provide an independent means of stabilizing the nonsense-containing mRNA. Western blotting of extracts from *upf1Δ* cells demonstrated that this alternative mode of stabilizing the *PGK1-MS2* mRNA did not enhance recovery of endogenous Sup35p in an MS2-Sxl IP [Fig. 2.12(d)], thereby implicating a specific MS2-Pab1p:Sup35p interaction.

Recovery of Sup35p, a termination factor known to interact with Pab1p and thought to play a role in the stability of conventional mRNAs (Uchida *et al.* 2002; Hosoda *et al.* 2003), suggested a role for this protein in the tethered-Pab1p-mediated reversal of NMD. This appears to be the case since tethered Sup35p also stabilized *PGK1* nonsense transcripts, albeit to a lesser extent than tethered Pab1p (Fig. 2.13). Similar experiments, in which Sup45p was the tethered component (Fig. 2.13), failed to stabilize the same mRNA significantly, indicating that regulatory aspects of termination played a key role in antagonizing NMD and that Pab1p's role in this process most likely reflected its function as a scaffold for post-transcriptional regulators (Mangus *et al.* 2003).

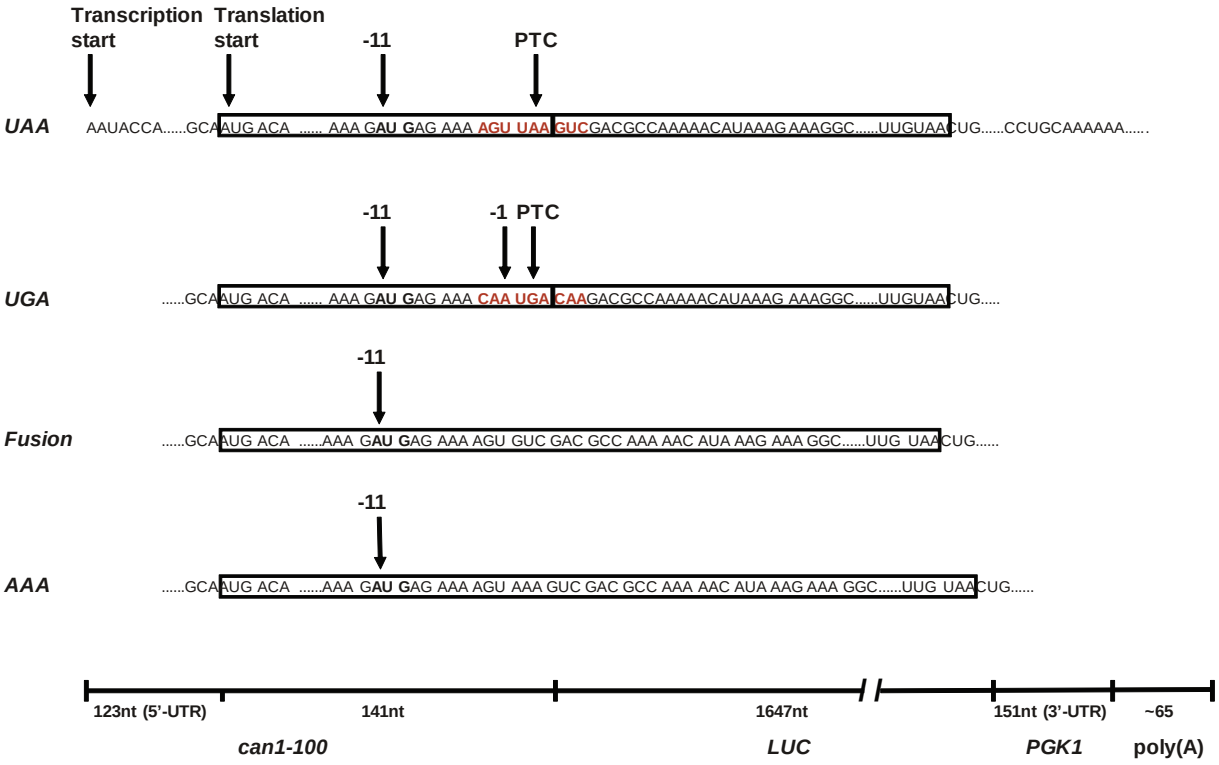

Fig. 2.1 : General schematic and sequences of selected regions of the *UAA*, *UGA*, *Fusion*, and *AAA CAN1/LUC* RNAs. PTC, denotes premature termination codon. Each RNA contains a the 5'-UTR and first 47 codons of the yeast *can-100* gene fused in frame with firefly *Luciferase* and the *PGK1* 3'-UTR followed by ~65 adenylate residues. -11, denotes position of the upstream AUG codon.

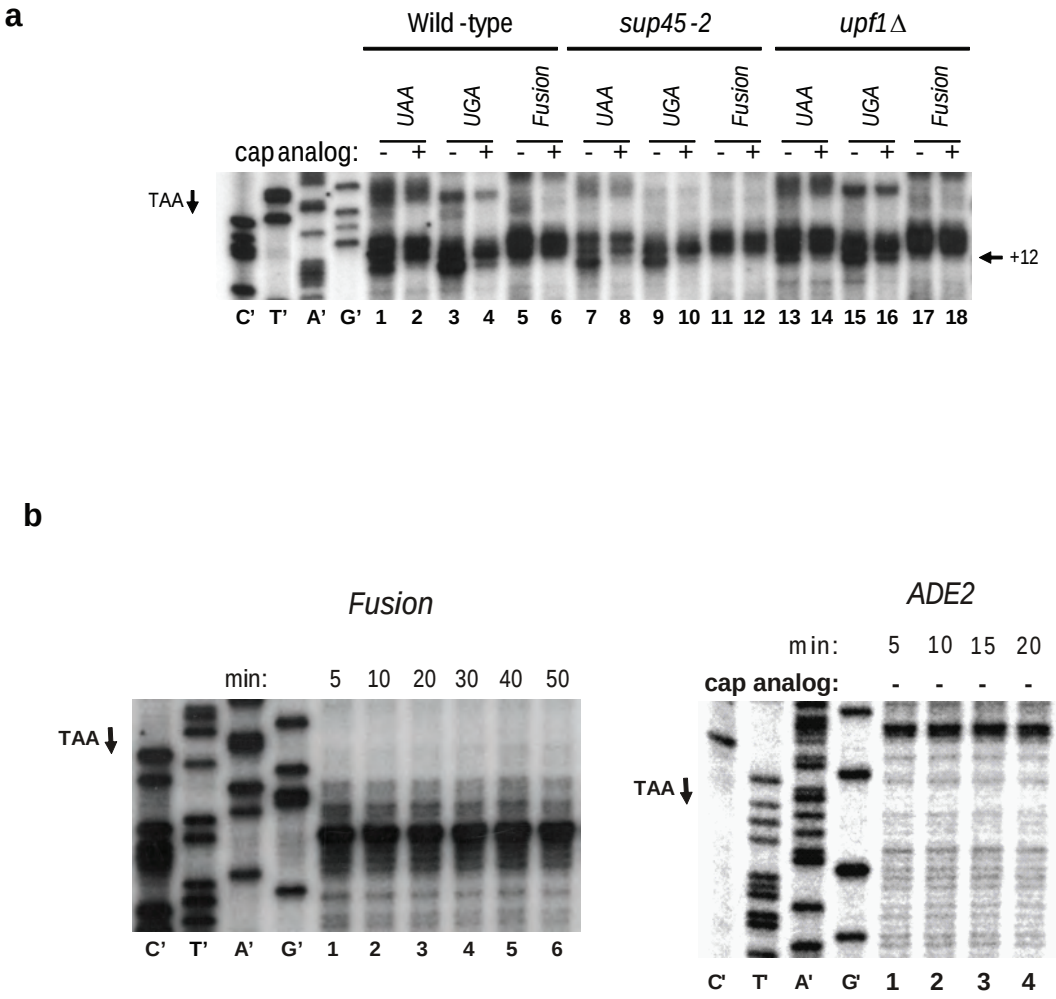

Fig. 2.2 : Toeprint analyses of termination in cell extracts in the absence of CHX. (**a**) PTC toeprints are detected during translation of *CAN1/LUC* RNAs in wild-type, *sup45-2*, and *upf1*Δ extracts in the absence of CHX. **(b)** No toeprints are detectable at normal terminators of the *Fusion* or *ADE2* RNAs in wild-type extracts in the absence of CHX. Sequence ladders on the left side of each panel correspond to the normal terminator region of each mRNA.

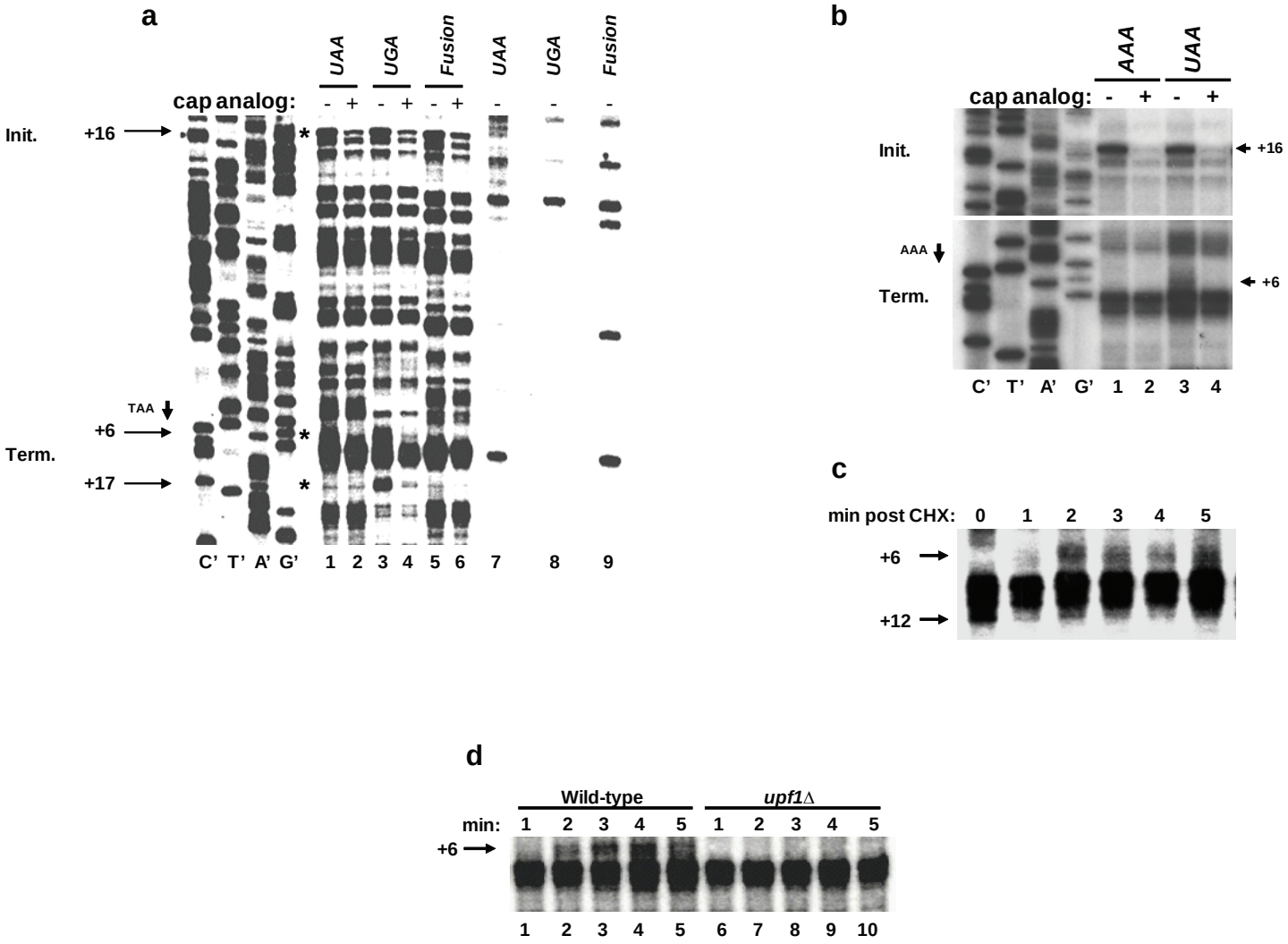

Fig. 2.3 : Toeprint analyses of initiation and termination in cell extracts in the presence of CHX. (**a**) CHX addition to wild-type extracts promotes the appearance of normal toeprints at initiator AUGs and aberrant toeprints in the vicinity of PTCs. Lanes 7-9 show products from reactions lacking added extract. (**b**) The +6 toeprint of the *UAA* RNA incubated in the presence of CHX is eliminated by a single nucleotide substitution. (**c**) The +6 toeprint in the *UAA* RNA appears subsequent to CHX-chasing of the PTC toeprint. CHX was added after 4 min of translation and samples were taken for toeprinting at the designated times. (**d**) *upf1*Δ extracts do not reveal the +6 toeprint of the *UAA* RNA when incubated for 1 to 5 min and terminated by the addition of CHX for 3 min. Positions of the toeprints are indicated with arrows. The left portions of panels (**a**) and (**b**) show dideoxynucleotide sequencing reactions for the UAA or AAA templates, respectively (with 5' to 3' sequence reading from the top to the bottom).

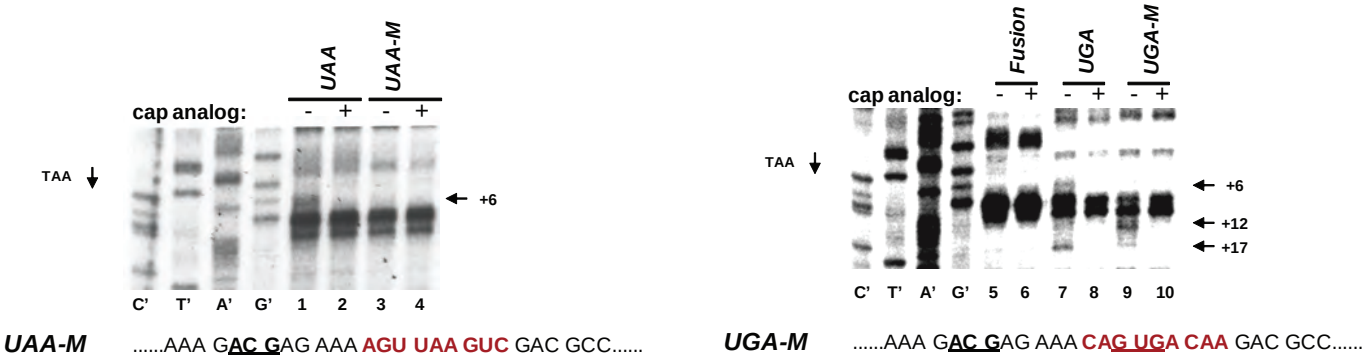

Fig. 2.4 : Aberrant toeprints derived from PTCs in wild-type extracts in the presence of CHX are dependent on upstream AUGs. Toeprint analyses of the *UAA, UAA-M* (left panel), or *Fusion, UGA,* and *UGA-M* (right panel) RNAs. CHX addition to wild-type extracts promotes the appearance of aberrant toeprints in the vicinity of PTCs. Pertinent sequences of mutated *CAN1/LUC* constructs are shown below each panel.

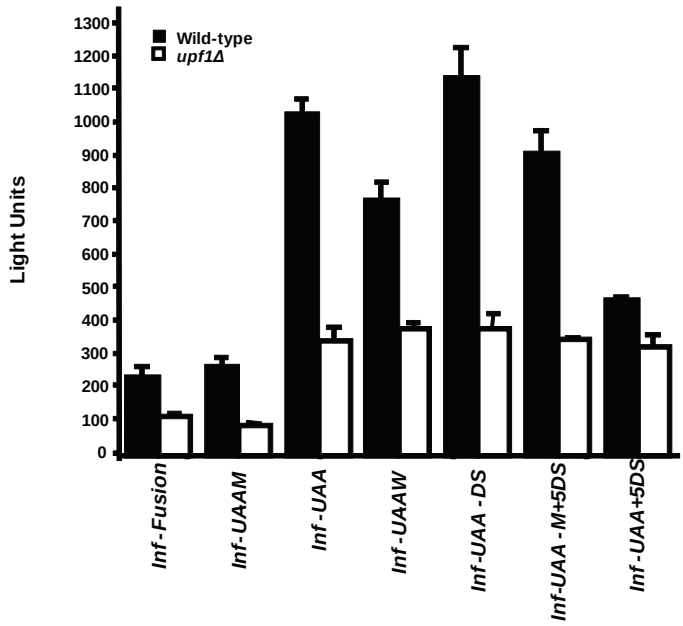

Inf-Fusion ..... CCA UUG AAA G**AUG** AGA AAA GUG UC**A** GAC GCC AAA AAC.....
-11

Inf-UAA-M ..... CCA UUG AAA G**ACG** AGA AAA GU**U AA**G UC**A** GAC GCC AAA AAC.....
-11

Inf-UAA ..... CCA UUG AAA G**AUG** AGA AAA GU**U AA**G UC**A** GAC GCC AAA AAC.....
-11

Inf-UAA-W ..... CCA UUG AAA G**AUG** AGA AAC AA**U AA**C AA**A** GAC GCC AAA AAC.....
-11

Inf-UAA-DS ..... CCA UUG AAA G**AUG** AGA AAA GU**U AA**G UC**A** G**AU G**CC AAA AAC.....
-11 +5

Inf-UAA-M+5DS ..... CCA UUG AAA G**AC G**AG AAA AGU **UAA** GUC G **AUG** CC**A** AAA AAC.....
+5

Inf-UAA+5DS ..... CCA UUG AAA G**AU G**AG AAA AGU **UAA** GUC **AUG** CC**A** AAA AAC.....
-11 +5

Fig. 2.5 : Ribosomes can reinitiate translation at AUG codons upstream or downstream of the stop codon. Translation reactions in wild-type (n=4) or *upf1*Δ (n=3) extracts were programmed with the respective in-frame *LUC* fusion (*Inf*) mRNAs and analyzed for luciferase activity. Sequences of pertinent segments of the *Inf* constructs are shown.

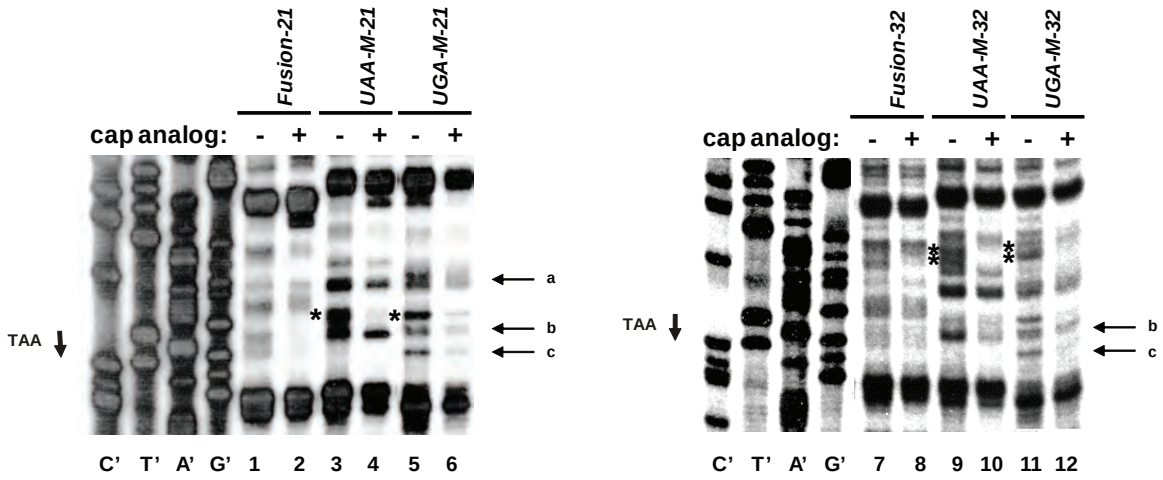

Fusion-21 ..... AGA CGU GGG UGA AUA **AUG** UUG AAA GAU GAG AAA AGU GUC GAC GCC.....
-21

UAA-M-21 ..... AGA CGU GGG UGA AUA **AUG** UUG AAA G**AC G**AG AAA **AGU UAA GUC** GAC GCC.....
-21

UGA-M-21 ..... AGA CGU GGG UGA AUA **AUG** UUG AAA G**AC G**AG AAA **CAG UGA CAA** GAC GCC.....
-21

Fusion-32 .....AGA C**AU G**GG UGA AUA CCA UUG AAA GAU GAG AAA AGU GUC GAC GCC.....
-32

UAA-M-32 ..... AGA C**AU G**GG UGA AUA CCA UUG AAA GAC GAG AAA **AGU UAA GUC** GAC GCC.....
-32

UGA-M-32 ..... AGA C**AU G**GG UGA AUA CCA UUG AAA GAC GAG AAA **CAG UGA CAA** GAC GCC.....
-32

Fig. 2.6 : Ribosomes can migrate to AUG codons 21 or 32 nt upstream of premature stop codons. The *Fusion-21 and Fusion-32* constructs, used as controls, lack PTCs, but contain the -21 or -32 AUGs, respectively. Sequences indicate mutational changes to the *Fusion*, *UAA-M*, or *UGA-M* RNAs (see Figs. 2.1 and 2.4 for original sequences). Asterisks (*) show toeprint bands 16-18 nt downstream of the -21 (left panel) or -32 (right panel) AUGs. Arrows a, b, and c are explained in the main text.

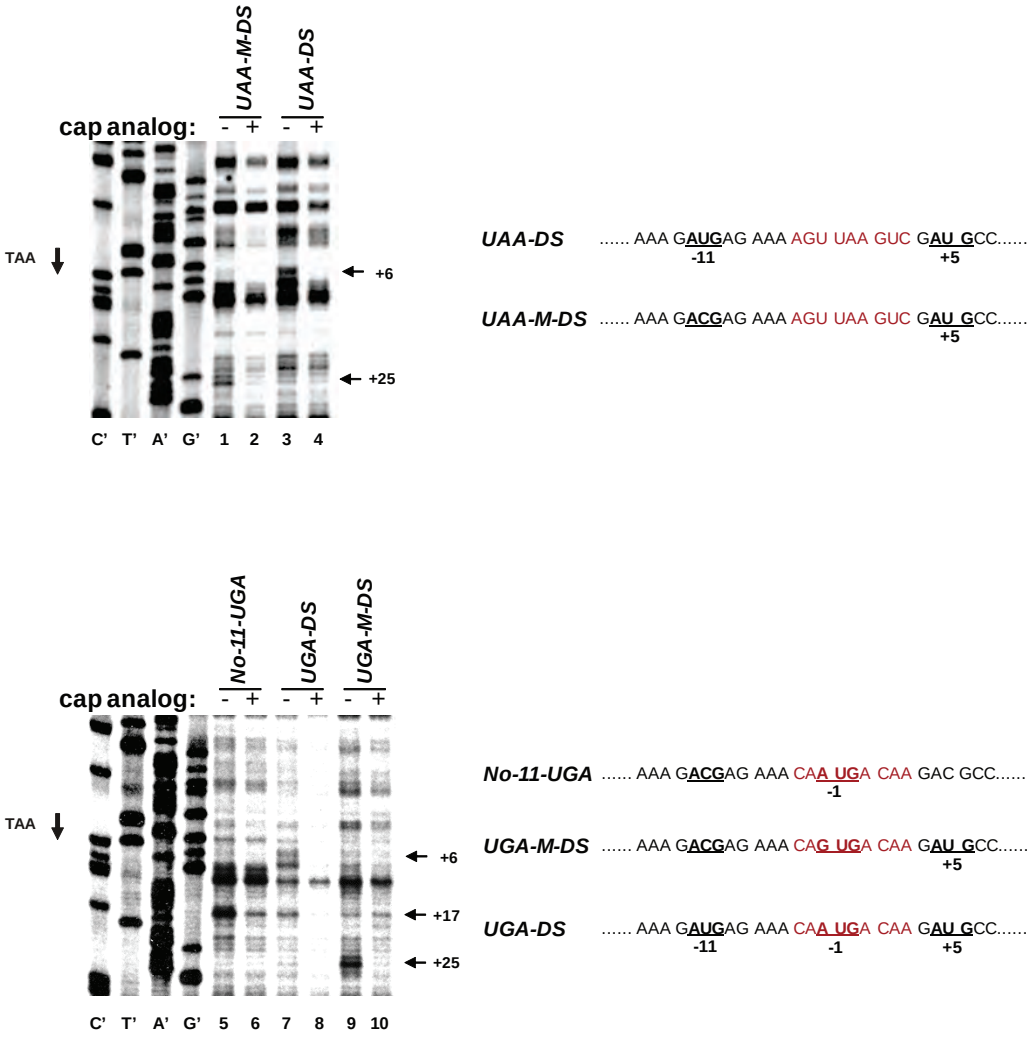

Fig. 2.7 : Reinitiation at upstream AUGs is favored over downstream reinitiation. Top panel: toeprint analyses of *UAA* RNA derivatives containing an additional downstream AUG 5 nt from the PTC with (*UAA-DS*) or without (*UAA-M-DS*) the -11 AUG. Bottom panel: *UGA* RNA derivatives lacking the –11 AUG (*No-11-UGA*), containing an additional AUG 5 nt 3' to the stop codon (*UGA-DS*), or containing the +5 AUG, but lacking the –11 and –1 AUGs (*UGA-M-DS*). Numbers under the AUGs denote position relative to the PTCs and numbers on the right of each panel indicate the positions of toeprints relative to PTCs.

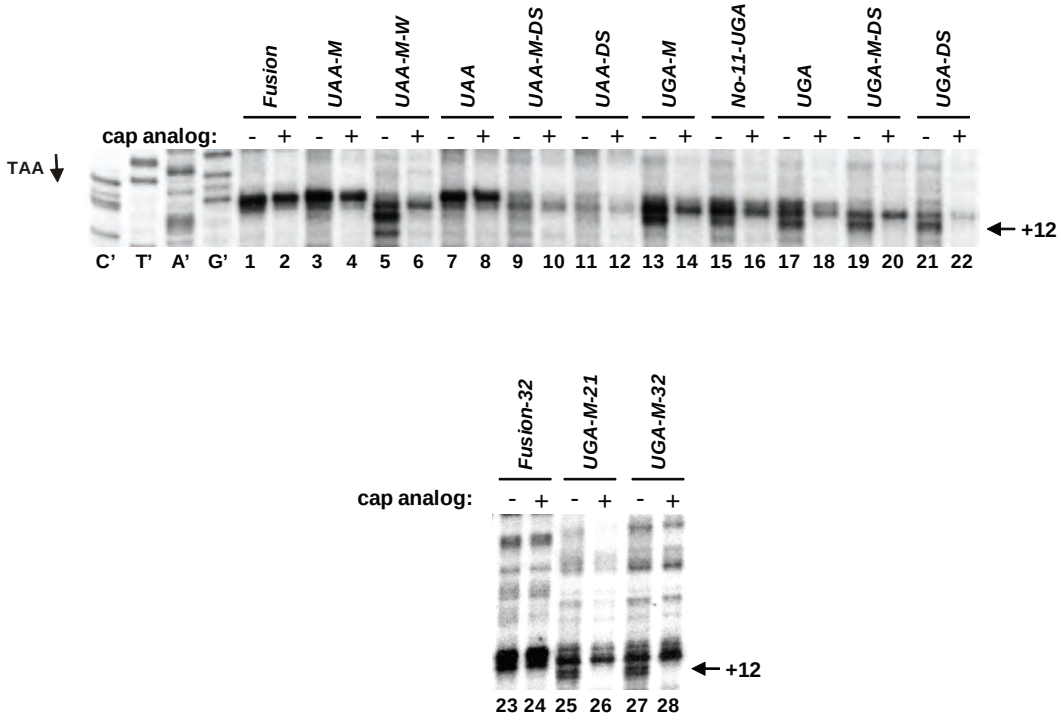

Fig. 2.8 : RNAs translated in *sup45-2* extracts in the presence of CHX yield only +12 toeprints. *UAA* and *UGA* RNAs and their derivatives with or without AUG codons 5' or 3' to the respective terminators (see Figs. 2.1, 2.4, 2.6, and 2.7) were subjected to toeprint analysis. *UAA-M-W* RNA is a construct containing the UAA codon in a weak termination context (CAA UAA CAA)[12]**.** The sequence ladder depicted are derived from the *UAA* template.

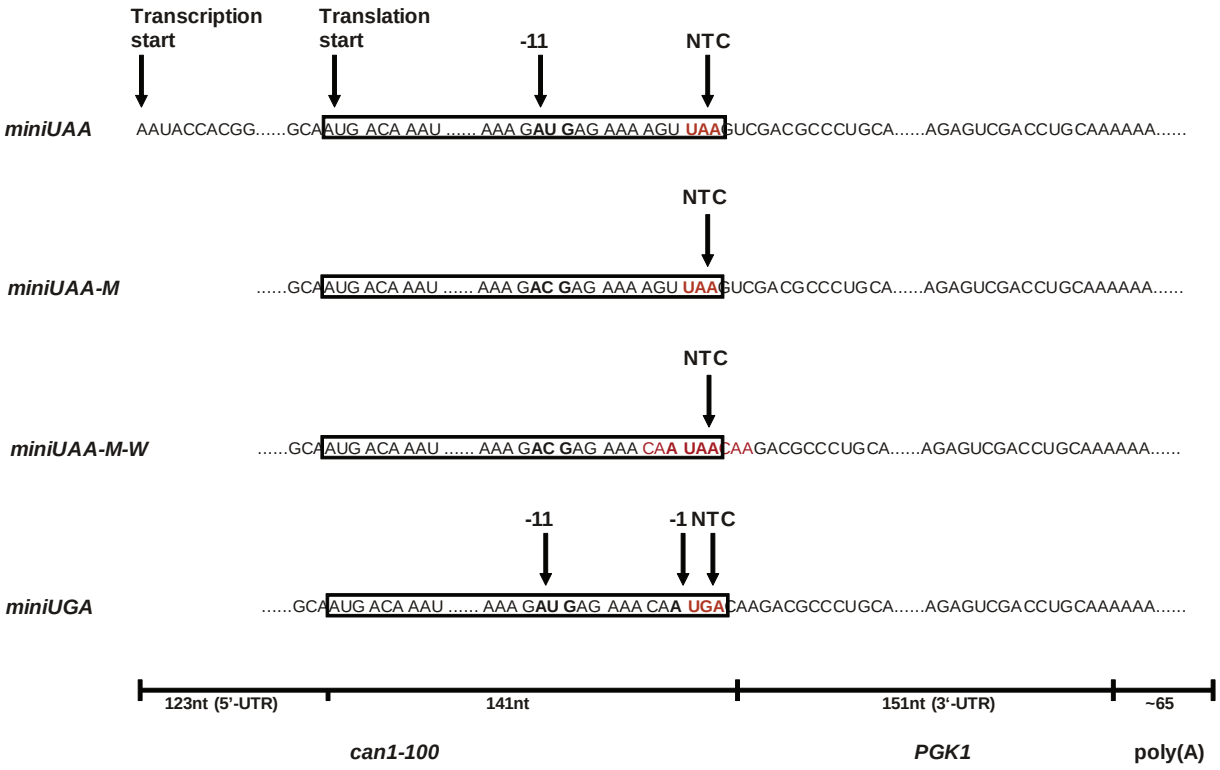

Fig. 2.9 : General schematic and sequences of the *mini* RNAs. NTC, denotes PTCs that have been converted to normal termination codons by virtue of coding region deletions.

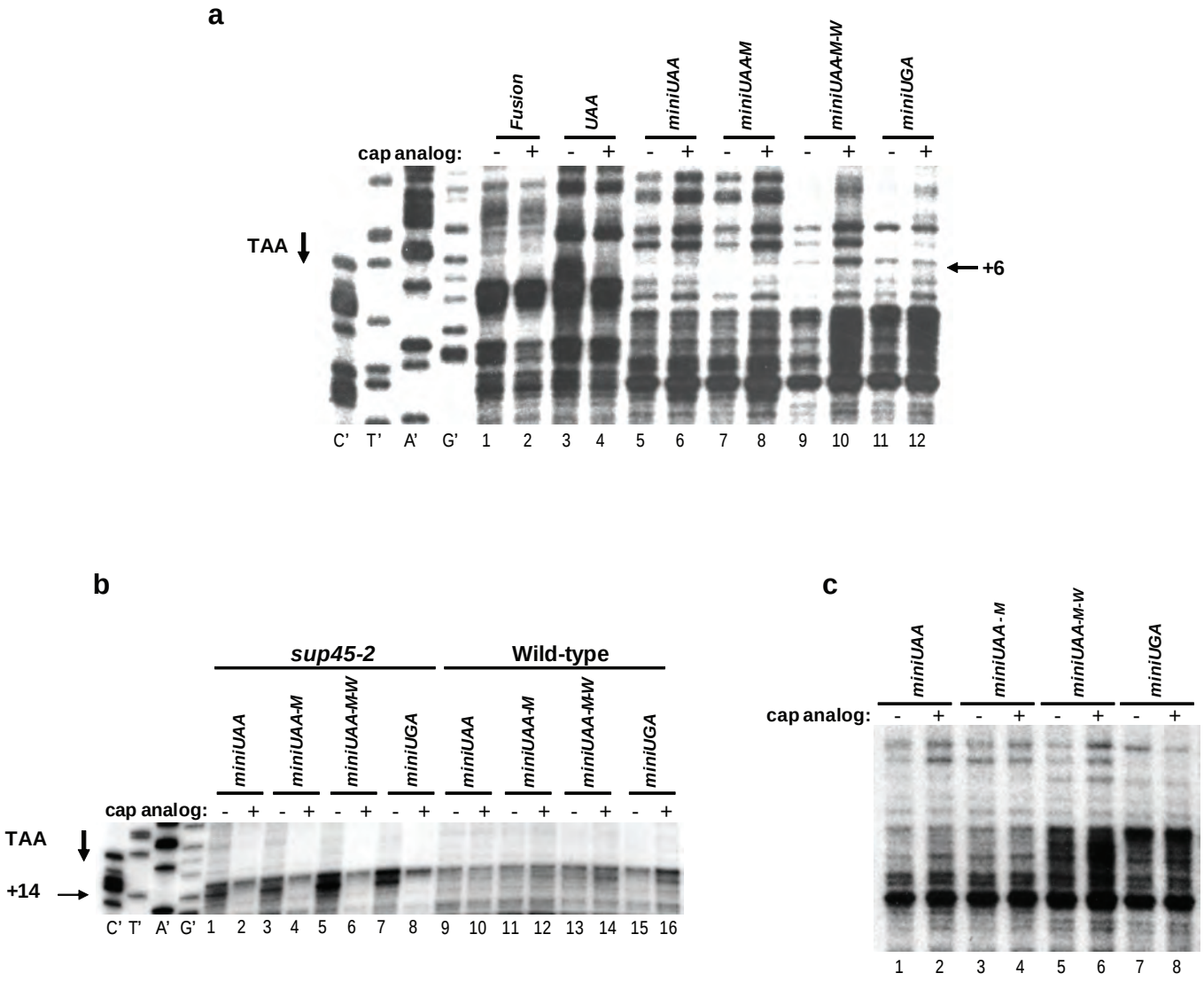

Fig. 2.10 : Aberrant toeprint signals are eliminated when PTCs are flanked by a normal 3'-UTR. (**a**) The +6 toeprints are not detected during translation of *mini* RNAs in wild-type extracts in the presence of CHX. The *UAA* and *Fusion* RNAs, used as controls, were toeprinted using oligoprimer #3029. (**b**) Translation of *mini* RNAs in the absence of CHX, in *sup45-2* extracts, but not in wild-type extracts yields +14 toeprints. The left portion of panels a and b show dideoxynucleotide sequencing reactions for the *miniUAA* template. (**c**) *mini* RNAs translated in *sup45-2* extracts in the presence of CHX yield no cap analog-sensitive toeprints.

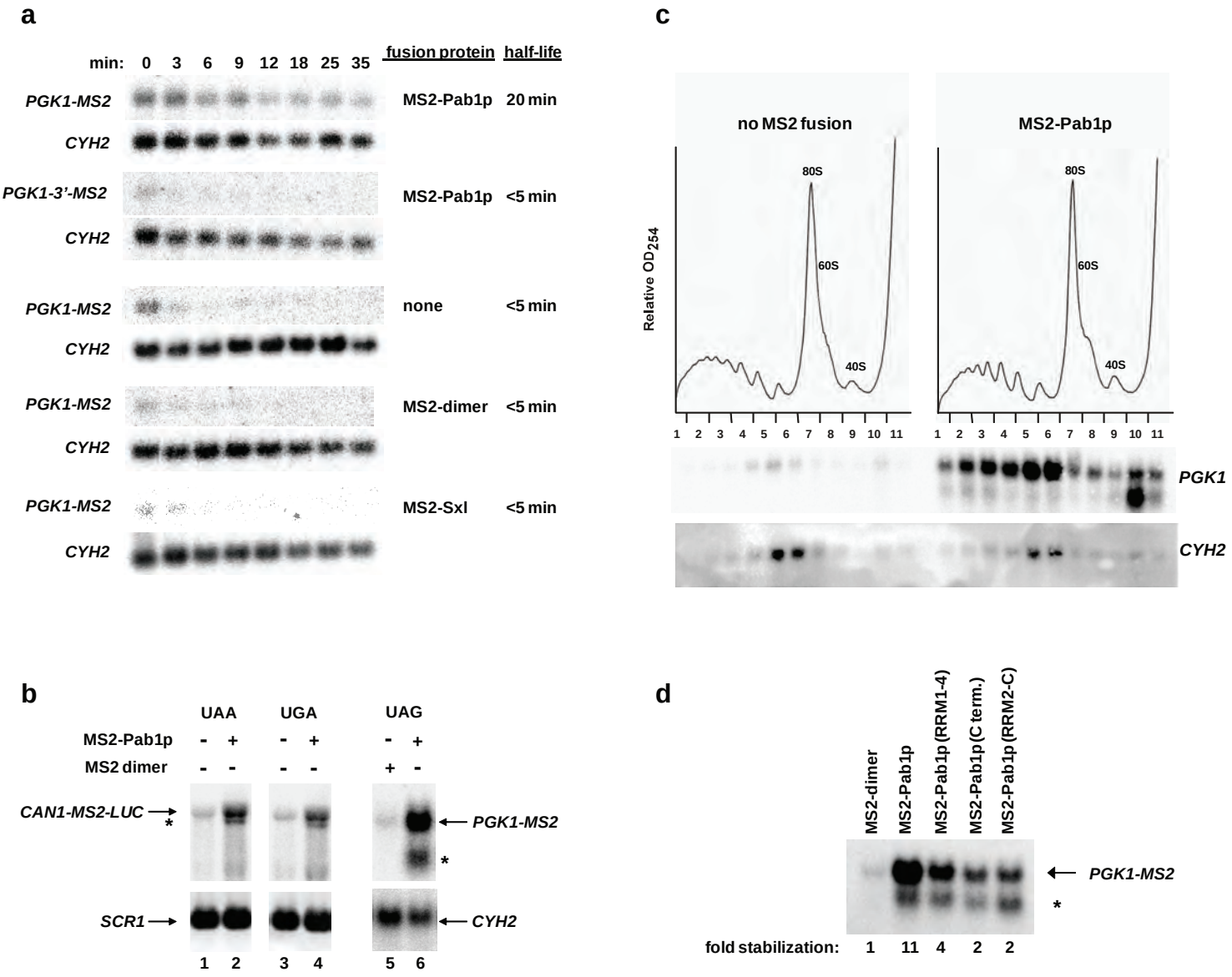

Fig. 2.11 : Stabilization of nonsense-containing mRNAs by tethered Pab1p. (**a**) Stabilization of the *PGK1-MS2* mRNA is dependent on the presence and proximity of tethered Pab1p. Half-lives of the *PGK1-MS2, PGK1-3'-MS2,* and *CYH2* mRNAs were assessed by northern blotting at different times (min) subsequent to transcription inhibition[19]. Cells expressed the mini-*PGK1* allele[19] containing an insertion of MS2 coat protein binding sites 37 nt (*PGK1-MS2*) or 164 nt (*PGK1-3'-MS2*) 3' of the premature UAG. (**b**) Cellular steady-state levels of PTC-containing *CAN1* (lanes 1-4) and *PGK1* (lanes 5 and 6) mRNAs with or without tethered Pab1p. Cells expressed UAA or UGA alleles of *CAN1/LUC* (see Fig. 2.1) or the mini-*PGK1* UAG allele, all of which contained insertions of MS2 coat protein binding sites. Levels of all transcripts were determined by northern blotting. The * denotes decay intermediates generated by 5' to 3' degradation up to the site of bound MS2-Pab1p. Simultaneous expression of MS2 fusion proteins in (**a**) and (**b**) are indicated. (**c**) Tethered Pab1p does not affect translation of the *PGK1-MS2* mRNA. Extracts from cells expressing the *PGK1-MS2* mRNA with (right) or without (left) co-expressed MS2-Pab1p were fractionated on sucrose gradients and subsequently analyzed by northern blotting. Top: OD profiles, with sedimentation proceeding from right to left. Bottom: northern analysis of the gradient fractions for *PGK1-MS2* mRNA and control *CYH2* mRNA. (**d**) Tethered fragments of Pab1p partially stabilize the *PGK1-MS2* mRNA. MS2 fusion proteins encompassing Pab1p full-length, RRM1-4 (residues 1-405); C-terminus only (residues 406-577); and RRM2 through the C-terminus (residues 119-577) were expressed and assessed as in part (**b**) for their effects on the steady-state level of *PGK1-MS2* mRNA.

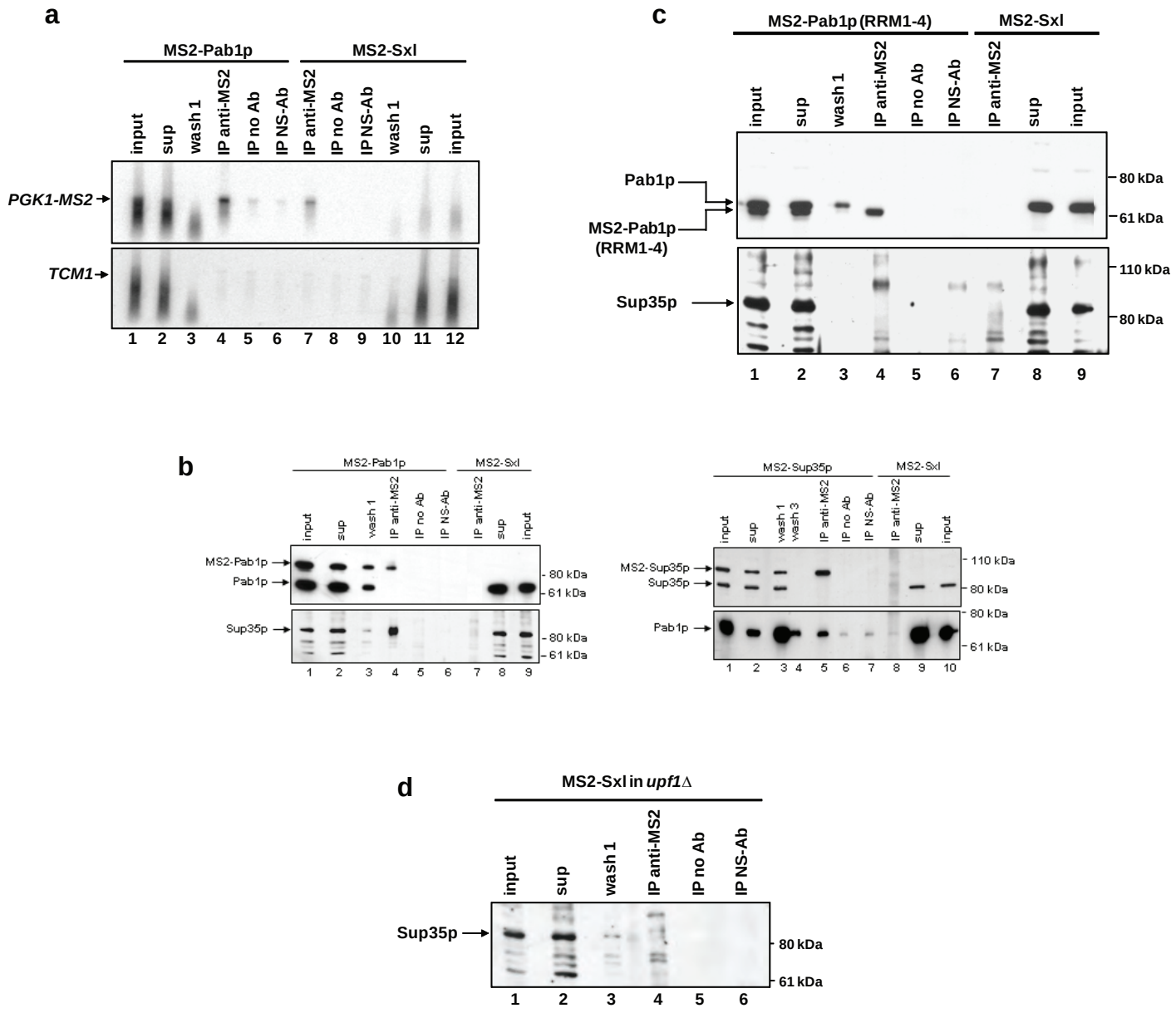

Fig. 2.12 : Tethered Pab1p interacts with Sup35p. (**a**) *PGK1-MS2* mRNA is selectively recovered in α-MS2 immunoprecipitates. RNA extracted from IP reactions using α-MS2 coat protein antibodies (IP anti-MS2), no antibodies (IP no Ab), or non-specific antibodies (IP NS-Ab) was analyzed by northern blotting for the presence of *PGK1-MS2* or control *TCM1* mRNA. *PGK1-MS2* mRNA is not stabilized in cells expressing MS2-Sxl fusion protein (lanes 7-12), thus rendering its signal weaker than in MS2-Pab1p-expressing cells (lanes 1-6). The loading for the input, the unbound fraction (sup), and the wash represent half of the loading of the different IP fractions. (**b**) Sup35p co-IPs with tethered MS2-Pab1p and vice versa. Left; western blot analysis of IP reactions described in (**a**) using antibodies that detect Pab1p (left upper panel) or Sup35p (left lower panel). Right: lysates from cells expressing *PGK1-MS2* and MS2-Sup35p were IP'd with α-MS2 antibodies and analyzed by western blotting for the presence of Sup35p (upper panel) or Pab1p (lower panel). The positions of Pab1p, MS2-Pab1p, Sup35p, MS2-Sup35p, and marker proteins are indicated. (**c**) Sup35p does not co-IP with MS2-Pab1p lacking the Sup35p-interacting domain. MS2-Pab1p harboring only PAB1 RRM1-4 was co-expressed with *PGK1-MS2* mRNA and analyzed for co-IP of Sup35p as in (**b**). (**d**) Sup35p does not co-IP with mRNPs stabilized by deletion of *UPF1*. Extracts of *upf1Δ* cells expressing *PGK1-MS2* mRNA and MS2-Sxl fusion protein were immunoprecipitated with anti-MS2 antibodies and characterized as in (**b**).

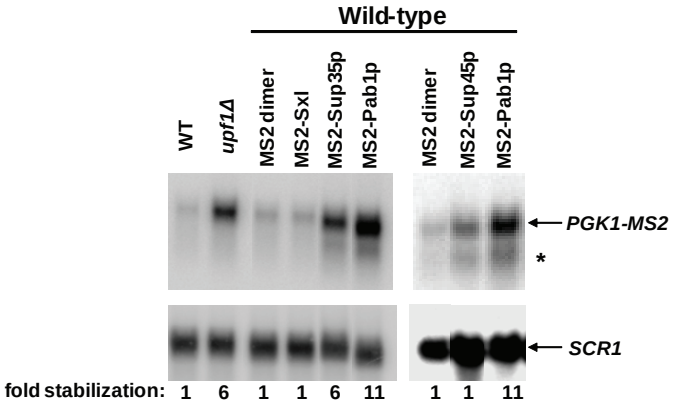

Fig. 2.13 : PTC-containing mRNA is stabilized by tethered Sup35p, but not by tethered Sup45p. RNA extracted from wild-type or *upf1Δ* cells expressing *PGK1-MS2* mRNA was analyzed by northern blotting. Cells used for the wild-type (WT) and *upf1*Δ samples contained no fusion protein whereas those of the remaining lanes contained the indicated MS2 fusion proteins. Fold stabilization, relative to the WT sample, was determined by phosphorimaging.

Chapter III

Translational competence of ribosomes released from a premature termination codon is modulated by NMD factors

The work presented in this chapter is currently under revision for publication in *RNA* as:

Ghosh S., Ganesan R., Amrani N., and Jacobson A. Translational competence of ribosomes released from a premature termination codon is modulated by NMD factors. *RNA* (submitted 2009; under revision).

SG performed all *in vitro* experiments.
In vivo assays were performed by R. Ganesan.

Chapter III – Translational competence of ribosomes released from a premature termination codon is modulated by NMD factors

Summary

In addition to their well-documented roles in the promotion of nonsense-mediated mRNA decay (NMD), the yeast Upf proteins (Upf1p, Upf2p/Nmd2p, and Upf3p) have also manifested translational regulatory functions, at least *in vitro*, including roles in premature translation termination (but not normal termination) and subsequent translational reinitiation. Using a *PGK1/LUC* reinitiation reporter, we have found that all *upf⊿* strains fail to reinitiate translation after encountering a PTC *in vivo*, a result that led us to seek a possible unifying mechanism for these collected translation phenomena. Comparing the *in vitro* translational activities of wild-type (WT) and *upf1Δ* extracts, we find that Upf1p appears to play a role in regulating the efficiency of post-termination ribosome reutilization. Relative to WT extracts, non-nucleased extracts lacking Upf1p manifest an almost 2-fold decrease in the translation of synthetic *CAN1/LUC* mRNA, a defect paralleled by fewer ribosomes per mRNA and reduced efficiency of the 60S joining step at initiation. We hypothesized that these deficiencies, which could be complemented by purified FLAG-Upf1p or 60S subunits, reflected diminished cycling of ribosomes from endogenous PTC-containing mRNAs to the exogenously added synthetic mRNA in the same extracts. This hypothesis was tested, and supported, by experiments in which nucleased WT or *upf1Δ* extracts were first challenged with high concentrations of synthetic mRNAs that were templates for either normal or premature translation termination and then assayed for their capacity to translate a normal mRNA.

Collectively, our results strongly suggest that Upf1p is required *in vitro* for efficient termination and release of ribosomes at a PTC and their subsequent reutilization for their next round of translation initiation.

Results

Mutations in a *PGK1/LUC* reporter attenuate its reinitiation activity

We have shown that, *in vitro*, yeast ribosomes will reinitiate translation subsequent to premature termination, provided that Upf1p is present in the translation reaction (Chapter II). This observation indicated that premature termination was inefficient and suggested that Upf1p might influence the extent to which prematurely terminating ribosomes remain associated with an mRNA (Chapter II). To determine whether Upf1p, and other NMD factors, play a similar role *in vivo*, we constructed a reinitiation reporter and evaluated its expression in wild-type yeast strains and in strains devoid of NMD function. The reporter, a chimeric *PGK1*/*LUC* gene (Fig. 3.1(a), construct 1) that encodes an mRNA subject to NMD [Fig. 3.1(b)], consists of the following: i) the *PGK1* 5'-untranslated region (UTR); ii) the first 5% of the *PGK1* open reading frame (ORF) followed by a UAG stop codon; iii) an 82 nt *PGK1* coding region sequence element whose first AUG codon, designated +19 AUG (relative to the U of the UAG), is out of frame with the upstream *PGK1* ORF; iv) the *LUC* ORF lacking its normal start codon, fused in frame with the +19 AUG; and v) the 3'-UTR of *PGK1*. Luciferase assays, performed on extracts of wild-type yeast strains bearing this construct, yielded activity that was assigned a value of 100% for purposes of comparison with subsequent experiments [Fig. 3.1(c)]. In this, and all other assays, luciferase activity was normalized to both total protein content of the sample, as well as to the level of the construct-specific mRNA. The derived values were thus expressed as relative light units (RLUs)/μg protein/unit mRNA.

Our analyses indicated that the luciferase activity derived from the reporter represented reinitiation from the +19 AUG codon downstream of the partial *PGK1* ORF or from one additional in-frame AUG located five codons downstream of the +19 AUG. First, we measured luciferase activity from cells containing construct 2 [Fig. 3.1(a)], in which the +19 AUG and the additional downstream AUG codon were deleted, and observed a 5-fold decrease in luciferase expression relative to construct 1 [Fig. 3.1(c)] . (The residual luciferase activity appears to derive from an in-frame AUG codon 82 nt into the *LUC* sequence (Fig. 3.2, construct 6). Second, in a separate construct, the *LUC* ORF was placed out of frame with respect to the +19 AUG, as well as out frame with the *PGK1* ORF (Fig. 3.1(a), construct 3). This construct yielded almost no luciferase activity [Fig. 3.1(c)], indicating that the *LUC* ORF has to be in-frame with the +19 AUG to produce functional luciferase protein. Finally, deletion of the *PGK1* stop codon (Fig. 3.1(a), construct 4), which allows translation until a termination codon 75 nt into the *LUC* coding region, also resulted in a substantial decrease in luciferase activity [Fig. 3.1(c)]. These results strongly implicate the +19 AUG codon in the expression of luciferase from a translational reinitiation event in the *PGK1/LUC* mRNA derived from construct 1.

Reinitiation on nonsense-containing *PGK1/LUC* mRNA is sensitive to mutations in the NMD pathway

To assess whether NMD factors influence reinitiation events *in vivo*, *PGK1/LUC* construct 1, on a YCp plasmid, was transformed into isogenic yeast strains bearing deletions of *UPF1*, *UPF2*/*NMD2*, or *UPF3*, and combinations thereof. Although the mRNA derived from this construct is sensitive to NMD, as indicated by the observation

that it is stabilized in yeast strains defective in this pathway [Fig. 3.1(b)], the expression of low-copy *PGK1/LUC* construct 1 in *upf*/*nmd* strains yielded a dramatic decrease in luciferase activity when compared to that in wild-type cells [Fig. 3.1(d)]. It was important to determine whether this apparent decrease in luciferase activity was simply due to the increased stability of the *PGK1*/*LUC* mRNA and consequent increase in its steady-state level in these strains without a parallel increase in luciferase protein. To clarify this question, *PGK1*/*LUC* construct 1 was inserted into a high-copy YEp vector and transformed into the wild-type and *upf/nmd* mutant strains. Normalized values for luciferase activity in strains harboring the YEp construct were very similar to those in cells harboring the construct on a YCp plasmid [Fig. 3.1(d)]. Notably, the increased levels of *PGK1/LUC* mRNA in wild-type cells [Fig. 3.1(b)] did not lead to any apparent decrease in normalized values of reinitiation activity, showing that mRNA levels do not affect overall reinitiation in this reporter. Additionally, the *upf/nmd* mutant strains showed a similar reduction in luciferase activity regardless of whether there was an increase in steady-state levels of the mRNA [Fig. 3.1(b)]. As an additional control, we utilized sucrose gradient analysis to evaluate the polysomal distribution of the *PGK1/LUC* mRNA in wild-type and *upf1Δ* cells. These experiments manifested indistinguishable polysomal profiles for the *PGK1/LUC* mRNA in wild-type and *upf1Δ* cells, with >90% of the mRNA on polysomes in both cases (data not shown). Collectively, these results indicate that the mutation-dependent variations in reinitiation activity evident in Fig. 3.1(d) are not simply a function of increases in the abundance of *PGK1/LUC* mRNA, or of decreases in its overall translatability, and that, as was seen previously in cell-free

translation reactions (Chapter II), reinitiation *in vivo* is decreased in the absence of the key NMD factors.

A small percentage of ribosomes reinitiate downstream of the premature stop codon

To determine the proportion of ribosomes that initiate at the normal *PGK1* AUG and are subsequently able to reinitiate, post-termination, on the *PGK1/LUC* mRNA, it was necessary to first assess the efficiency with which ribosomes initiated at the *PGK1* AUG. We made a construct in which the premature *PGK1* stop codon plus one nucleotide were deleted, resulting in a fusion ORF which begins at the *PGK1* start codon and ends at the normal *LUC* terminator (Fig. 3.2(a), construct 5). The luciferase activity of construct 1 was found to be approximately 2.5% that of construct 5 [Fig. 3.2(b)], a comparison indicating that approximately one in forty ribosomes reinitiated translation after encountering the premature *PGK1* nonsense codon.

NMD is independent of translation reinitiation

Since our data indicated that reinitiation efficiency is directly affected by the NMD factors, and other experiments have shown that reinitiation can affect NMD (Zhang and Maquat 1997), it was of interest to determine whether rapid mRNA decay still occurred in the absence of reinitiation. To address this question, we introduced a strong stem-loop structure (ΔG = 58.3 kcal/mol) between the *PGK1* stop codon and the *PGK1* downstream +19 AUG (Fig. 3.3(a), construct 7). This stem-loop structure bears a 25-nt-pair stem and 4 nt loop and is preceded by a 30 nt spacer between the stop codon and

the stem-loop to ensure that the structure does not interfere with termination. mRNA derived from construct 7 displayed almost no luciferase activity [Fig. 3.3(b)], but continued to undergo NMD since it could be stabilized in an *nmd2Δ* strain [Fig. 3.3(c)]. Further insight into the potency of the stem-loop structure used in these experiments was obtained from an additional construct that contains the stem-loop, but lacks the premature *PGK1* stop codon, generating an ORF that extends from the *PGK1* initiator AUG, through the stem loop and *PGK1* downstream sequence, to the *LUC* terminator (Fig. 3.3(a) construct 8). Luciferase activity derived from construct 8 was only 25% that of construct 5, which is identical but lacks the stem-loop [Fig. 3.3(b)]. Collectively, the results of Fig. 3.3 suggest that the strong stem-loop disrupts reinitiation (and presumably ribosome scanning), and substantially inhibits elongation, but is not sufficient to prevent NMD. Thus, we conclude that neither reinitiation, nor any form of ribosome scanning beyond the termination codon, is required for the promotion of NMD.

NMD-deficient extracts manifest a translation defect *in vitro*

The *in vivo* results of Figs. 3.1 - 3.3 are consistent with our earlier *in vitro* data (Chapter II) and suggest that factors regulating NMD have an as yet undefined function that affects translation reinitiation. To characterize this role further, we returned to the analysis of yeast cell-free translation and evaluated the ability of non-nucleased extracts prepared from WT or *upf/nmd* mutant strains to translate a synthetic *CAN1/LUC* fusion mRNA [Fig. 3.4(a)] that harbors a full-length open reading frame and which remains stable during the course of *in vitro* translation (Chapter II). Fig. 3.4(b) shows that, relative to WT extracts, extracts from strains lacking Upf1p activity manifested reduced

luciferase expression from the *CAN1/LUC* mRNA. Similar results were observed with extracts lacking Upf2p/Nmd2p or Upf3p (data not shown). Northern analyses of WT and *upf1Δ* translation reactions fractionated on sucrose gradients demonstrated that the WT extract had higher relative amounts of *CAN1/LUC* mRNA in the heavier polysome fractions, thus confirming the relatively poor translation activity of the mutant extracts and suggesting that they initiated translation inefficiently [Fig. 3.4(c)].

Further evidence for a translational deficiency in extracts from *upf/nmd* mutant strains followed from experiments that we dubbed ribosome reutilization assays. Here, translation of an extract's endogenous mRNA was allowed to proceed and, at regular intervals, the translation reaction was supplemented with *CAN1/LUC* mRNA and incubated for 25 additional minutes to allow for synthesis of the luciferase fusion protein. Thus, luciferase activity at each time point should reflect the relative ability of ribosomes and factors to initiate and translate the exogenously added reporter mRNA. As shown in Fig. 3.4(d), WT extracts exhibit enhanced translatability of the reporter mRNA over time, whereas *upf1Δ* extracts (as well as *nmd2Δ*, and *upfΔ3* extracts; data not shown) fail to do so. These results suggest that, upon preincubation, WT extracts increase the availability or activity of a limiting component of the translation system whereas the mutant extracts maintain over time a smaller and relatively unchanged pool of the functionally available component. One possible explanation for this observation, considered below, is that the increase in translation activity in WT extracts arises from translation termination and dissociation of ribosomal subunits from endogenous mRNAs. Thus, ribosomes in WT extracts might readily enter the pool of functional ribosomes over time, leading to an overall increase in *CAN1/LUC* expression, whereas

the reutilization of ribosomes that were previously engaged in translation is somehow compromised in the mutant extracts.

Upf1p affects translation *in vitro*

To test whether the decrease in translation of the *CAN1/LUC* reporter mRNA observed in *upf1Δ* extracts was due to the absence of Upf1p, or resulted from an indirect effect of the lack of a functional NMD pathway, we assessed translation of the *CAN1/LUC* mRNA in *upf1Δ* extracts supplemented with either purified FLAG-Upf1p or BSA (as a control). As shown in Fig. 3.5(a), purified FLAG-Upf1p was sufficient to restore the translation activity of a *upf1Δ* extract to that approaching the activity of a WT extract. In addition, purified FLAG-Upf1p was also able to stimulate the translational capacity of a *upf1Δ* extract at different time points in a ribosome reutilization assay (Fig. 3.5(b), compare white boxes to gray boxes at each time point). These results suggest that Upf1p may play a direct role in enabling or enhancing the availability of functional ribosomes *in vitro*.

Translation initiation is compromised in *upf1Δ* extracts

To evaluate the relative efficiency of translation initiation on the *CAN1/LUC* mRNA in different extracts, we used a primer extension inhibition (toeprinting) assay (Dmitriev *et al.* 2003; Amrani *et al.* 2004). WT and *upf1Δ* extracts were preincubated for different lengths of time and then supplemented with *CAN1/LUC* mRNA, as in Fig. 3.4(d). After incubating the extracts with the mRNA for 25 min, cycloheximide (CHX) was added to terminate the reactions and stall elongating 80S ribosomes. Toeprinting

reactions were then performed using a radiolabeled oligonucleotide that allowed visualization of a gel band corresponding to a ribosome positioned at the initiator AUG codon (Fig. 3.6(a), upper panel). Accumulation of this "toeprint" was sensitive to cap analog (Fig.3.6(a), upper panel), indicating that it arose from initiation activity, and WT extracts routinely showed a more intense toeprint than the *upf1Δ* extracts (Fig. 3.6(a), upper and lower panels), reflecting better translation initiation.

Since the AUG toeprints could arise as a consequence of both *de novo* initiation, as well as recycling of ribosomes post-termination, we modified the assay such that CHX was added at the same time as the *CAN1/LUC* mRNA. Thus, only ribosomes undergoing *de novo* initiation would contribute to the AUG toeprints. Fig. 3.6(b) shows that, using this approach, only WT extracts exhibit a significant increase in the AUG toeprint within the first twenty minutes, whereas *upf1Δ* extracts fail to show any appreciable increase in the AUG toeprint band even at late timepoints, suggesting an absence of 80S ribosomes at the initiator AUG. This result indicates further that the availability of functional ribosomes may be diminished in the absence of Upf1p. To determine whether Upf1p affects an early or late step in initiation, we repeated the same assay, replacing CHX with the nonhydrolyzable GTP analog, GMP-PNP, which allows 48S formation, but inhibits joining of the 60S ribosomal subunit [Fig. 3.6(c)] (Dmitriev *et al.* 2003). In this experiment we observed that both WT and *upf1Δ* extracts exhibited strong AUG toeprint bands in the presence of GMP-PNP, indicative of the presence of 40S ribosomal subunits on the RNA, with the *upf1Δ* extracts showing a slightly diminished signal. Taken together, these results suggest that, although 40S loading is

slightly impaired in *upf1Δ* extracts, Upf1p is likely to influence a late stage of translation initiation, namely the joining of the 60S subunit to the 48S complex.

Initiation efficiency depends on prior termination events

The results depicted in Figs. 3.4-3.6 implicate Upf1p in the determination of translational initiation efficiency *in vitro*, but the mechanism underlying this activity, and its relationship to the reinitiation defects seen *in vivo* (Figs. 3.1-3.3) and *in vitro* (Amrani *et al.* 2004), were unclear. Our translation reactions are carried out in the absence of any prior nuclease treatment and the ongoing translation of endogenous mRNAs includes that of a substantial number of mRNAs that are NMD substrates (He *et al.* 2003; Johansson *et al.* 2007). Since premature termination on the latter transcripts is altered in the absence of *UPF1* (Chapter II) we considered the possibility that these events might influence subsequent translation initiation activity in the extracts. Accordingly, we devised an assay to monitor translation of the *CAN1/LUC* reporter mRNA by ribosomes that had undergone a prior termination event at either a normal or a premature termination codon. To achieve this, we first treated WT and *upf1Δ* extracts with micrococcal nuclease to eliminate endogenous mRNAs. With this treatment, the ability of *upf1Δ* extracts to translate the *CAN1/LUC* mRNA *in vitro* resembled that of WT extracts [3.7(a)], confirming our earlier observation that MN-treated extracts showed similar AUG toeprints of the *CAN1/LUC* transcript (Amrani *et al.* 2004). We then primed these extracts with different amounts of synthetic WT *CAN1* mRNA, or its nonsense-containing counterpart (*can1-100* mRNA), in order to generate extracts in which ribosomes were preferentially undergoing either normal or premature translation

termination events. We rationalized that ribosomes undergoing one termination event or the other might be differentially predisposed for further rounds of translation in these extracts, a difference that we could test by measuring the luciferase activity generated by the subsequent addition of the *CAN1/LUC* reporter mRNA. Fig. 3.7(b) depicts the ratios of luciferase activity obtained in WT and *upf1Δ* extracts from reactions that were first primed with *can1-100* or *CAN1* mRNAs. The results of this experiment indicate that WT extracts manifest as much as twofold more translation of the *CAN1/LUC* reporter mRNA when primed with high levels of the *can1-100* mRNA *vs.* the *CAN1* mRNA, but that translation of the reporter mRNA in *upf1Δ* extracts is unaffected by the nature of the priming mRNA. This result suggests that in WT extracts, but not in *upf1Δ* extracts, the termination and release of ribosomes from premature stop codons generates a pool of ribosomes with greater "recycling" ability than ribosomes released from the normal terminator.

In principle, the size of the ORF, rather than the nature of the termination event, could be responsible for the increased luciferase activity in translation reactions primed with the *can1-100* mRNA in WT extracts. Hence, we repeated the assay in WT extracts using either the *can1-100* mRNA or the *miniUAA* mRNA (Fig. 2.9 and Chapter II). The latter is a transcript that contains the same ORF as the *can1-100* mRNA, but which has a normal termination event because the short ORF is followed by a normal 3'-UTR (Chapter II). A comparison of the ratios of luciferase activities obtained with the two RNAs showed that priming with the *can1-100* mRNA yielded enhanced translation of the *CAN1/LUC* mRNA relative to priming with the *miniUAA* mRNA (Fig. 3.7(c), middle box). The experiments in Fig. 3.7(c) [right box] also demonstrate that the luciferase

output obtained when reactions were primed with the *miniUAA* mRNA were comparable to those primed with the *CAN1* mRNA. Taken together, these results indicate that premature termination events, not the length of the ORF, are responsible for the increased luciferase activity, and reflect the possibility that more ribosomes, or more active ribosomes, were released from the nonsense-containing transcript than from the WT or pseudo-WT mRNA.

To test whether Upf1p is involved in the increase of translation activity subsequent to premature termination, we primed *upf1Δ* extracts with the *CAN1* or *can1-100* mRNAs in the presence of purified FLAG-Upf1p or BSA and measured the responses of the respective extracts to *CAN1/LUC* mRNA that was added subsequently. We found that addition of purified FLAG-Upf1p was sufficient to enhance luciferase activity in *upf1Δ* extracts primed with *can1-100* mRNA, similar to that observed with WT extracts (Fig. 3.8(a), compare gray boxes in WT+BSA and *upf1Δ*+FLAG-Upf1p). To further analyze the translation status of the *CAN1/LUC* mRNA in reactions primed with the *can1-100* mRNA in the presence of FLAG-Upf1p or BSA, we fractionated the translation reactions on sucrose gradients and analyzed the fractions by northern blotting for their levels of specific transcripts. These experiments showed that, in WT extracts (supplemented with BSA), the *CAN1/LUC* mRNA was distributed throughout the sucrose gradient, including the polysomes and lighter fractions (Fig. 3.8(b), left panel). In *upf1Δ* extracts (supplemented with BSA) there was significantly less *CAN1/LUC* mRNA in the polysome fractions, with most of the mRNA being confined to the sub-80S fractions. However, addition of FLAG-Upf1p to the *upf1Δ* extracts restored the polysome distribution of the *CAN1/LUC* mRNA to that seen in the

WT control. To determine whether the decreased translation of the secondary *CAN1/LUC* mRNA was due to overall decreased translational capacity of the nuclease-treated *upf1Δ* extracts, we also analyzed the distribution of the *can1-100* mRNA (Fig. 3.8(b), right panel) used to prime the reactions. We observed a similar distribution pattern for the primary *can1-100* mRNA in extracts containing or lacking Upf1p, further indicating that decreased *CAN1/LUC* translation in *upf1Δ* extracts is most likely a consequence of translational termination at a PTC in the absence of Upf1p.

Addition of WT ribosomal subunits enhances translation in *upf1Δ* extracts

Although Upf1p has been shown to cosediment with polyribosomes (Peltz *et al.* 1993; Atkin *et al.* 1995; Yamashita *et al.* 2009), little is known about the nature of this association. Since the results of Figs. 3.7 and 3.8 suggested that Upf1p might enhance the ability of ribosomes to recycle to another round of translation, we evaluated the effect of adding purified WT ribosomal subunits to *upf1Δ* extracts. We reasoned that the absence of Upf1p in these extracts might lead to the accumulation of defective 40S and/or 60S subunits and that the possible amelioration of the translation defects upon addition of the WT subunits would shed light on which subunit was affected in the absence of Upf1p. Fig. 3.9(a) [right panel] shows that addition of purified 40S or 60S subunits to non-nucleased *upf1Δ* extracts was sufficient to increase the translation of the *CAN1/LUC* mRNA. WT extracts (Fig. 3.9(a), left panel), on the other hand, did not show any increases in translation upon addition of either ribosomal subunit. The stimulatory activity of 40S and 60S subunits in *upf1Δ* extracts suggested that either both subunits were affected by the absence of Upf1p, or that only one subunit was affected

but that the other contained bound Upf1p. Indeed, Fig. 3.9(b) shows that Upf1p preferentially copurified with 40S subunits, although the amount of Upf1p associated with the ribosomal subunits is much lower than the total WT Upf1p present in a translation reaction (Fig. 3.9(b), compare 40S lanes vs. WT extract lane) or the purified FLAG-Upf1p required for complementation *in vitro* (the 11 ng lane represents 4% of the purified FLAG-Upf1p used per translation reaction). Since the subunit purification protocol (Algire *et al.* 2002) involves high salt washes, this result indicates that Upf1p can form a stable association with 40S subunits, and may account in part for the increase in luciferase activity observed upon their addition to *upf1Δ* extracts. Comparison of the amount of Upf1p present in association with ribosomal subunits to the amount of purified FLAG-Upf1p [Fig. 3.9(b)] used in the complementation assays in Figs. 3.5, 3.8, and 3.9 suggests that 40S-associated Upf1p may retain more activity than the purified FLAG-Upf1p or that 40S subunits themselves may have a slight defect. In turn, this suggests that the stimulatory activity of the purified 60S subunits may reflect a relative inactivity of such subunits in *upf1Δ* extracts. It should be noted that the 60S subunit sample also contains a polypeptide band in the approximate position of Upf1p, but this band is significantly less abundant than that associated with the 40S sample and does not show a linear increase with overall protein loaded on the gel.

Fig. 3.1

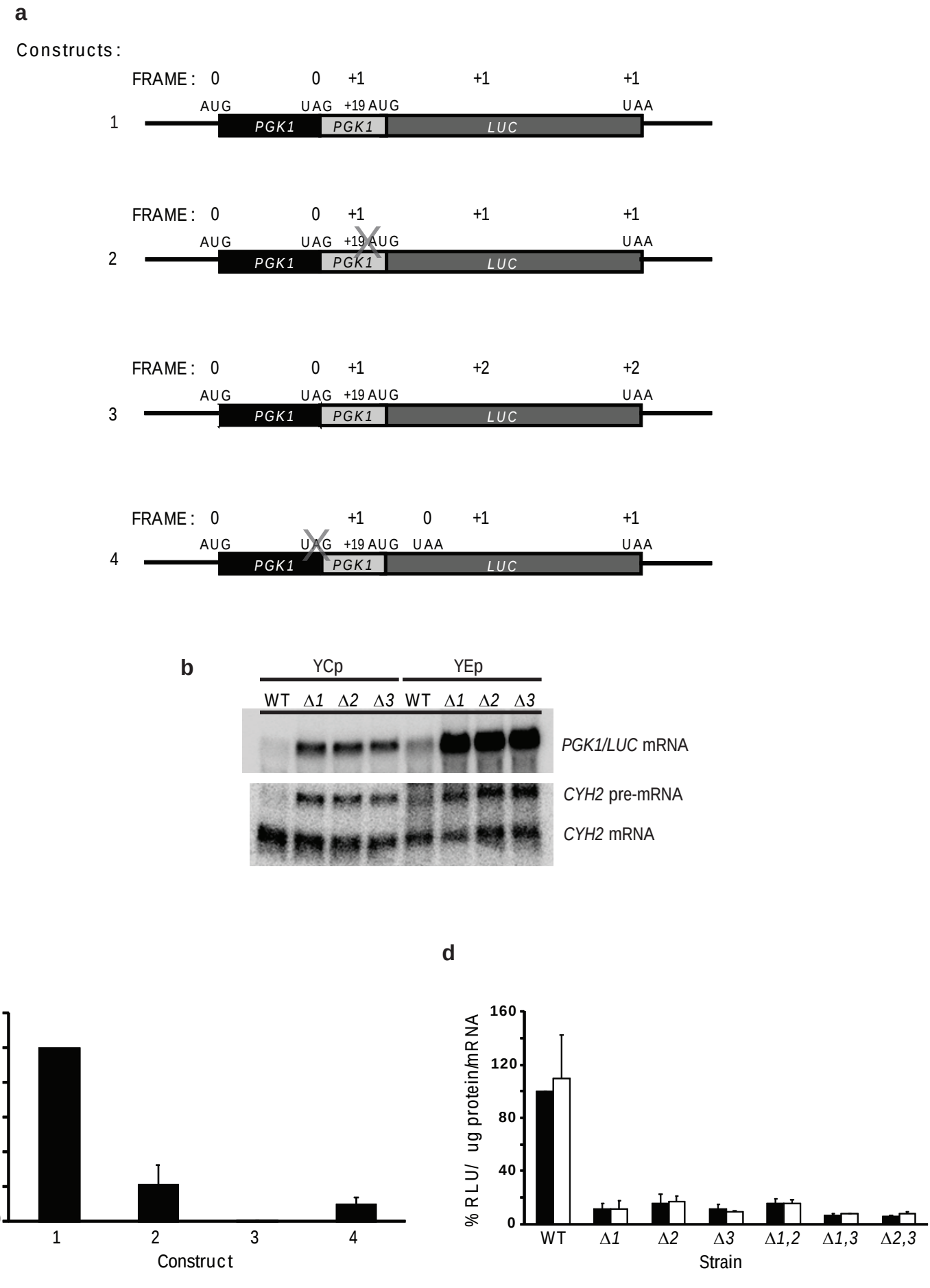
a
Constructs:
FRAME: 0 0 +1 +1 +1
AUG UAG +19 AUG UAA
1
PGK1 PGK1 LUC
FRAME: 0 0 +1 +1 +1
AUG UAG +19 AUG UAA
2
PGK1 PGK1 LUC
FRAME: 0 0 +1 +2 +2
AUG UAG +19 AUG UAA
3
PGK1 PGK1 LUC
FRAME: 0 +1 0 +1 +1
AUG UAG +19 AUG UAA UAA
4
PGK1 PGK1 LUC
b
YCp YEp
WT Δ1 Δ2 Δ3 WT Δ1 Δ2 Δ3
PGK1/LUC mRNA
CYH2 pre-mRNA
CYH2 mRNA
c
% RLU/ug protein/mRNA
120
100
80
60
40
20
0
1 2 3 4
Construct
d
% RLU/ ug protein/mRNA
160
120
80
40
0
WT Δ1 Δ2 Δ3 Δ1,2 Δ1,3 Δ2,3
Strain

Fig. 3.1 : Reinitiation activity is reduced in strains bearing mutations in the NMD pathway. (**a**) Schematic representation of *PGK1/LUC* chimeric constructs 1-4. Start and stop codons are indicated, as are their reading frames and that of the *LUC* coding region, relative to the *PGK1* start codon. "X" indicates deletion or mutation of a particular feature. "+19 AUG" denotes the first of two in-frame *PGK1* AUGs downstream of the PTC. Details of the constructs are given in Table 2. (**b**) Northern analysis of the *PGK1/LUC* mRNA expressed from either a low-copy (YCp) or high-copy (YEp) vector in WT cells or in isogenic cells harboring deletions of *UPF1*, *UPF2/NMD2*, or *UPF3*. Blots were stripped and reprobed for *CYH2* transcripts as an internal control for NMD function (*CYH2* pre-mRNA) and loading (*CYH2* mRNA). (**c**) Relative luciferase activities of constructs 1-4 normalized for protein content and mRNA levels in the WT strain HFY114. The luciferase activity of construct 1 was assigned a value of 100%. (**d**) Reinitiation activity. Construct 1 was inserted into either a low-copy (YCp) or high-copy (YEp) vector and transformed into the indicated strains. Relative luciferase activities, normalized for protein content and mRNA levels, are shown for YCp-bearing strains in black boxes and for YEp-bearing strains in white boxes. The luciferase activity of construct 1 on a YCp plasmid in a WT strain was assigned a value of 100%. The symbol Δ*1* represents *upf1*Δ*;* Δ*2, nmd2*Δ*;* Δ*3, upf3*Δ; and combinations thereof. Vertical bars represent standard error of the mean.

a

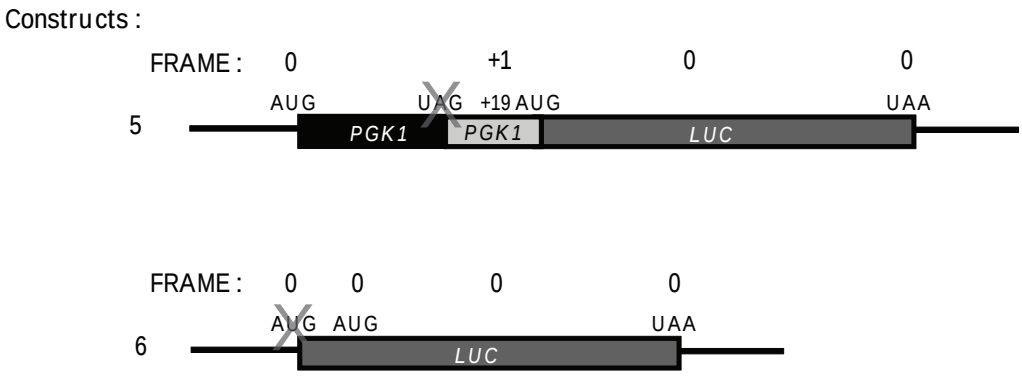

b

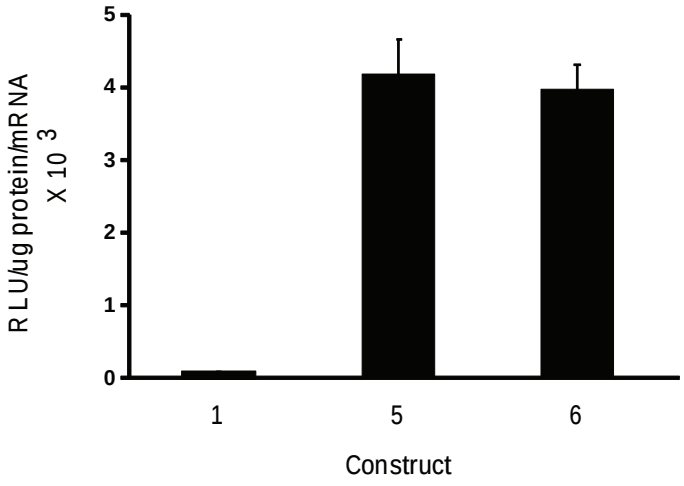

Fig. 3.2 : Determination of ribosomal initiation efficiency and proportion of ribosomes that reinitiate downstream of the *PGK1* stop codon. (**a**) Schematic representations of chimeric *PGK1/LUC* constructs 5 and 6. Labeling of start and stop codons and reading frame is as depicted in Fig. 3.1, with "X" indicating deletion or mutation of a particular feature. (**b**) Luciferase activities of constructs 5 and 6 in the wild type strain HFY114. Activity is expressed as RLU/μg protein/unit mRNA. The activity of construct 1 (Fig. 1) is shown for purposes of comparison. Vertical bars represent standard error of the mean.

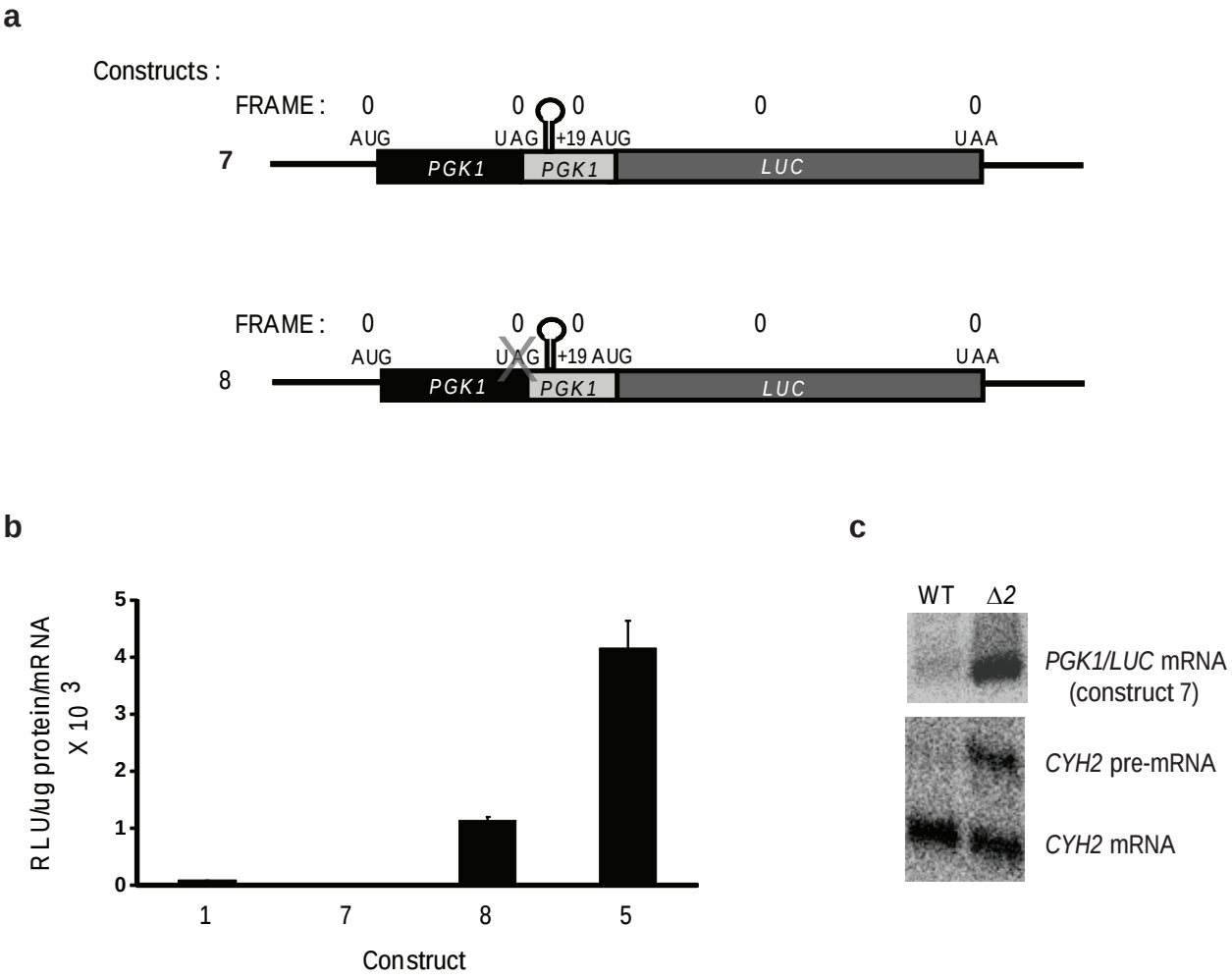

Fig. 3.3 : A strong stem loop structure does not eliminate nonsense-mediated mRNA decay. (**a**) Schematic representations of chimeric *PGK1/LUC* constructs 7 and 8. Labeling of start and stop codons and reading frame is as depicted in Fig. 1, with "X" indicating deletion or mutation of a particular feature. (**b**) Luciferase activities of constructs 7 and 8 in the WT strain HFY114. Activity is expressed as RLU/μg protein/unit mRNA. Activities of constructs 1 and 5 are shown for purposes of comparison. Vertical bars represent standard error of the mean. (**c**) Northern analysis of *PGK1/LUC* construct 7 mRNA expressed from a low-copy (YCp) vector in WT cells or in isogenic cells harboring a deletion of *UPF2/NMD2*. Blots were stripped and reprobed for *CYH2* transcripts as an internal control for NMD function (*CYH2* pre-mRNA) and loading (*CYH2* mRNA).

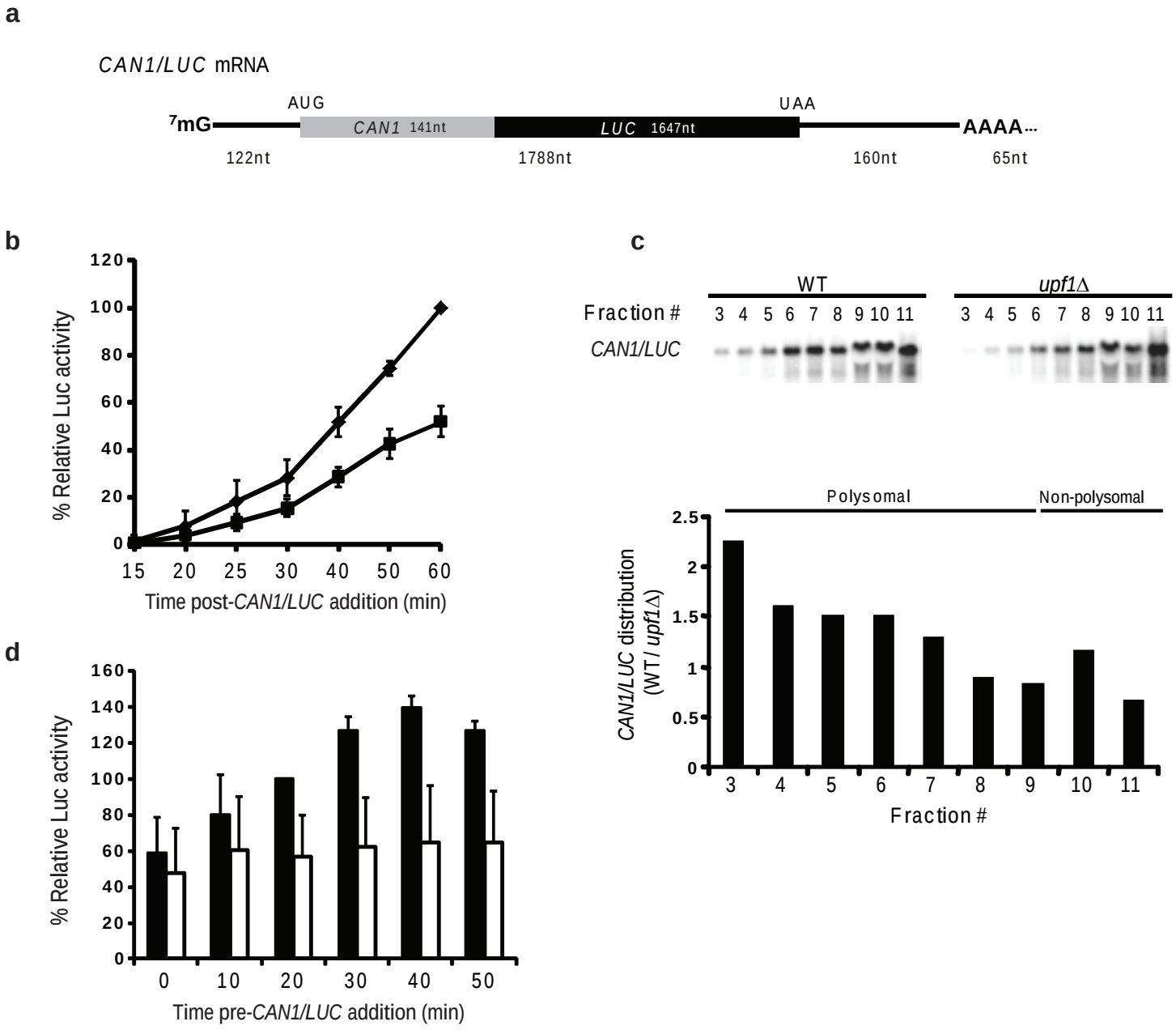

Fig. 3.4 : Translation of *CAN1/LUC* mRNA is decreased in *upf1*Δ, *nmd2*Δ, and *upf3*Δ extracts. (**a**) Schematic representation of the *CAN1/LUC* fusion mRNA. (**b**) Luciferase activities of WT (diamonds) and *upf1*Δ (squares) extracts prepared without micrococcal nuclease (MN) treatment and incubated with 100ng *CAN1/LUC* mRNA at 18oC for the indicated times. Relative luciferase activity was calculated using the WT 60 min values as 100%. (**c**) Upper panel - northern analysis of polysomal distribution of *CAN1/LUC* mRNA translated *in vitro* in WT or *upf1*Δ extracts. Lower panel - ratio of the polysomal distributions of the *CAN1/LUC* mRNA during *in vitro* translation. WT and *upf1*Δ extracts, prepared without MN treatment, were incubated with synthetic *CAN1/LUC* mRNA at 18oC for 30 min and then analyzed by fractionation on 7-47% sucrose gradients and subsequent northern blotting using a probe specific for the *CAN1/LUC* mRNA. The amount of *CAN1/LUC* mRNA (in arbitrary units) in each gradient fraction was determined by phosphorimaging and the Y-axis depicts the ratios of those amounts in WT vs. *upf1*Δ extracts. Sedimentation of the gradients was from right to left; the bars at the top of the panel indicate the polysomal and non-polysomal fractions. (**d**) Relative luciferase activities of WT (black boxes) and upf1Δ (white boxes) extracts treated as in (**b**) and incubated for 25 min after addition of *CAN1/LUC* mRNA at the indicated times. Relative luciferase activities were measured using WT 20 min values as 100%. Vertical bars in (**b**) and (**d**) depict standard deviation.

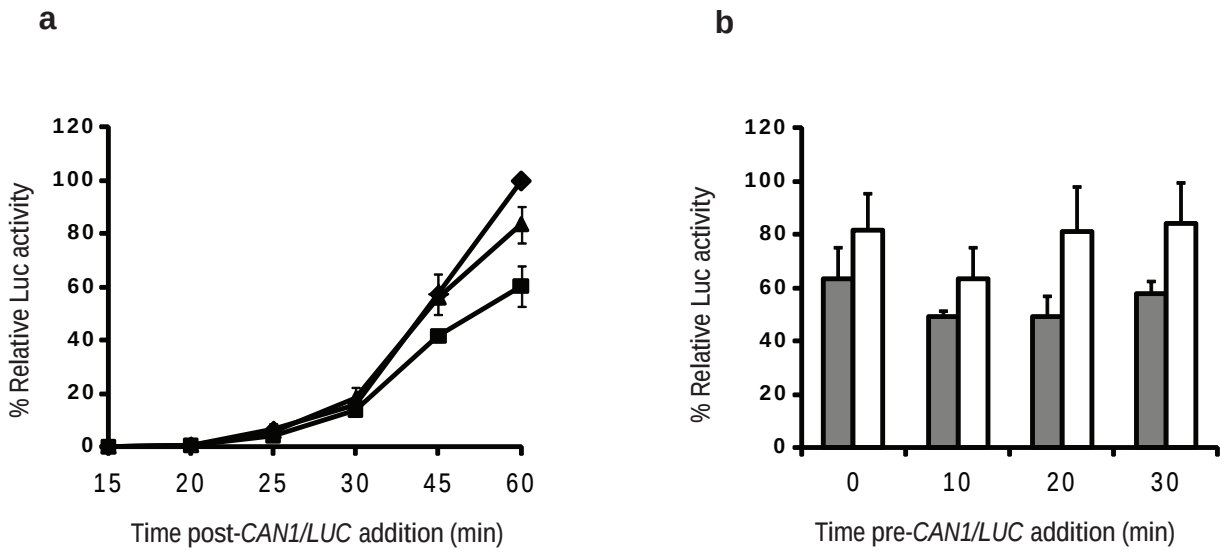

Fig. 3.5 : Purified FLAG-Upf1p can complement translation defects in vitro. Cell-free translation extracts were prepared from WT or *upf1*Δ cells without MN treatment and preincubated on ice for 10 min with 270-360ng BSA or purified FLAG-Upf1p, followed by incubation at 18oC in either of two modes: (**a**) addition of 100ng *CAN1/LUC* mRNA at t=0 min and sampling for luciferase activity at the indicated time points or (**b**) addition of 100ng *CAN1/LUC* mRNA at the indicated time points and translation at 18oC for 25 min prior to measurement of luciferase activity. **(a**) Relative luciferase values were calculated as in Fig.3.4b for WT extracts supplemented with BSA (diamonds), *upf1*Δ extracts supplemented with BSA (squares) or *upf1*Δ extracts supplemented with FLAG-Upf1p (triangles). (**b**) Relative luciferase activites of *upf1*Δ extracts supplemented with BSA (gray boxes) or FLAG-Upf1p (white boxes) normalized to the corresponding WT+BSA values at each given time point. Vertical bars in (**a**) and (**b**) depict standard deviation.

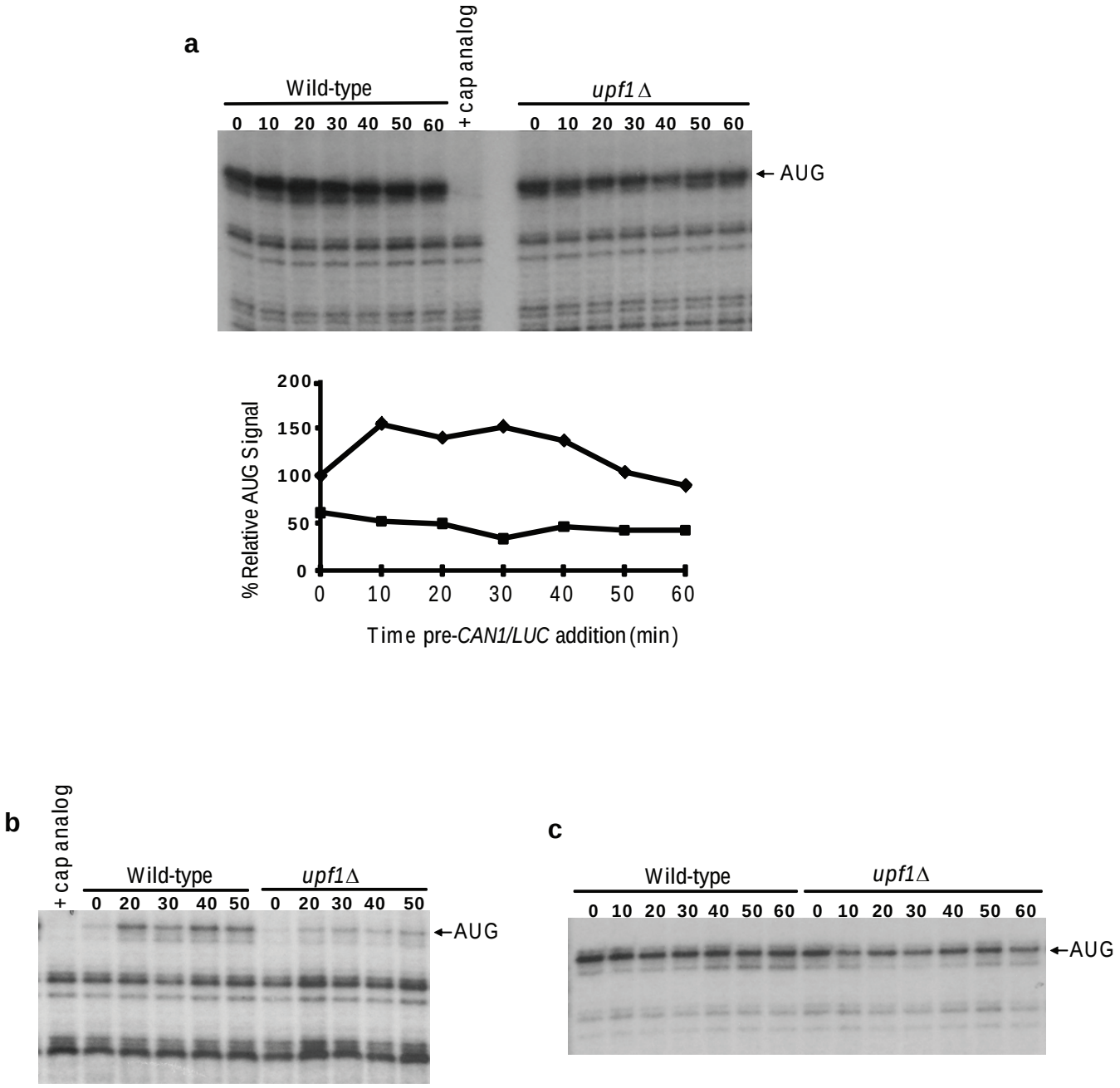

Fig. 3.6 : Formation of 80S toeprints is diminished in upf1Δ extracts. (**a**) Cell-free translation extracts, prepared from WT and *upf1*Δ cells without MN treatment, were incubated at 18oC. *CAN1/LUC* mRNA (100ng) was added at the indicated time points and reactions were further incubated for 25 min, followed by addition of 2 mM cycloheximide (CHX) for 3 min. Reactions were frozen and subsequently analyzed by toeprinting. The upper panel shows the autoradiograph, and the lower panel depicts the densitometry of the AUG band in WT (diamonds) and *upf1*Δ (squares) reactions normalized to the WT 0 min value. (**b**) Translation conditions were as in (**a**), except that 2 mM CHX was added with 100ng *CAN1/LUC* mRNA at each time point, followed by incubation for 25 min. Lanes in (**a**) and (**b**) in which control reactions contained 2.7mM cap analog are indicated. (**c**) Translation and incubation conditions were as in (**b**), except that CHX was replaced with 2 mM GMP-PNP.

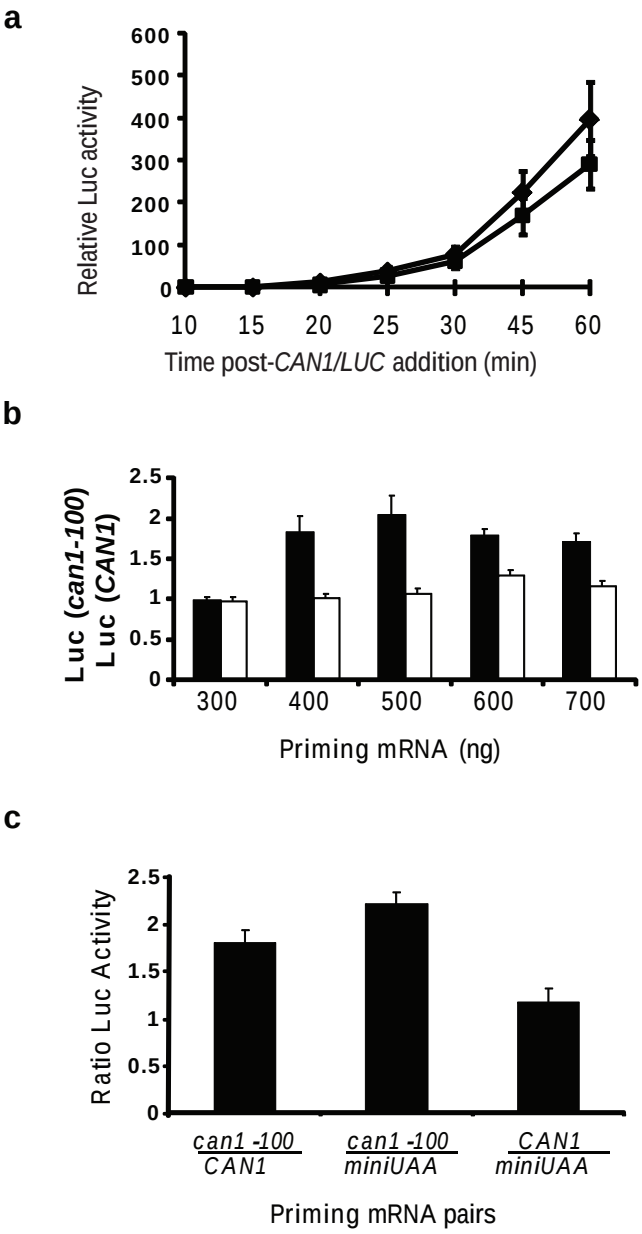

Fig. 3.7 : Initiation efficiency depends on prior termination events. Translation extracts prepared from WT or *upf1*Δ cells were treated with MN for 5 min at 25oC. (**a**) Luciferase activities of WT (diamonds) and *upf1*Δ (squares) extracts incubated with 100ng *CAN1/LUC* mRNA at 18oC for the indicated times. (**b**) Treated extracts were incubated with the designated concentrations of the priming *CAN1* or *can1-100* mRNA for 7 min at 18oC, followed by addition of 300ng of *CAN1/LUC* mRNA and incubation for an additional 25 min. Ratios of luciferase activities calculated from reactions programmed with *can1-100* and *CAN1* mRNAs are shown for WT (black boxes) and *upf1*Δ (white boxes) extracts. (**c**) *CAN1* or *can1-100* mRNA (500ng of either), or 50ng of *miniUAA* mRNA, was incubated with WT extracts for 7 min, followed by addition of 300ng *CAN1/LUC* mRNA and further incubation for 25 min at 18oC. Ratios of luciferase activity were calculated as designated on the X-axis. Vertical bars all panels depict standard deviation.

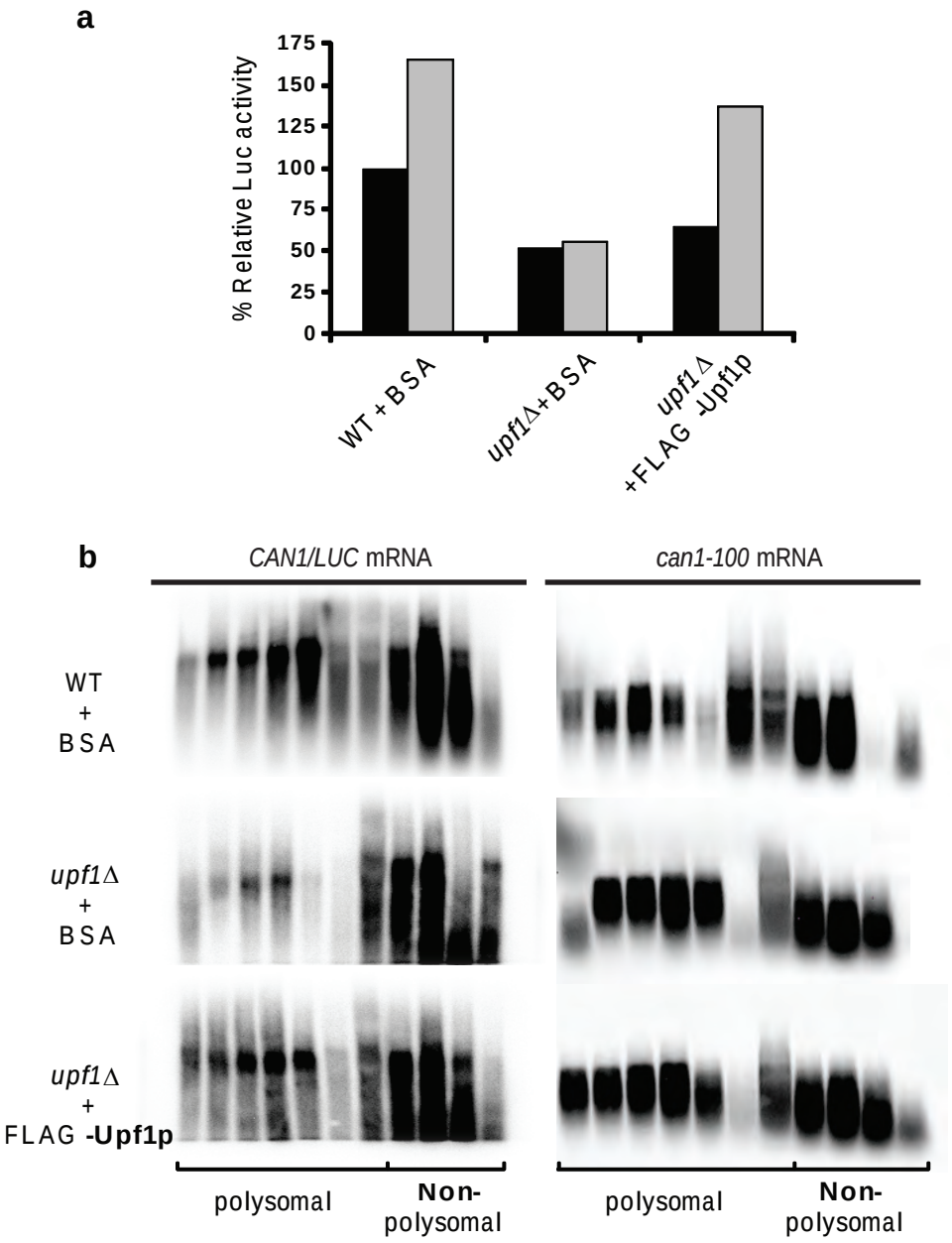

Fig. 3.8 : Purified FLAG-Upf1 restores efficient translational activity to upf1Δ extracts. Cell-free translation extracts were prepared from WT or *upf1*Δ cells and treated with MN for 5 min at 25oC. Extracts were incubated with 270ng of BSA or FLAG-Upf1p on ice for 10 min and added to translation mixes containing 500ng of *CAN1* (**a**) or *can1-100* (**a** and **b**) mRNA and incubated for 7 min at 18oC. *CAN1/LUC* mRNA (300ng) was then added and reactions were further incubated for 25 min at 18oC. (**a**) Relative luciferase activities in the respective reactions as detailed on the X-axis. Black and gray boxes indicate reactions primed with the *CAN1* or *can1-100* mRNAs, respectively. (**b**) *can1-100*-primed translation reactions were set up as in (**a**), terminated by the addition of CHX (2 mM), and subsequently fractionated on sucrose gradients. The fractions were then analyzed by northern blotting using a DNA probe specific for the *CAN1/LUC* (left panel) or the *can1-100* (right panel) mRNA.

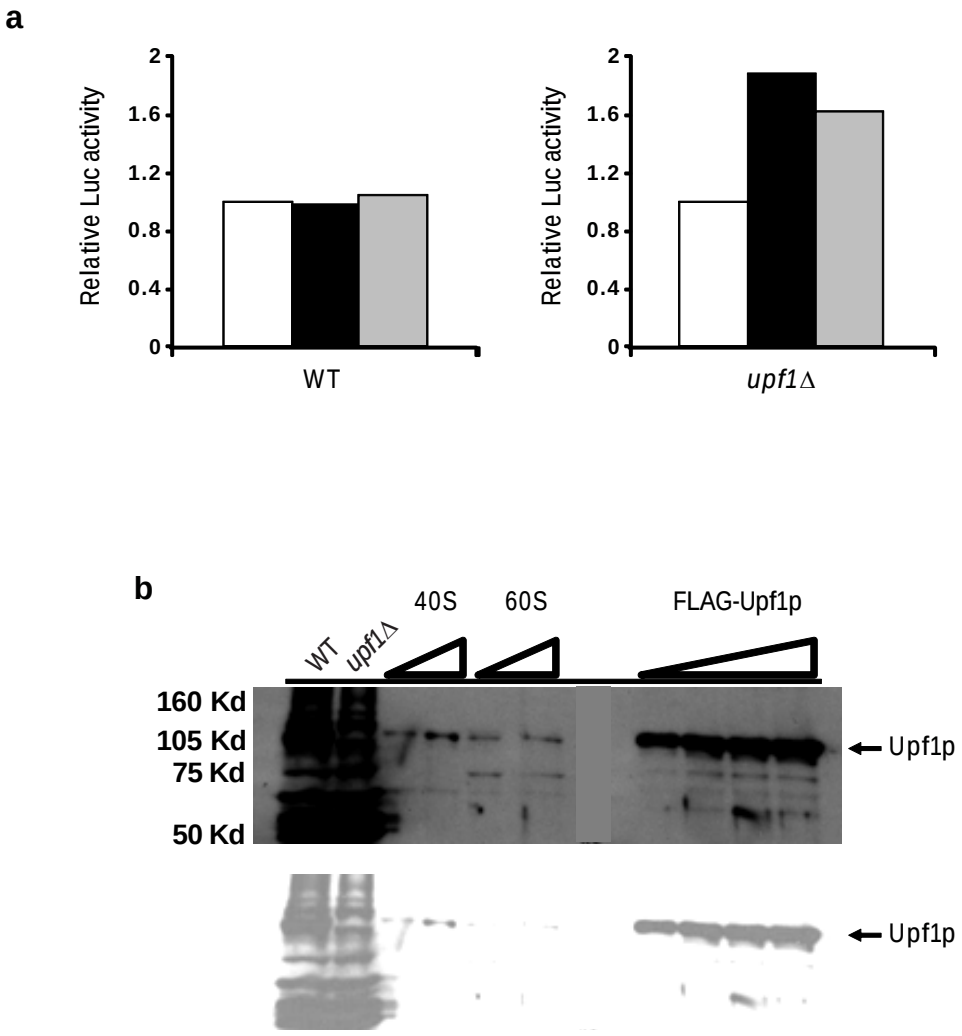

Fig. 3.9 : 40S and 60S ribosomal subunits enhance translation in *upf1*Δ extracts. Cell-free translation extracts were prepared from WT or *upf1*Δ cells. In (**a**) extracts were supplemented with 100ng *CAN1/LUC* mRNA and then incubated with BSA (white boxes), purified 40S subunits (black boxes), or purified 60S subunits (gray boxes) at 18oC for 60 min. Luciferase activity is depicted relative to the value obtained with the BSA control for each extract. The graph depicts the average of two experiments. (**b**) Western blot of increasing amounts of purified 40S subunits (5 and 10 µg), 60S subunits (10 and 20 µg), and FLAG-Upf1p (11, 22, 45 and 90 ng) probed with polyclonal anti-Upf1p antibody. WT and *upf1*Δ extracts (5 µg each) were run as controls. The bottom panel is a lighter exposure of the top panel to allow visualization of the Upf1p band in the WT extract lane.

Chapter IV

Translation factors promote formation of two states of the closed loop mRNP

The work presented in this chapter has been published as:

Amrani N., **Ghosh S.**, Mangus D.A., Jacobson A. (2008). Translation factors promote formation of two states of the closed loop mRNP. Nature **453**(7199):1276-80.

SG's contributions to this work include extract preparation, handling and processing of toeprint gels, all sucrose density gradient experiments, and northern blotting.

Chapter IV - Translation factors promote formation of two states of the closed loop mRNP

Summary

Efficient translation initiation and optimal stability of most eukaryotic mRNAs depends on the formation of a closed loop structure and the resulting synergistic interplay between the 5' m^7G cap and the 3' poly(A) tail (Gallie 1991; Jacobson 1996). Evidence of eIF4G and Pab1p interaction supports the notion of a closed loop mRNP (Wells *et al.* 1998), but the mechanistic events that lead to its formation and maintenance are still unknown. Here we have used toeprinting and polysome profiling assays to delineate ribosome positioning at initiator AUG codons and ribosome:mRNA association, respectively, and find that two distinct stable (cap analog resistant) closed loop structures are formed during initiation in yeast cell-free extracts. The integrity of both forms requires the mRNA cap and poly(A) tail, as well as eIF4E, eIF4G, Pab1p, and eIF3, and is dependent on the length of both the mRNA and the poly(A) tail. Formation of the first structure requires the 48S ribosomal complex whereas the second requires an 80S ribosome and the termination factors eRF3/Sup35p and eRF1/Sup45p. Surprisingly, the involvement of the termination factors is independent of a termination event.

Results

Responsiveness of the yeast cell-free translation system to the presence or absence of a 5' cap and/or a 3' poly(A) tail on *LUC* mRNA

The mRNA 5' cap and 3' poly(A) tail have previously been shown to enhance mRNA translational efficiency synergistically (Gallie 1991). Fig. 4.1 shows that the yeast cell-free translation system utilized for this study recapitulates this phenomenon. In the absence of both the 5' cap and the 3' poly(A) tail, the *LUC* mRNA is barely translated, but the addition of either a cap or a poly(A) tail enhances its translation several fold. The simultaneous presence of both a cap and a poly(A) tail stimulate luciferase production to a much larger extent than the sum of the two effects, i.e., the two mRNA appendages provide a synergisitic effect.

AUG toeprints and cap analog resistance are specific and independent of the polynucleotide concentration

Our *in vitro* translation reactions utilizing synthetic mRNAs derived from yeast transcripts were also able to recapitulate competitive inhibition of translation initiation by m^7GpppG (cap analog), and analyses of ribosome positioning or mRNA association by toeprinting and sucrose gradient sedimentation. Addition of the elongation inhibitor, cycloheximide (CHX), to translation reactions programmed by the 2135nt *AAA* and *UAA* mRNAs containing long or short ORFs, respectively, (Fig. 4.2) allowed detection of CHX-dependent initiator AUG toeprints that reflect 80S ribosomes protecting 16-18 nt 3' of the AUG (Dmitriev *et al.* 2003; Amrani *et al.* 2004; Wu *et al.* 2007) (Fig. 4.3(a), left

and right panels, lanes 1 and 3). A shorter mRNA (*miniUAA1*, 488nt, Fig. 4.2) also yielded the AUG toeprint (Fig. 4.3(b) upper panel, lane 1), but this band was resistant to 2.7mM cap analog (lane 2) and only manifested sensitivity at higher concentrations (Fig. 4.3(c) lower panel). These toeprints were dependent on initiation codon recognition, the presence of yeast extract, and concurrent mRNA translation (Fig.4.4). Translation reactions in wild-type extracts were incubated with either capped and polyadenylated *miniUAA1* or *AAA* mRNAs, or with both the capped and polyadenylated *miniUAA1* mixed with the non-capped, non-polyadenylated *AAA* mRNA for 4 min, followed incubation with CHX for 3 min. Toeprints corresponding to ribosomes stalled with the AUG codon in their P sites were obtained with the *miniUAA1* and *AAA* RNAs at the expected position, 16-18 nt downstream of the start codons (Fig. 4.4(a), lanes 1-4). The toeprint bands were dependent on the presence of the start codon, because they were absent in the *No-iATG* mRNA [a derivative of *miniUAA1* mRNA with a deletion of the initiator AUG codon; Fig. 4.4(c)], and dependent on mRNA translation, because they were not detected in the absence of the mRNAs (Fig. 4.4(a), lane 5) or in the absence of the extract (Fig.4.4(a), lanes 6 [contains *miniUAA1* mRNA] and 7 [contains *AAA* mRNA]). Supporting the latter conclusion, toeprints were almost completely eliminated by 2.7mM cap analog, a concentration that distinguished *bona fide* toeprints from background bands (Fig. 4.3(a), lanes 2 and 4). Lower cap analog concentrations also inhibited AUG toeprint accumulation, with 70% and 96% sensitivity obtained at 0.05mM and 0.5mM, respectively (Fig. 4.3(c), left panel).

Resistance to cap analog is mRNA size dependent but is not mRNA sequence dependent

In wild-type extracts, the short capped and polyadenylated *miniUAA1* mRNA is ~160-fold more resistant to cap analog than the longer *AAA* mRNA [Fig.4.3(c)]. Translation and toeprinting analyses of *miniADE2* mRNA (485nt) and full-length *ADE2* mRNA (2070nt), which have the same 5'-UTR and 3'-UTR, show the expected AUG toeprint bands (Fig. 4.5(a), lanes 1 and 3). However, addition of 2.7mM of cap analog had no effect on the *miniADE2* AUG toeprints (lane 2) whereas the *ADE2* AUG toeprints were eliminated in the presence of the same concentration of the drug (lane 4). These data are consistent with the results obtained with the *miniUAA1* and *AAA* mRNAs (Fig. 4.3), which are, respectively, similar in size to the *miniADE2* and *ADE2* mRNAs, and demonstrate that resistance to cap analog is mRNA size dependent *in vitro,* not mRNA sequence dependent. Consistent with the apparent mRNA size dependence of cap analog resistance *in vitro,* mRNAs with intermediate sizes (from 488nt to 2135nt), but with the same stability [Fig. 4.5(c)], showed intermediate phenotypes, with approximately 40% sensitivity to 2.7mM cap analog obtained with an 882nt mRNA, 60% sensitivity with an 1105nt mRNA, and near maximal sensitivity reached with a 1336nt mRNA [Fig. 4.5(b)].

Cap analog resistance is not due to cap-independent translation

To rule out cap-independent translation as the basis for cap analog resistance, we translated and toeprinted a polyadenylated *miniUAA1* mRNA with no 5' cap. This mRNA, which is stable during translation [Fig 4.6(c)], initiates inefficiently in wild-type

extracts (Fig. 4.6(a), lane 1), strongly suggesting that translation of our reporter mRNAs is cap-dependent. As reported previously (Tarun and Sachs 1995; De Gregorio *et al.* 1998) the addition of cap analog stimulates translation of uncapped mRNA (Fig. 4.6(a), lane 2), possibly because it titrates other inhibitors. Collectively, these data suggest that interactions between the eIF4F cap-binding complex and the 5' m^7G cap of the *mini* mRNAs are much stronger than those occurring with the long mRNAs.

Translation of poly(A)-deficient mRNA is sensitive to cap analog

Short mRNAs may be preferentially resistant to cap analog because they form a more stable closed loop mRNP than long mRNAs, possibly by promoting increased affinity of mRNP factors for each other or for mRNA structures such as the 5' cap (Christensen *et al.* 1987; Wells *et al.* 1998; Sachs 2000; Karim *et al.* 2006). To test the relationship of the closed loop state to m^7GpppG resistance, we analyzed the toeprinting of capped, poly(A)$^-$ *miniUAA1* mRNA. This transcript showed strong sensitivity to cap analog (Fig. 4.6(b), lane 2). Further analyses of *miniUAA1* mRNAs having different poly(A) tail lengths [but identical stabilities; Fig 4.6(e)] showed that *miniUAA1* mRNA with a poly(A) tail of 14 or 18As (Fig. 4.6(d), lanes 1-4) displayed a phenotype similar to poly(A)-deficient mRNA (>95% sensitivity to 2.7mM cap analog). Increasing the poly(A) tail length to 22, 25, or 33 residues yielded an intermediate phenotype (~80% sensitivity to cap analog; lanes 5-10), whereas a *miniUAA1* mRNA with 57 As showed no sensitivity to 2.7mM cap analog (lanes 11 and 12). These results correlate cap analog resistance with poly(A) length, a result consistent with closed loop formation. Since Pab1p:poly(A) association requires a minimum of 12 adenosines, and

multiple Pab1p molecules can bind the same poly(A) tract in a 27nt repeating unit (Baer and Kornberg 1983; Sachs *et al.* 1986; Sachs *et al.* 1987), it appears that at least two Pab1p molecules are required for a stable closed loop structure. Consistent with this conclusion, previous studies showed that an A_{15} tail did not suffice to stimulate translation in *Drosophila* (Gebauer *et al.* 1999) and mammalian (Munroe and Jacobson 1990) extracts, but that longer poly(A) tails promoted strong translational enhancement.

Pab1p is required for cap analog resistance of the *miniUAA1* mRNA

Toeprinting of the *miniUAA1* mRNA after translation in Pab1p-deficient (*pab1*Δ*/pbp1*Δ) extracts reinforced the notion of a critical role for Pab1p in cap analog resistance. Translation initiation in these extracts was highly sensitive to cap analog (Fig. 4.7(a), lanes 3 and 4; compare to extracts from wild-type [lanes 1 and 2] or *pbp1*Δ [a *pab1*Δ suppressor] cells [lanes 5 and 6]). Toeprinting of *miniUAA1* mRNA after translation in Pab1p-deficient (*pab1*Δ*/pbp1*Δ) extracts indicated an 80-fold increase in cap analog sensitivity [Fig. 4.3(c) and Fig.4.7(c)] that was directly attributable to the absence of Pab1p because supplementation with 15pmole of recombinant Pab1p, but not the same amount of BSA, restored cap analog resistance to wild-type levels [Fig. 4.7(b)]. While Pab1p is essential for cap analog resistance, its level must be well balanced since excess Pab1p, i.e., the addition of 15pmole Pab1p to wild-type extracts (lanes 3 and 4) or 38pmole Pab1p to *pab1*Δ*/pbp1*Δ extracts (data not shown), reduces the extent of cap analog resistance.

Cell-free extracts derived from mutants defective in Pab1p activity, or the activity of Pab1p-interacting proteins, are markedly sensitive to cap analog

To further evaluate the relationship between cap analog resistance and closed loop formation, we determined whether the same regions of Pab1p were required for both phenomena. Extracts derived from *pab1-134* cells, where Pab1p has wild-type affinity for eIF4G1 but reduced affinity for eIF4G2 [yeast has two eIF4G isoforms encoded by the functionally redundant *TIF4631* and *TIF4632* genes, respectively (Goyer *et al.* 1993; Otero *et al.* 1999)], showed a wild-type phenotype (Fig. 4.7(a), lanes 7 and 8). However, toeprinting analyses in *pab1-184* extracts, in which Pab1p does not bind to eIF4G1 or eIF4G2 (Otero *et al.* 1999), revealed a strong sensitivity to cap analog (Fig. 4.7(a), lanes 9 and 10). Similarly, extracts of *pab1-ΔRRM1* cells, in which Pab1p has lost the ability to interact with the poly(A) tail, and probably with either isoform of eIF4G as well (Kessler and Sachs 1998), also exhibit strong sensitivity to cap analog (Fig. 4.7(a), lanes 11 and 12), but not to the same concentration of GTP [Fig. 4.7(d)]. Both *pab1-184* and *pab1-ΔRRM1* extracts show about 10-fold more sensitivity to cap analog than those obtained from cells lacking the *PAB1* gene [Fig. 4.7(c)]), possibly indicating dominant-negative effects of the mutant proteins. To determine whether Pab1p interaction with the termination factor eRF3/Sup35p (Cosson *et al.* 2002) is also required for cap analog resistance, we analyzed extracts of *pab1-ΔC-term* cells. Fig. 4.7(a) [lanes 13 and 14] shows that this mutation also confers cap analog sensitivity, albeit 2.5-fold less sensitivity than that observed in *pab1Δpbp1Δ* extracts [Figs. 4.7(c) and 4.9(b)]. In addition, the pattern of toeprint inhibition with the *pab1-ΔC-term* extract appears different from that seen with other *pab1* mutants [Figs. 4.7(c) and 4.9(b)],

suggesting that the Pab1p C-terminal domain may be involved in a step distinct from that involving the other domains. All of the *pab1* mutant extracts show full sensitivity to cap analog when programmed with poly(A)$^-$ *miniUAA1* mRNA [Fig. 4.7(e)], but recombinant Pab1p could not complement the phenotypes of these extracts, further suggesting dominant-negative effects of the mutated proteins (data not shown).

The differences in cap analog sensitivity of the different *pab1* extracts are consistent with the loss of interactions characteristic of specific Pab1p domains (Mangus *et al.* 2003) being involved in closed loop mRNP formation and stabilization. Accordingly, we analyzed *miniUAA1* mRNA toeprints in extracts from strains harboring mutations in genes encoding different Pab1p-interacting proteins. Extracts of *eIF4G1-ΔN300* cells (Otero *et al.* 1999), in which there is no eIF4G2 and Pab1p:eIF4G1 interaction is disrupted, show strong sensitivity to cap analog and correlate well with the cap analog sensitivity phenotype of *pab1-184* extracts (Figs. 4.7(c) and 4.8). Likewise, extracts harboring mutated eRF3 (*sup35-R419G*) (Salas-Marco and Bedwell 2004) or eRF1 (*sup45-2*) (Stansfield *et al.* 1997) termination factors show both sensitivity to cap analog (but not to GTP [Fig. 4.7(d)]) and toeprint patterns that are strikingly similar to those obtained with the *pab1-ΔC-term* extract (Fig. 4.9), with the exception that they also yield two extra bands 5' of the AUG toeprint (asterisks) that are suggestive of initiation anomalies. Control reactions demonstrated that the termination mutant extracts were fully sensitive to cap analog when programmed with poly(A)$^-$ *miniUAA1* mRNA (Fig. 4.10) and that the addition of extra Mg^{2+} to the different translation reactions (to compensate for a possible titration by cap analog) had no affect on their toeprint phenotypes (Fig. 4.11). These results, and the observation that toeprinting of *miniUAA1*

mRNA after translation in extracts defective in eIF3 and eIF4E also exhibited more sensitivity to cap analog than did wild-type extracts (Fig. 4.12), imply that cap analog resistance results from formation of a stable closed loop structure.

Cap analog resistance is independent of translation termination

Further insights into closed loop formation followed from experiments using extracts supplemented with mutant transcripts or different competitive inhibitors, or independent analytical methods. First, we evaluated whether the role of eIF4G:PABP:eRF3 interactions in closed loop formation, and possibly ribosome recycling (Uchida *et al.* 2002), was also dependent on translation termination (Uchida *et al.* 2002). We prepared a *mini* mRNA with no stop codon and analyzed its response to cap analog in extracts derived from wild-type or termination-defective cells. Translation of nonstop*miniUAA1* in wild-type extracts showed strong cap analog resistance (Fig. 4.13, lanes 1 and 2), suggesting that conventional termination steps are not required for a stable closed loop mRNP. In contrast, *sup35-R419G* and *sup45-2* extracts programmed with nonstop*miniUAA1* RNA exhibit strong sensitivity to cap analog (Fig. 4.13, lanes 3-6), indicating that, while termination *per se* is not required, *de novo* formation of a stable closed loop structure in yeast is dependent on the principal termination factors.

Cap analog resistance or sensitivity of *miniUAA1* mRNA appears at the onset of translation

Second, since there was no requirement for termination, we considered the possibility that closed loop formation precedes the first round of mRNA translation and thus analyzed the toeprinting of *miniUAA1* mRNA after two-minute time courses of translation in wild-type or Pab1p-mutant extracts. In wild-type extracts, cap analog-resistant AUG toeprints were obtained within 30 sec of incubation with *miniUAA1* mRNA. Similarly, in *pab1-184* and *pab1-*Δ*RRM1* extracts, sensitivity to cap analog was observed at the same time point (Fig. 4.14).

Polysome profiling of ribosome:mRNA association in wild-type and mutant extracts

Third, to monitor mRNA:ribosome association by an independent method, we fractionated translation reactions by velocity sedimentation in sucrose gradients and utilized northern blotting to analyze the gradient fractions for their respective content of different mRNAs. Fig. 4.15 shows the A_{254} profile of a representative gradient. For simplicity, all fractions from the top of the gradient up to the size of 80S ribosomes were designed “non-polysomal” and the remaining part of the gradient, including mRNAs associated with one or more ribosomes, was designated “polysomal”. Application of this methodology to translation reactions incubated for 4 min in the absence of cap analog, followed by 3 min of incubation with CHX, demonstrated that 60-70% of the *miniUAA1* mRNA was distributed across the polysomal fractions in all extracts tested (Fig. 4.16(a), left panel). However, when the same reactions were supplemented with cap analog, the

mutant extracts (*pab1-ΔRRM1*, *sup35-R419G,* and *sup45-2*) displayed 2- to 4-fold less mRNA in the polysomal fractions while the distribution of mRNA in the wild-type extract showed essentially the same distribution as in the absence of the drug (Fig. 4.16(a), right panel). These data provide important additional evidence that the translation of capped and polyadenylated *miniUAA1* mRNA is resistant to cap analog in wild-type extracts, but sensitive to the drug in extracts derived from *pab1* cells or those of termination mutants. Additional experiments, in which GMP-PNP, the non-hydrolyzable GTP analog that blocks 48S to 80S conversion *in vitro*, was added at the beginning of a 5 min translation reaction showed that all extracts tested had similar distributions of the *miniUAA1* mRNA in the absence of cap analog (Fig. 4.16(b), left panel). The distributions differed from those observed in CHX-treated extracts (i.e., the relative percentage of non-polysomal mRNA was considerably higher; compare Fig. 4.16(a) and Fig. 4.16(b), left panels), but this result was expected since GMP-PNP blocks the joining of the 60S subunit to form an 80S complex (Dmitriev *et al.* 2003). Further, the addition of cap analog to the GMP-PNP-treated extracts had no significant effects on the mRNA distributions in wild-type and termination mutant extracts whereas the *pab1-ΔRRM1* mutant extract manifested a substantial shift of the *miniUAA1* mRNA to the free fractions (Fig. 4.16(b), right panel). These data suggest that, in the presence of cap analog, 48S complex formation proceeds in both the wild-type and termination mutant extracts, but not in the *pab1-ΔRRM1* extract.

Two states of the closed loop structure of mRNA can be distinguished

The previous observations are consistent with the notion that interactions between the mRNP 5' and 3' ends are established early in the translation process (Figs. 4.13 and 4.14). Hence, we sought to identify the step of translation initiation associated with closed loop formation. The toeprinting assays described above utilized CHX to stabilize the 80S ribosome on the initiator AUG (Dmitriev *et al.* 2003) and thus monitored a late step in initiation. To determine whether closed loop mRNP formation occurred earlier, we analyzed mRNA toeprints in extracts supplemented with GMP-PNP (Dmitriev *et al.* 2003). In both wild-type and *pbp1Δ* extracts, translation of *miniUAA1* mRNA in the presence of GMP-PNP gave the same results observed with CHX, namely, full resistance to 2.7mM cap analog (Fig. 4.17(a), lanes 1, 2 and 5, 6). This result implies that steps essential to establishing the closed loop phenotype occur prior to or during formation of the 48S complex.

As observed with CHX toeprinting, cap analog sensitivity of *miniUAA1* mRNA in the presence of GMP-PNP was dependent on a poly(A) tail (data not shown) and the availability of functional Pab1p and eIF4G (Figs. 4.17(a), lanes 3, 4, 7-16; and 4.17(b), lanes 5-8). However, alterations in termination factor activity yielded different toeprint phenotypes. Extracts of termination factor mutants supplemented with GMP-PNP either at the beginning of the reaction (data not shown), or after 4 min of translation, were fully resistant to cap analog and lacked the upstream toeprints detected with CHX [Fig. 4.17(c)]. Consistent with these results, sucrose gradient analyses of mRNA:ribosome association in extracts supplemented with GMP-PNP at the onset of the reaction showed no differences between the wild-type and the termination mutant extracts in the

presence or absence of cap analog while the *pab1-ΔRRM1* extract manifested a phenotype characteristic of cap analog inhibition of translation initiation [Fig. 4.16(b)]. Thus, while eRF1 and eRF3 do not appear to affect the rate of translation initiation as assayed by one-minute time courses of AUG toeprinting (in the presence of CHX) with the *miniUAA1* mRNA. (Fig. 4.18) or the formation of the closed loop mRNP that includes only the 48S complex, they are required upon 80S formation to generate a second state of the closed loop structure.

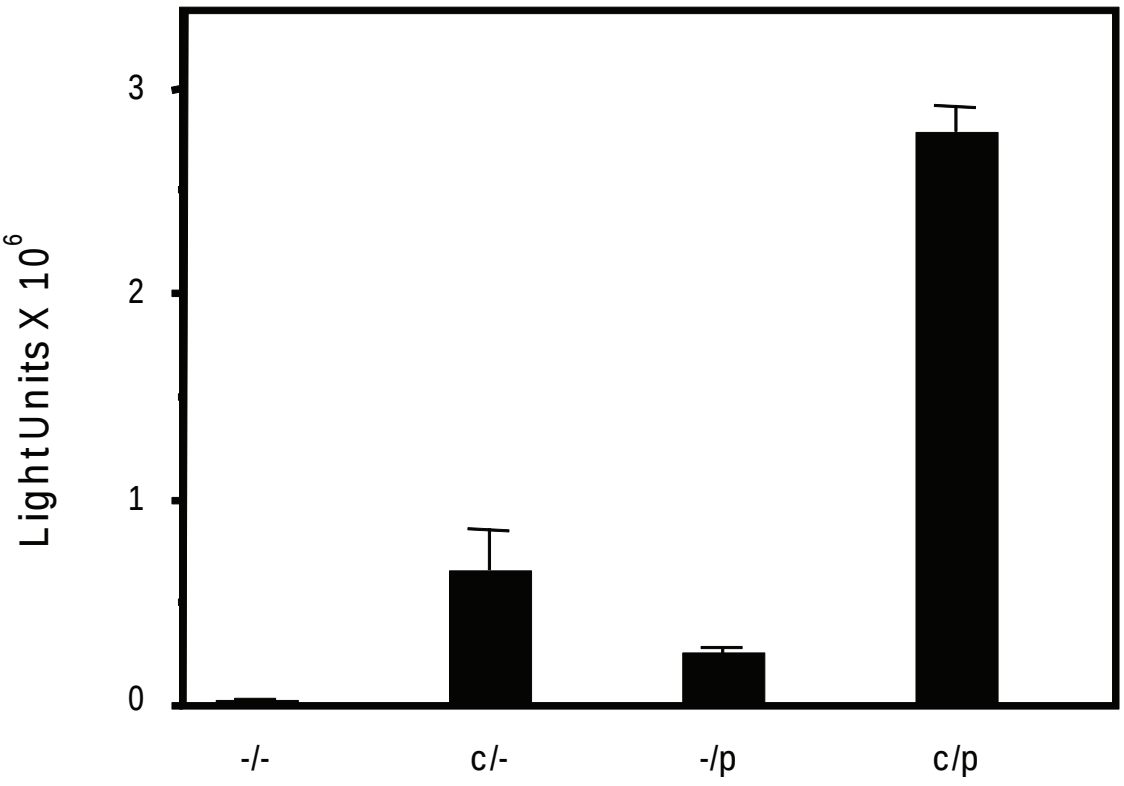

Fig. 4.1 : **Yeast cell extracts recapitulate the synergy between the cap structure and the poly(A) tail *in vitro*.** The presence of both the cap structure and the poly(A) tail stimulate translation of *LUC* mRNA in wild-type extracts.

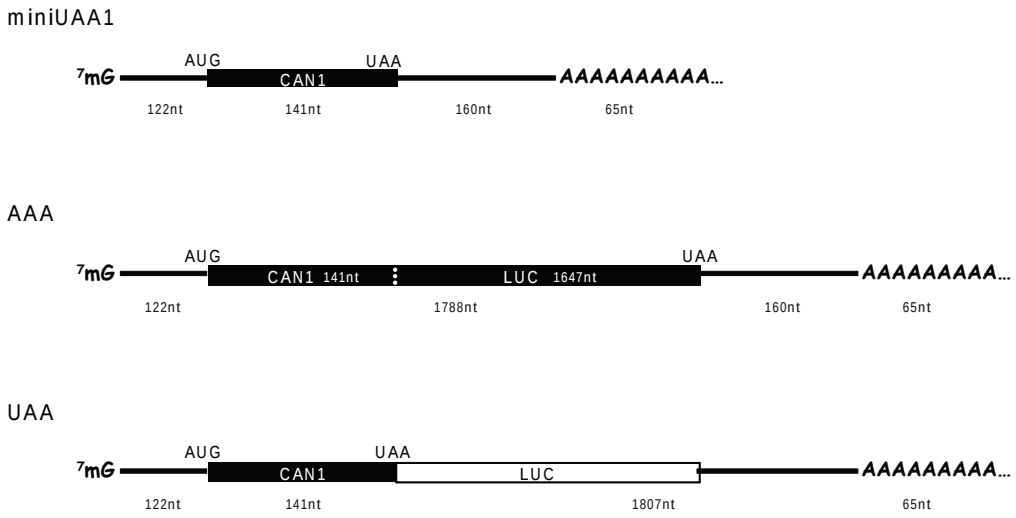

Fig. 4.2 : General schematic of the *miniUAA1*, *UAA*, and *AAA* mRNAs. Sizes (in nt) listed under each construct respectively refer to the length of the 5' UTR, the coding region, the 3' UTR, and the poly(A) tail.

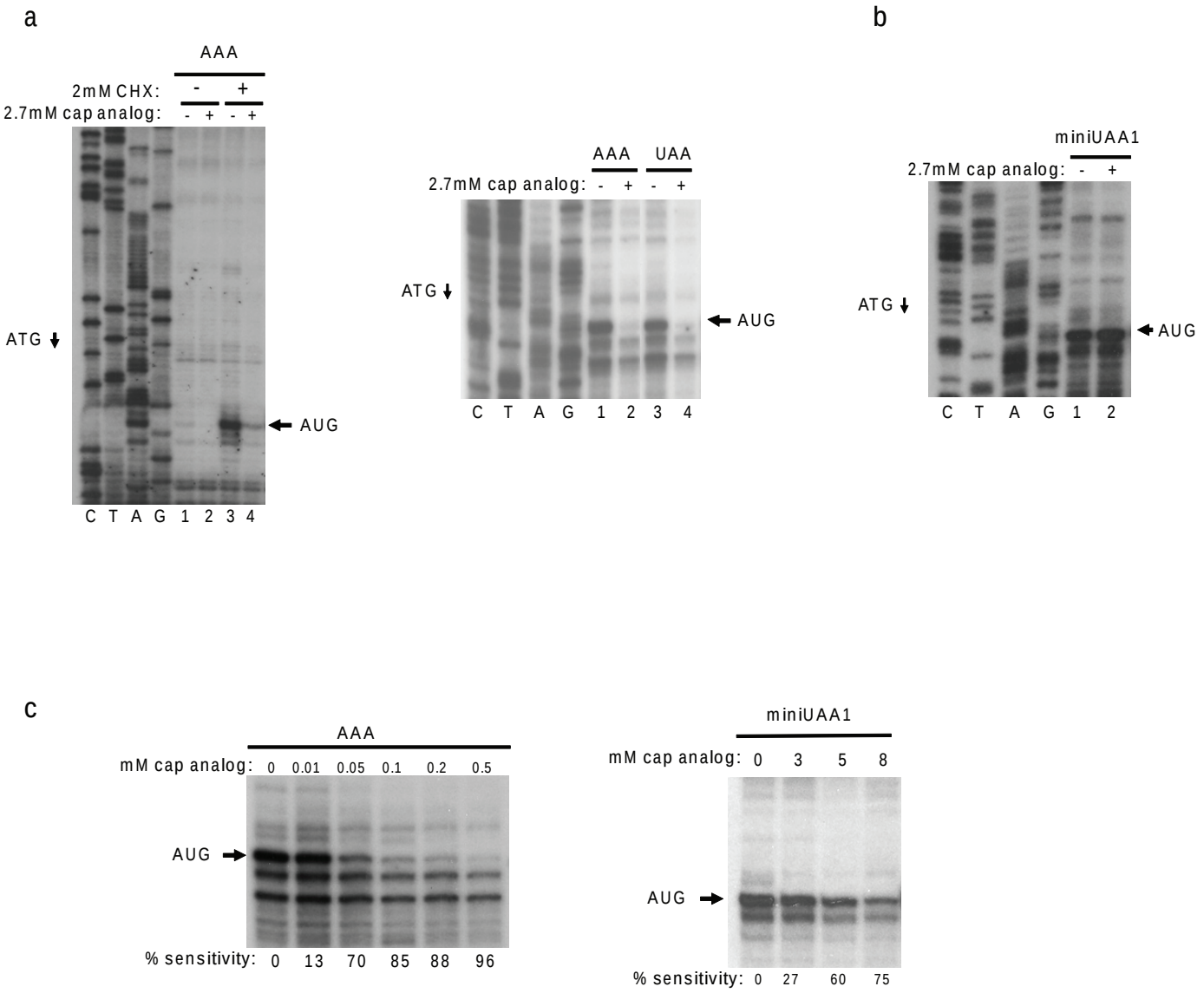

Fig. 4.3 : Toeprint analyses of initiation on long and short mRNAs in the presence of CHX in wild-type extracts. (**a**) Addition of cap analog to *AAA* (left) and *UAA* (right) mRNAs inhibits accumulation of the AUG toeprint bands. (**b**) *miniUAA1* mRNA AUG toeprints are resistant to 2.7mM cap analog. The left portions of panels in (**a**) and (**b**) show dideoxynucleotide sequencing reactions for the *AAA* or *miniUAA1* templates (with 5' to 3' sequence reading from the top to the bottom). (**c**) Cap analog sensitivities of the *AAA* (left) and *miniUAA1* (right) mRNAs.

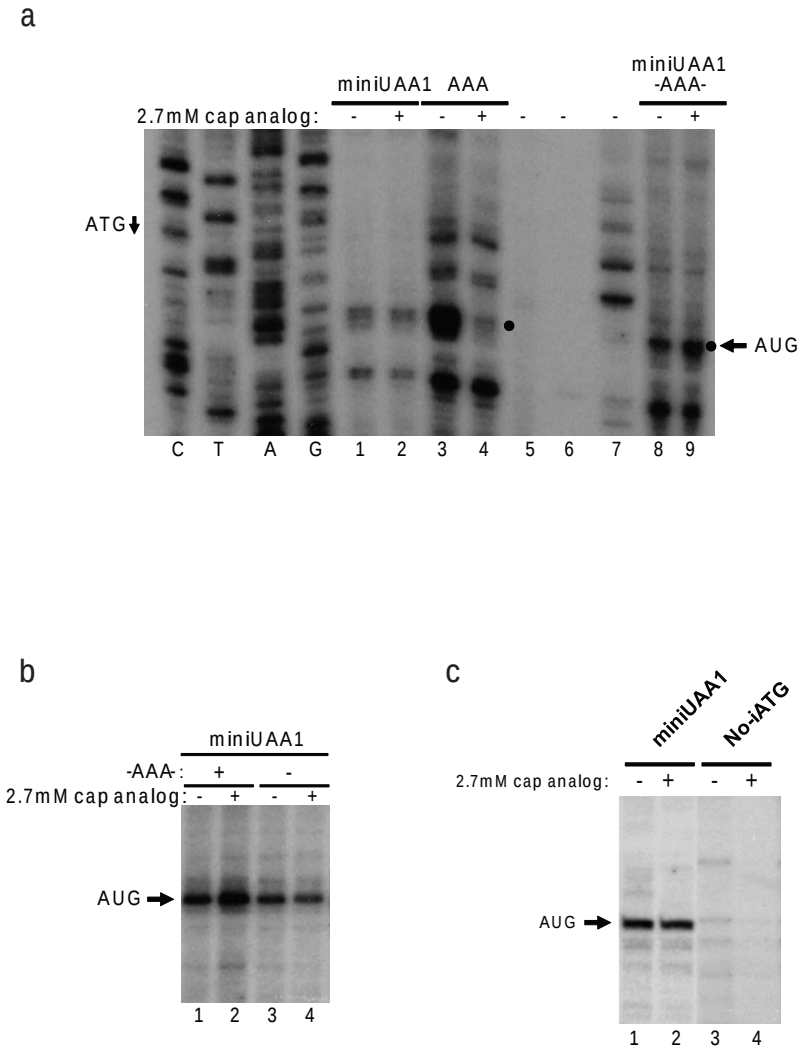

Fig. 4.4 : AUG toeprints and cap analog resistance are specific and independent of polynucleotide concentration. (**a**) Toeprinting of *miniUAA1*, *AAA*, or a mix of *miniUAA1* (10 ng) and non-capped non-polyadenylated *AAA* mRNA [-*AAA*-] (40 ng) with primer #105. (**b**) Toeprinting analyses of *miniUAA1* mRNA alone or mixed with non-capped non-polyadenylated *AAA* mRNA [-*AAA*-] using primer #55, to assay for ability of cap status of the *miniUAA1* mRNA. (**c**) Toeprinting analyses of *No-iATG* mRNA, a derivative of *miniUAA1* mRNA with a deletion of the initiator AUG codon.

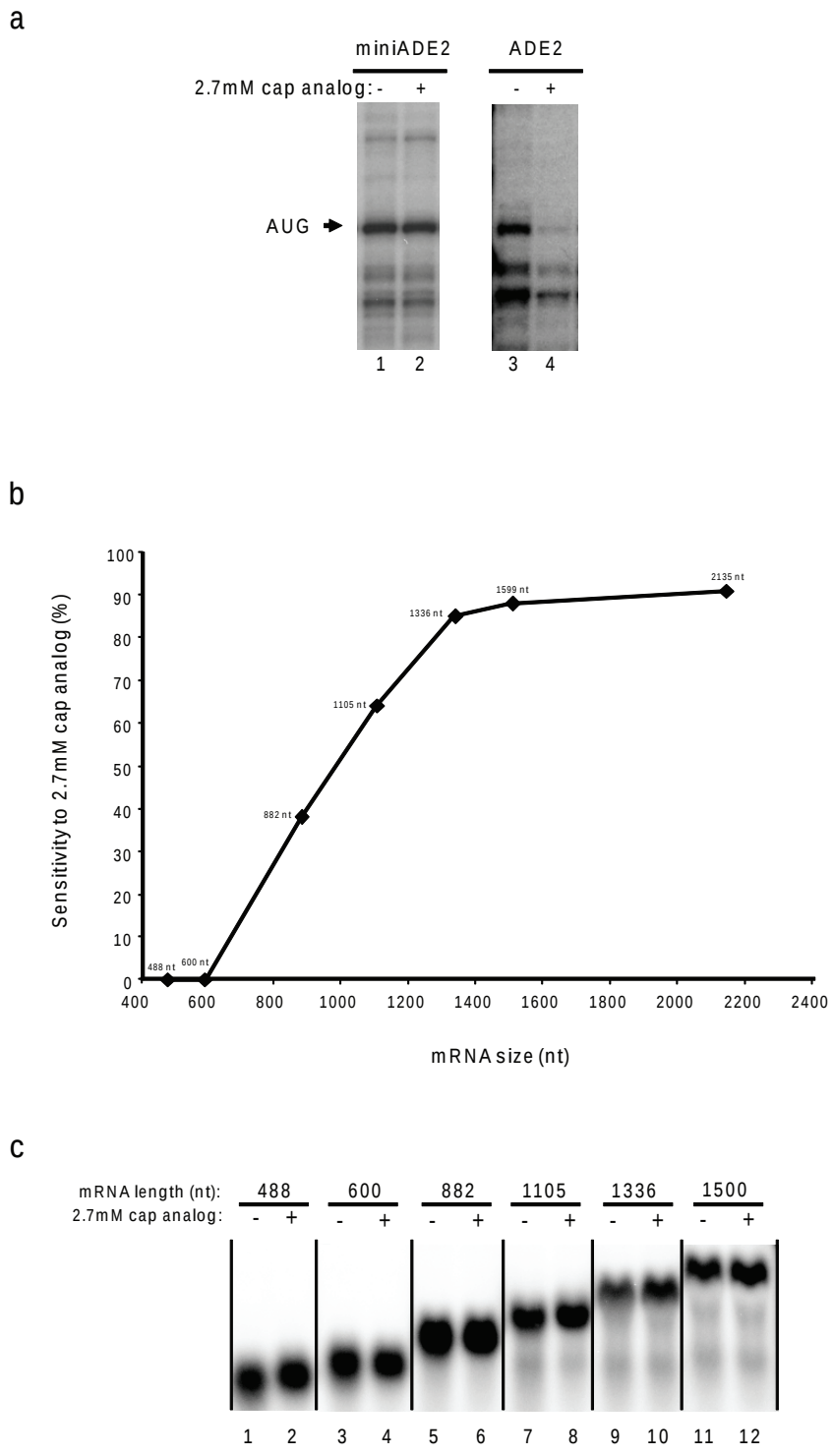

Fig. 4.5 : Cap analog sensitivity in the presence of CHX in wild-type extracts is mRNA size dependent. (**a**) Toeprinting analyses of *miniADE2* mRNA (485nt) and full-length *ADE2* mRNA (2070nt) in the presence or absence of cap analog. (**b**) Sensitivity to 2.7 mM cap analog for mRNAs of increasing length. The values on the graph are the average of two independent experiments. (**c**) Cap analog resistance depends on the size of the mRNA and the presence of a poly(A) tail. mRNAs of different sizes, monitored by northern blotting, are equally stable during translation *in vitro*.

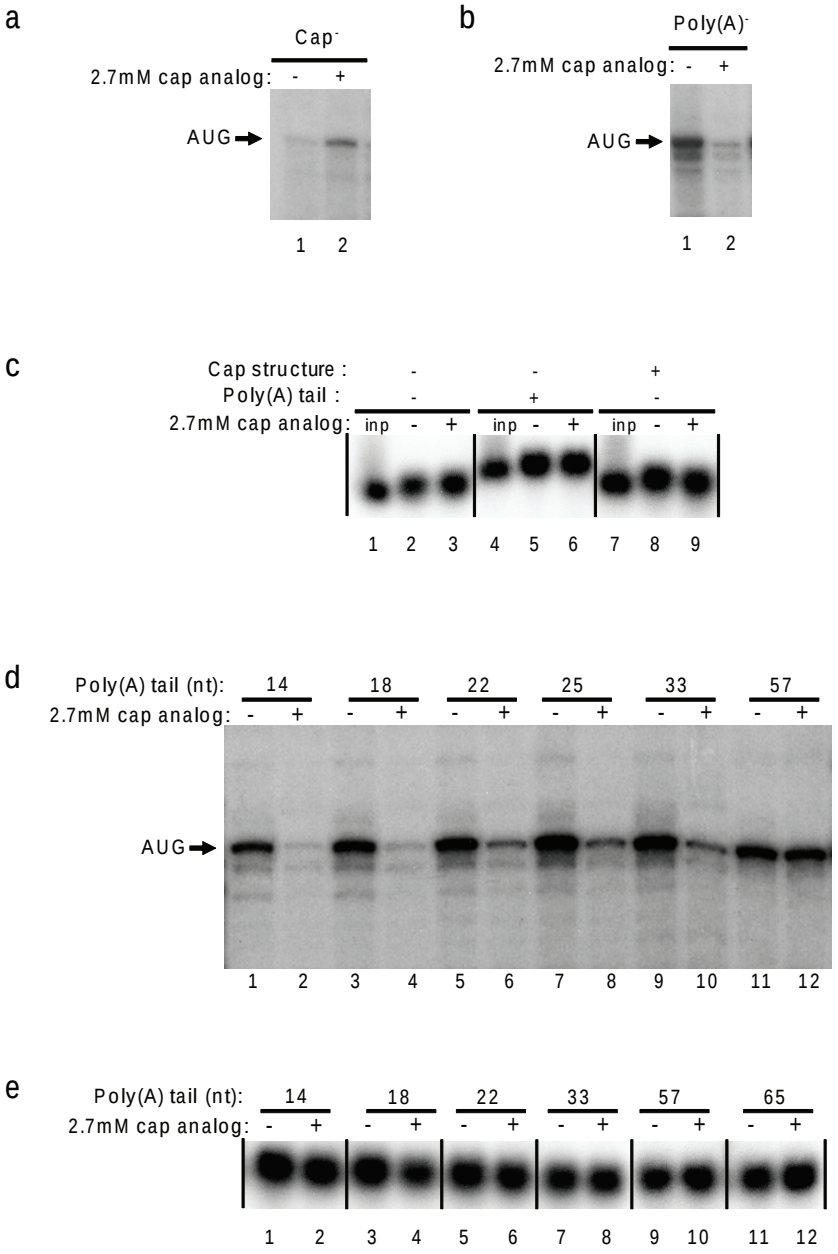

Fig. 4.6 : Cap analog resistance of the *miniUAA1* mRNA is cap and poly(A) dependent in wild-type extracts and suggests formation of a stable closed loop structure. (**a**) AUG toeprint analyses of uncapped mRNA. (**b**) AUG toeprint analyses of poly(A)-deficient mRNAs. (**c**) Northern blot of *miniUAA1* mRNAs containing either a cap structure or poly(A) tail, or both, after translation *in vitro*. (**d**) AUG toeprint analyses of *miniUAA1* mRNAs with poly(A) tails of differing sizes. (**e**) Northern blot of *miniUAA1* mRNAs with different poly(A) tail lengths translated *in vitro*.

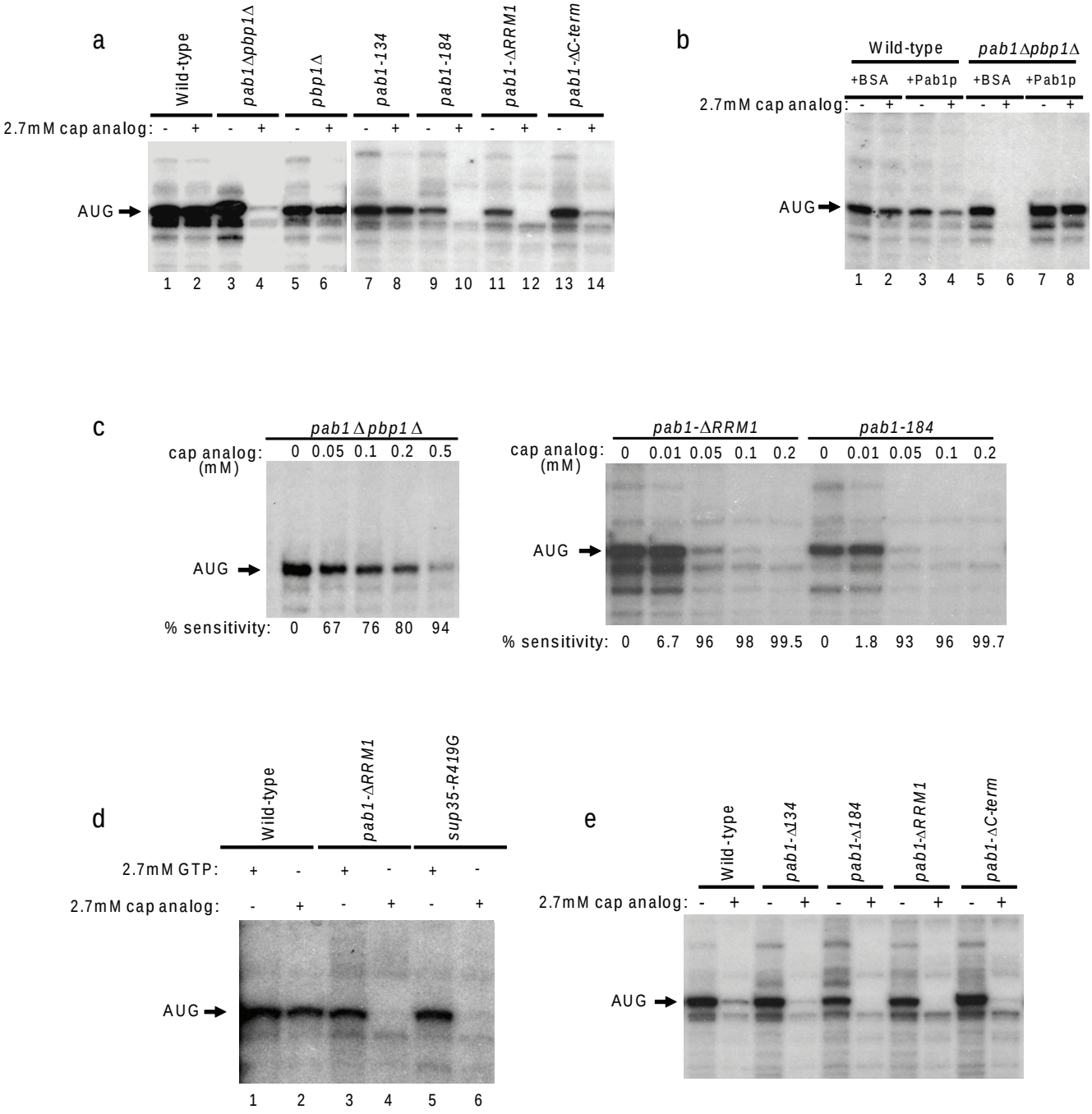

Fig. 4.7 : Formation of a stable closed-loop structure on a capped and polyadenylated mRNA in the presence of an 80S complex requires Pab1p interactions with eIF4G, mRNA, and Sup35p. (**a**) Toeprinting analyses of *miniUAA1* mRNA in Pab1p-defective, wild–type, or *pbp1Δ* extracts. (**b**) Toeprinting analyses of *miniUAA1* mRNA after the addition of recombinant Pab1p to *pab1Δpbp1Δ* extracts. (**c**) Toeprinting analyses of cap analog sensitivities of *miniUAA1* mRNA in Pab1p-defective extracts. (**d**) Toeprinting analyses of *miniUAA1* mRNA in the presence of excess GTP. (e) Toeprinting analyses of poly(A)- *miniUAA1* mRNA translated in wild-type or *pab1* extracts.

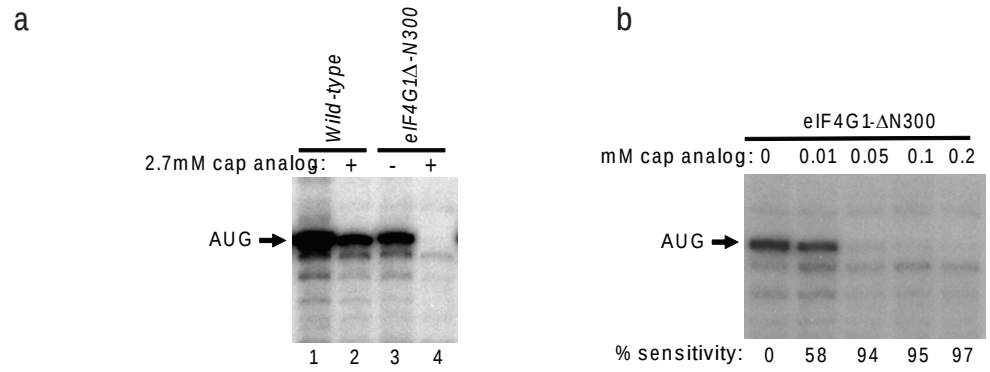

Fig. 4.8 : Formation of a stable closed-loop structure on a capped and polyadenylated mRNA in the presence of an 80S complex requires Pab1p interactions with eIF4G. (**a**) Toeprinting analyes of *miniUAA1* mRNA in the *eIF4G1Δ-300* mutant incapable of Pab1p interaction. (**b**) Toeprinting analyes of sensitivity to cap analog in the *eIF4G1Δ-300* mutant incapable of Pab1p interaction.

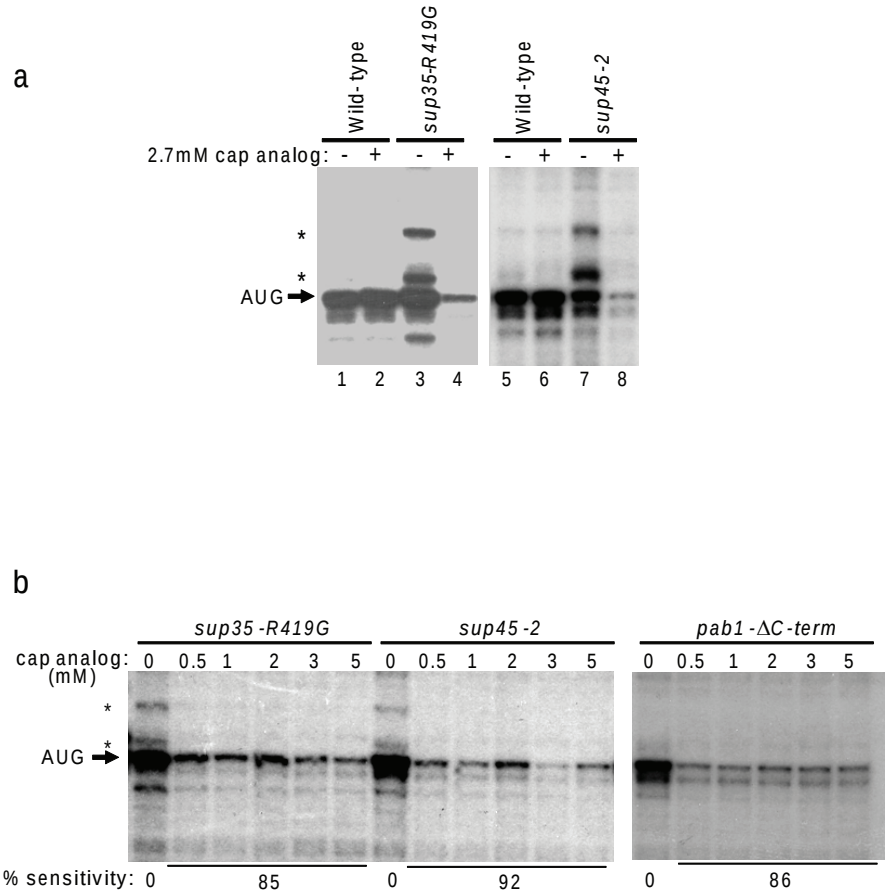

Fig. 4.9 : Formation of a stable closed-loop structure on a capped and polyadenylated mRNA in the presence of an 80S complex requires Sup35p. (**a**) Toeprinting analyses of *sup35-R419G* and *sup45-2* mutants show sensitivity to cap analog and additional toeprint bands upstream of the initiator AUG. (**b**)Toeprinting analyses of with differening concentrations of cap analog in *sup35-R419G* and *sup45-2* mutants show sensitivity to cap analog and additional toeprint bands (*) upstream of the initiator AUG.

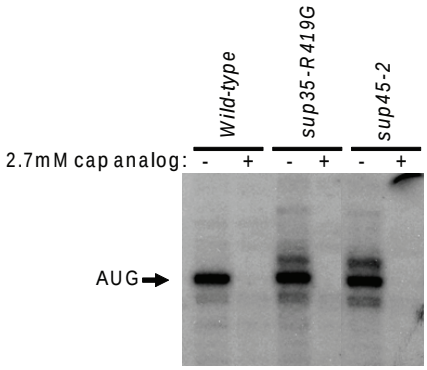

Fig. 4.10 : Cap analog resistance depends on the presence of a poly(A) tail. Toeprinting analyses of poly(A)$^-$ *miniUAA1* mRNA translated in termination-defective extracts.

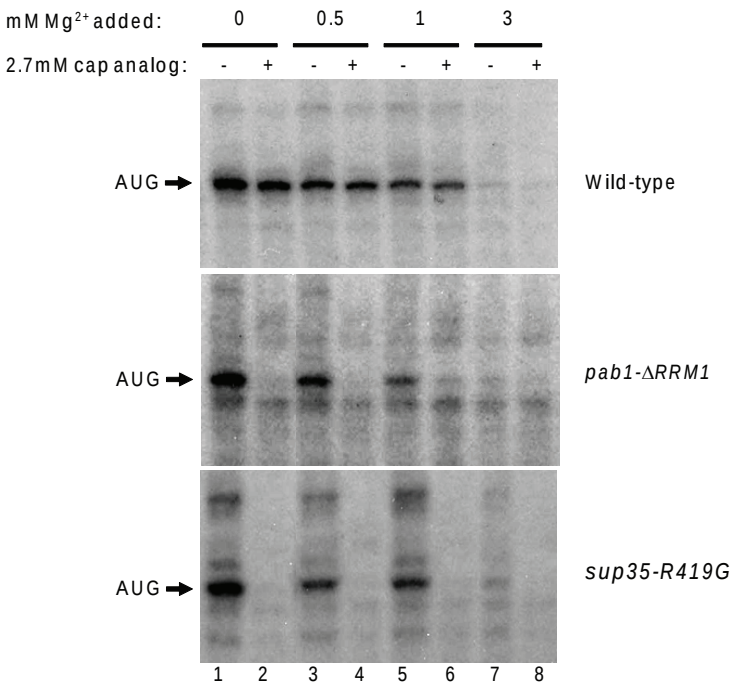

Fig. 4.11 : Increased Mg^{2+} concentration does not affect sensitivity or resistance to cap analog in different extracts. Toeprinting analyses of wild-type, *pab1*-defective, or eRF3-defective extracts in the presence of increasing magnesium concentration.

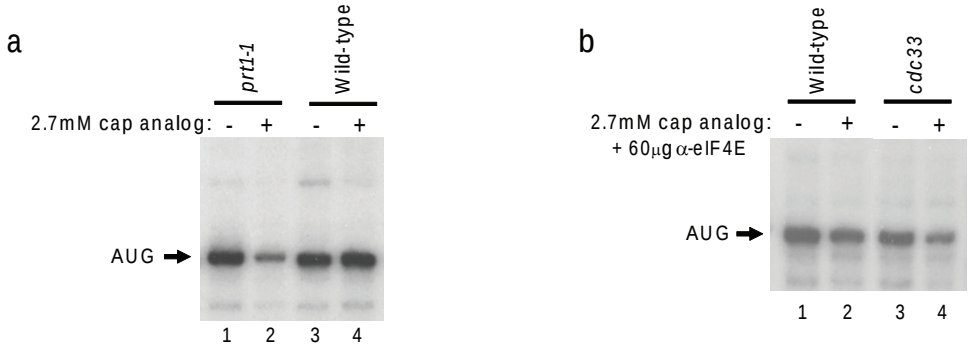

Fig. 4.12 : Toeprinting analyses of *miniUAA1* mRNA in initiation-defective extracts. (**a**) Sensitivity to cap analog in *prt1-1* extracts heated to 35°C. (**b**) Sensitivity to cap analog in *cdc33* extracts supplemented with anti-eIF4E antibodies.

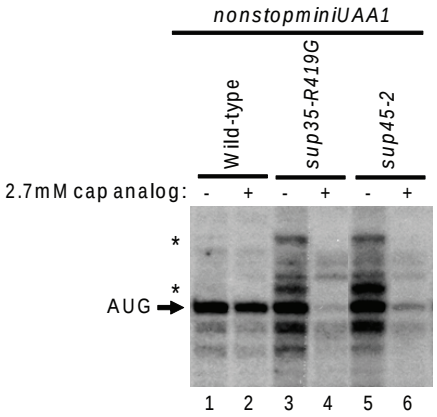

Fig. 4.13 : Sensitivity to cap analog is independent of the termination event. Toeprint analyses pf wild-type or termination-defective extracts programed with the *nonstopminiUAA1* mRNA that lacks a stop codon.

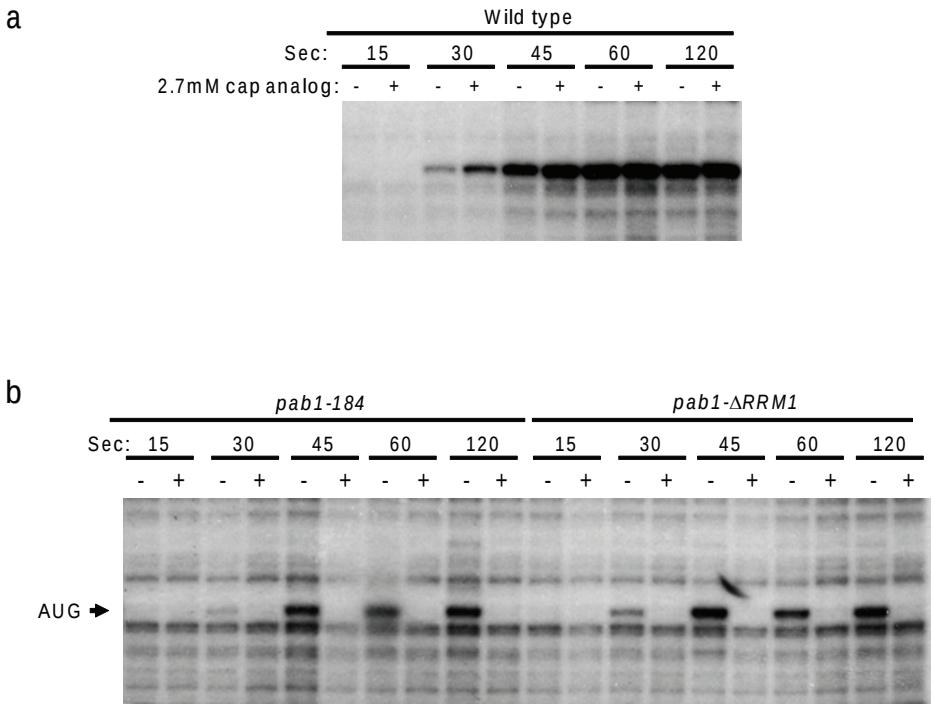

Fig. 4.14 : Cap analog resistance or sensitivity of the *miniUAA1* mRNA appears at the onset of translation. Toeprint analyses of the the *miniUAA1* mRNA translated for upto two minutes in wild-type (**a**) or *pab1* mutants (**b**).

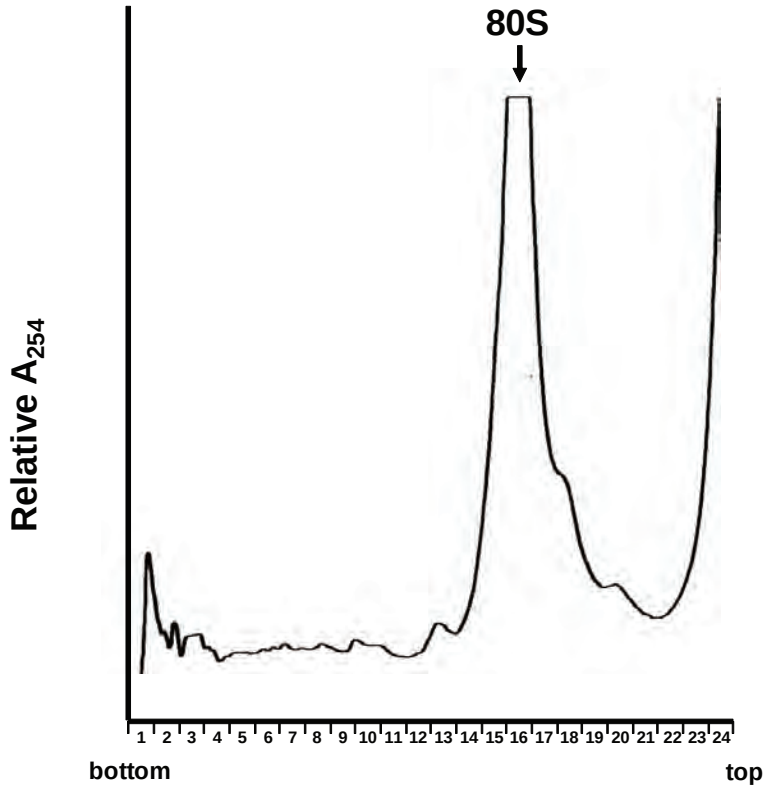

Fig. 4.15 : Typical polysome profile of an extract after micrococcal nuclease treatment and translation of the *miniUAA1* mRNA. Numbers on the X-axis represent fractions collected in decreasing order of density, such that “bottom” corresponds to the heaviest and “top” to the lightest fractions.

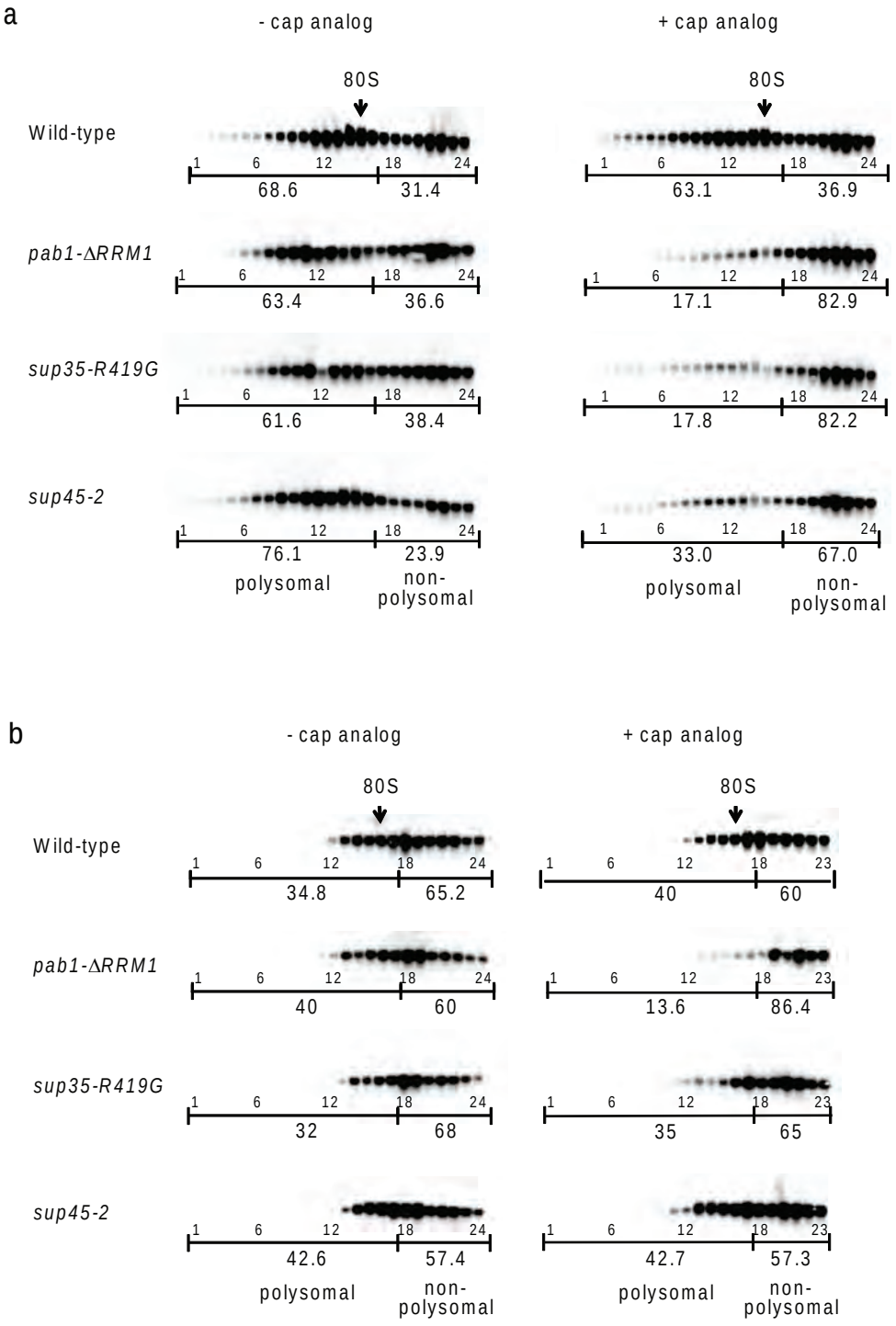

Fig. 4.16 : Translation of the *miniUAA1* mRNA as assayed by sucrose density centrifugation and northern blot analysis. Sucrose gradient fractionation of *miniUAA1* mRNA translated in wild-type and mutant extracts in the absence and presence of cap analog, and in the presence of CHX (**a**) or GMP-PNP (**b**). The values above the horizontal line depict fraction numbers and those below the line denote the respective percentages of mRNA associated with polysomal or non-polysomal fractions.

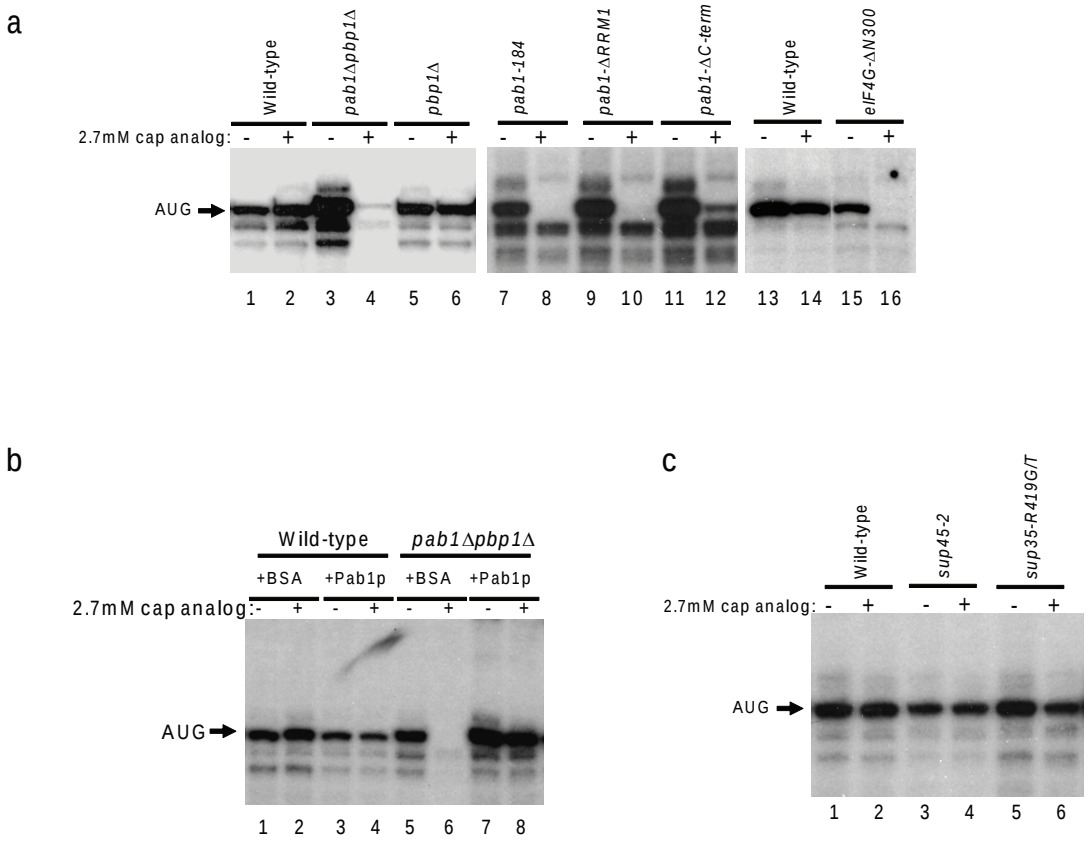

Fig. 4.17 : Stabilization of the closed-loop structure on a capped and polyadenylated mRNA in the presence of a 48S complex requires Pab1p interactions with eIF4G and *miniUAA1* mRNA. (**a**) Toeprinting analyses of extracts from Pab1p- and eIF4G1-deficient strains in the presence of GMP-PNP. (**b**) Toeprinting analyses of resistance to cap analog in *pab1Δpbp1Δ* extracts in the presence of GMP-PNP after addition of recombinant Pab1p. (**c**) Toeprinting analyses of *sup35-R419G* and *sup45-2* termination mutant extracts in the presence of GMP-PNP.

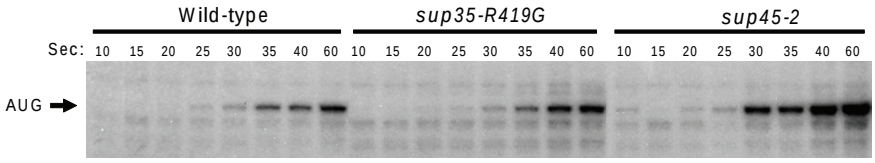

Fig. 4.18 : Termination-defective extracts manifest normal rates of ribosome recruitment. Toeprint analyses of the the *miniUAA1* mRNA translated for upto one minute in wild-type or termination-defective extracts.

Chapter V

Discussion

Chapter V - Discussion

Elaborating the “closed loop” model

The 5' cap and 3’ poly(A) tail act synergistically to promote the stability and translatability of an mRNP (Mangus *et al.* 2003). Here we show that both elements are required for optimum translation of a synthetic mRNA in our cell-free translation system (Fig. 4.1), supporting the idea that the 5' cap and 3’ poly(A) tail of an mRNA may exert this effect by forming a closed loop structure (Jacobson 1996), evidence for which has also been provided by electron microscopy (Wells *et al.* 1998; Kopeina *et al.* 2008). Most evidence for the presence of a circularized mRNP structure comes from evaluations of reporter RNAs lacking certain *cis* elements to be expressed in translation systems under different conditions (Munroe and Jacobson 1990; Gallie 1991). These data, although informative, are the end result of polypeptide synthesis and release and are indirect measures of structural aspects of events leading up to the expression of the reporter RNAs. In order to more easily monitor and characterize the formation of a circularized mRNA and early events in the translation cycle, we developed a toeprinting assay that allowed us to visualize 80S ribosomes that initiate translation on a synthetic reporter mRNA *in vitro* (Figs. 4.3-4.5). Translation of a long mRNA demonstrated sensitivity to cap analog as expected, suggesting that the drug is able to effectively compete for binding of the eIF4E cap-binding protein to the 5’ cap of the mRNA, resulting in disruption of the closed loop, and reduced translation initiation (leading to the loss of the AUG toeprint). On the other hand, a short mRNA was resistant to the

loss of the AUG toeprint at a similar cap analog concentration (Fig. 4.3-4.5), suggesting that decreasing the length of an mRNA may allow a tighter interaction of eIF4E to the capped mRNA and possibly the formation of a stronger closed loop, an idea supported by testing mRNAs of varying lengths for cap analog sensitivity (Fig. 4.5). Polysome profiling experiments showed that this cap analog resistance correlated well with the ability of the mRNA to be translated (Fig. 4.16). The idea of a closed loop being formed was supported by the observations that cap analog resistance was dependent on the mRNA containing a poly(A) tail (Fig. 4.6 and 4.10), the presence of Pab1p capable of interacting with eIF4G (Fig. 4.7), eIF4G capable of interacting with Pab1p (Fig. 4.8), eIF3 (Fig. 4.12), and eIF4E (Fig.4.12), all of which support earlier observations (Munroe and Jacobson 1990; Jacobson 1996; Tarun and Sachs 1996; Wells *et al.* 1998; Sachs 2000), except that we were able to more clearly define the requirement for at least two molecules of Pab1p to be associated with the mRNA [Fig. 4.6(d)]. Surprisingly, we observed a requirement for the eRF1 and eRF3 translation termination factors in maintaining this 80S-dependent cap analog-resistance phenotype even though a termination event *per se* did not appear to be required (Fig. 4.13). Accordingly, a *pab1* mutant deleted for its eRF3 binding domain was also susceptible to the effects of cap analog (Fig. 4.7) suggesting that eRF association with the “closed loop complex” may be mediated through Pab1p interaction. Further inquiry into what stages of translation initiation were dependent on the presence of the eRFs demonstrated that two forms of the stable closed loop structure can be distinguished during initiation on short mRNAs *in vitro*. The integrity of both forms requires the mRNA cap and poly(A) tail, as well as eIF4E, eIF4G, Pab1p, and eIF3, and is dependent on the length of both the mRNA and

the poly(A) tail. The first requires the preinitiation 48S complex but not eRF1 and eRF3 (Figs. 4.16 and 4.17), whereas the second is formed after 60S joining and requires the two eRFs as well as all the other components of the first structure. An intriguing possibility is whether the Pab1p-eRF1-eRF3 complex present as part of the closed loop structure maintains a local pool of termination factors in the vicinity of the normal termination codon thus enabling the rapid and highly efficient termination events thought to occur at normal terminators. The requirement for at least two molecules of Pab1p for cap analog resistance of the small mRNAs suggests that Pab1p interaction with both eIF4G and eRF3 simultaneously contributes to maintaining the strength of the closed loop. This hypothesis predicts that Pab1p-eRF3 interaction may confer protection of the poly(A) tail from deadenylation and disruption of the loop. Indeed, overexpression of a Pab1p-interacting N-terminal fragment of eRF3 decreases the rates of deadenylation of a reporter mRNA in yeast and mammalian cells (Hosoda *et al.* 2003; Funakoshi *et al.* 2007). Further analyses demonstrated that eRF3 mediated deadenylation through the Pan2p-Pan3p and Caf1p-Ccr4p deadenylases in yeast and human cells and that eRF3 binding to PABPC1 was in competition with hPan2-hPan3 in a manner that was translation-dependent (Funakoshi *et al.* 2007). These findings are consistent with a model wherein eRF1 and eRF3 are present as part of a stable closed loop complex and also act to antagonize deadenylase activity through their interaction with Pab1p. Moreover, the efficiency with which ribosomes at the normal termination codon undergo termination events, including subunit dissociation and possibly subunit recycling to the 5’ end, may be enhanced by the proximity and ready availability of the closed loop-associated eRFs (Fig. 5.1).

One can also imagine that usage of such localized eRFs in translation termination may allow their dissociation from Pab1p (and the closed loop complex), leading to a change in mRNP structure that would allow deadenylases to access the poly(A) tail through an interaction with Pab1p. This event may be further regulated by other 3'-UTR-associated factors or recruitment of additional molecules of eRF1 and eRF3 to maintain closed loop stability and continued translation termination efficiency. Thus, deadenylation mediated by eRF cycling would require active translation and termination to allow dissociation of the eRFs, and the ability of the cytoplasmic deadenylases to interact with Pab1p would be in direct competition with factors (such as eRF3) that prevent that association.

Normal and premature termination are biochemically distinct events

In light of the closed loop model, it is not inconceivable that distal sequences and factors bound to them can influence events occurring at more upstream locations on an mRNA. As suggested by the *faux* 3'-UTR model (Jacobson and Peltz 2000; Maderazo *et al.* 2003), proper termination of translation and normal rates of mRNA decay are likely to require interactions between a terminating ribosome and a specific RNP structure or set of factors (including Pab1p and Sup35p) localized 3' to the stop codon. Some of the evidence for this model is based on studies examining the effects of PTC positioning with respect to the normal terminator, and by observing decay phenotypes of mRNAs that eliminate sequences between a PTC and the 3'-UTR (Losson and Lacroute 1979; Peltz *et al.* 1993; Hagan *et al.* 1995; Yun and Sherman 1995; Zhang *et al.* 1995). In our studies, we utilized a tethering approach to show that localizing Pab1p in the vicinity of

an otherwise NMD-sensitive PTC stabilized the nonsense-containing mRNA (Fig. 2.11). Since the tethered Pab1p coimmunoprecipitated with eRF3 (Fig. 2.12), it was possible that part of Pab1p's role might be to stabilize eRF3 on the terminating ribosome to effect efficient termination (Hoshino *et al.* 1999; Cosson *et al.* 2002). Indeed, tethering eRF3, but not eRF1, was able to stabilize the nonsense reporter mRNA, although not to the extent that tethering Pab1p did (Fig. 2.13). Thus, decreasing the physical distance between an NMD-sensitive stop codon and 3'-bound Pab1p leads to the nonsense codon being regarded as normal. It has now been demonstrated that this phenomenon is not limited to yeast and can occur in a wide variety of organisms (Behm-Ansmant *et al.* 2007; Eberle *et al.* 2008; Silva *et al.* 2008; Singh *et al.* 2008).

Given that differential mRNA stability effects arise when a stop codon is located at a "normal" *vs.* "premature" position, we speculated that there might be differential effects on translation termination at each of those positions. Our results indicated that not all termination events are equivalent, a notion that is further strengthened by the recent discovery of a small molecule drug (ataluren) that is specifically able to elicit readthrough of premature, but not normal, nonsense codons both *in vitro* and *in vivo* (Welch et al. 2007). Utilizing our *in vitro* translation/toeprinting system, we found that termination at a PTC was aberrant, occurring more inefficiently, and could be toeprinted (Fig. 2.2), whereas no toeprints could be observed for termination codons located at their "normal" positions in an mRNA (Fig. 2.2). The latter could be toeprinted if eRF1 (sup45p) was defective (Fig. 2.10), reflecting the ability of wild-type terminating ribosomes to dissociate rapidly at a normal stop codon. The addition of CHX to the translation reactions resulted in an interesting phenomenon – the repositioning of the

ribosome at nearby AUGs (Figs. 2.3 and 2.7). Since the newly positioned ribosomes appeared to arise from ribosomes that had previously been positioned at the PTC [Fig. 2.3(c)] this phenomenon was indicative of post-termination reinitiation (Fig. 2.5). Based on reinitiation models for the *GCN4* mRNA (Hinnebusch 2005), it is likely that upon termination at a PTC, dissociation of the 60S subunit takes place, leaving the 40S subunit to scan for a nearby start codon. The observed retro-reinitiation as well as normal reinitiation phenotypes suggest that the ribosomal subunit is able to oscillate back and forth for varying distances until it encounters an AUG codon from which to reinitiate (Figs. 2.5-2.7). This aberrant post-termination event is somehow related to NMD, since ribosomes could not reinitiate in the absence of Upf1p (Figs. 2.3 and 2.5). The latter event must only be a symptom of aberrant termination, not a cause of NMD, because elimination of reinitiation site AUGs does not alter the decay rate of nonsense-containing mRNAs (data not shown). However, the failure to effectively release a terminating ribosome may be a stimulus for NMD, promoted, perhaps, by the ribosome's failure to recycle in *cis* (Uchida *et al.* 2002) and/or by the recruitment of Upf1p to the aberrant termination event or to a bound negative regulatory factor. At a minimum, the absence of aberrant termination toeprints in extracts prepared from *upf1Δ* cells links aberrant termination to NMD, and suggests that inactivation of this factor may preclude or perturb events that regulate ribosome stability and movement at a premature stop codon. The *in vivo* implications of the *in vitro* retro-reinitiation phenotype are still unclear. Whether or not such backward movements of ribosomes occur in a physiological context remains to be tested, but one can envision that retro-reinitiation coupled to subsequent in-frame premature termination could serve to amplify an NMD-

triggering signal for a given mRNA. A caveat to this hypothesis is the presence of 80S ribosomes upstream of the post-termination scanning 40S subunit. However, evidence suggesting that nonsense substrates may be translationally repressed *in vivo* (Muhlrad and Parker 1999) may preclude this obstacle.

In light of these observations, a slightly revised *faux* 3'-UTR model suggests that at a PTC, the absence of proximal Pab1p leads to inefficient termination and stable binding of the Upf proteins, which are prerequisites for decapping and subsequent Xrn1p-mediated degradation. In yeast, the mechanism of Upfp recruitment at PTC is still unclear. Of the several models that have been put forth, one posits that Upf2p/Nmd2p and Upf3p associate with nonsense substrates only after Upf1p-mediated localization to P bodies (Sheth and Parker 2006).

Finally, it is unlikely that the mechanism of NMD is fundamentally different in yeast and metazoans. The demonstration of a role for PTC-proximal PABPC in antagonizing NMD suggests a common underlying mechanism for nonsense recognition in eukaryotes (Behm-Ansmant *et al.* 2007; Eberle *et al.* 2008; Silva *et al.* 2008; Singh *et al.* 2008). Metazoans have probably evolved a more extensive regulatory mechanism to take into account additional steps of gene expression, such as splicing, to ensure that only correctly processed transcripts get expressed (Kawashima *et al.* 2009). If aberrant termination is also the trigger for NMD in higher organisms, Upf1p associated with the SURF complex may be stably associated with the termination complex in the absence of proximal PABPC (Kashima *et al.* 2006). The exon-junction complexes (EJC) deposited during splicing of mammalian pre-mRNAs may not reflect a specialized mRNA decay apparatus poised for activation in an early round of translation (Le Hir *et*

al. 2000; Kim *et al.* 2001; Gatfield *et al.* 2003; Gehring *et al.* 2003; LeBlanc and Beemon 2004). Rather, the EJC factors may function like the proteins associated with a normal 3'-UTR in yeast and render an mRNA competent for proper translation when present in an appropriate context and may serve to mediate NMD by enhancing translation of the substrate mRNAs (Nott *et al.* 2004). Alternatively, the EJC may act as a mark to enhance NMD (Stalder and Muhlemann 2008) through the associated Upf2p and Upf3p. In support of this model, it has been shown that that certain mRNAs undergo EJC-independent NMD that is dependent on the distance between the termination codon and the poly(A) tail (Buhler *et al.* 2006). Additionally, even though Upf2p and Upf3p are associated with the EJC and are known to promote phosphorylation of Upf1p, a necessary step for Upf1p function in metazoans, there exist examples of NMD occurring in a Upf2p- or Upf3p-independent manner (Gehring *et al.* 2005; Chan *et al.* 2007).

A role for Upf1p in translation

Results from both yeast and mammalian cells have implicated possible roles for Upf1p, Upf2p/Nmd2p, and Upf3p in the regulation of translational termination, repression, and reinitiation (Czaplinski *et al.* 1998; Muhlrad and Parker 1999; Maderazo *et al.* 2000; Wang *et al.* 2001; Isken *et al.* 2008; Ivanov *et al.* 2008). To consider the possible general translational involvement of these factors in yeast, we sought to examine whether the *in vitro* results supporting a Upfp role in translational reinitiation in Chapter II could be recapitulated *in vivo.* Using a series of *PGK1/LUC* reporter constructs, we defined a cell-based assay in which approximately 2.5% of the ribosomes that prematurely terminate the *PGK1* ORF subsequently reinitiate and

translate the *LUC* ORF. Relative to wild-type cells, strains that lacked the function of any one of the three *UPF* genes manifested markedly reduced reinitiation activity in this assay [Fig. 3.1(d)], but reinitiation *per se* played no role in activating NMD (Fig. 3.3). These observations not only served to confirm and elaborate the earlier results we had obtained in cell-free extracts (Chapter II), but led us to investigate in greater detail the mechanism by which the Upf proteins influence translational activity.

Prior studies indicated that Upf1p regulation of translation might not be limited to nonsense-containing mRNAs. For example, yeast cells expressing WT-like ("normal") *CUP1* reporters showed reduced Cup1p levels when *UPF1* was deleted (Muhlrad and Parker 1999). Further, *in vitro* translation of synthetic *CAN1/LUC* (WT) mRNA in yeast extracts was found to require Upf1p (Chapter II), and mammalian cell-free extracts containing hyperphosphorylated Upf1p showed reduced translation of synthetic *Renilla LUC* mRNA (Isken *et al.* 2008). Consistent with these observations, we not only confirmed that optimal translation of the *CAN1/LUC* mRNA is Upf1p-dependent, but that Upf2p/Nmd2p and Upf3p are also required (Fig. 3.4 and data not shown). Moreover, using a novel assay for ribosome reutilization, we found that elimination of any one of the Upf proteins led to reduced translation initiation on *CAN1/LUC* mRNA (Fig. 3.4(d) and data not shown). The significance of these results was underscored by the observation that the translational defect(s) of *upf1*Δ extracts could be overcome by the addition of purified recombinant Upf1p (Figs. 3.5 and 3.8). Collectively, these experiments suggested that Upf1p plays a direct role in regulating the initiation efficiency of ribosomes that enter a new cycle of translation.

A further understanding of the apparent initiation defect was obtained by attempting to identify the stage of initiation that was impaired. Toeprinting analyses of the *CAN1/LUC* initiator AUG codon indicated that although *upf1Δ* extracts had fewer 80S ribosomes at the AUG than did WT extracts, the two extracts exhibited similar 40S recruitment, suggesting that a loss of Upf1p affects subunit joining (Fig. 3.6). Indeed, the addition of purified WT 40S or 60S ribosomal subunits to *upf1Δ* extracts stimulated translation in these extracts, but not in WT extracts [Fig. 3.9(a)]. Further analyses showed that Upf1p was preferentially associated with 40S subunits suggesting that enhanced translation observed upon 40S addition may in part be due to the bound Upf1p [Fig. 3.9(b)]. In combination with the toeprinting results, these data implied that: i) the increase in luciferase activity detected upon addition of 40S subunits to *upf1Δ* extracts was most likely Upf1p-mediated and ii) the stimulation of translation occurring in *upf1Δ* extracts upon addition of 60S subunits was probably attributable to the accumulation of inactive 60S subunits in those extracts.

It is becoming increasingly apparent that factors involved in regulating translation may have multiple functions and that this multitasking may link the initiation pathway to those for termination and/or NMD (Amrani *et al.* 2008; Saini *et al.* 2009). Moreover, it has been shown that: i) eIF3, eIF1, and eIF1A, as well as the eIF3j subunit, not only play a role in initiation, but also stimulate the *in vitro* dissociation of post-termination 80S complexes (Pisarev *et al.* 2007); ii) at elevated temperatures, yeast strains harboring the temperature-sensitive *prt1-1* mutation (in eIF3) lose their abilities to both initiate translation and promote NMD (Welch and Jacobson 1999); iii) yeast cells with mutations in both *SUI1* (encoding eIF1) and *UPF1* manifest synthetic lethality (Harger and Dinman

2004); and iv) phosphorylated mammalian Upf1p can interact with eIF3 and this interaction appears to inhibit cap-dependent *in vitro* translation (Isken *et al.* 2008). Consistent with these observations, we find that yeast *upf1Δ* extracts are unable to recycle ribosomes efficiently from a nonsense-containing mRNA (Figs. 3.7 and 3.8), a result suggesting that events at termination can influence the subsequent activity of ribosomal subunits. Since our *in vitro* translation system does not support NMD (e.g., see Fig. 3.8(b) and Chapter II), we hypothesize that Upf1p's role in promoting ribosome dissociation and/or recycling from nonsense-containing mRNAs represents an independent function that occurs concurrently or prior to its role in promoting decapping (Fig. 5.2). How these events may be linked remains to be elucidated. Since premature termination in yeast is considerably less efficient than normal termination (Chapter II), one possibility is that the post-peptide hydrolysis recruitment of eIF3, and perhaps other initiation factors, to a prematurely terminating ribosome is Upf1p-dependent and that inclusion of Upf1p allows termination complex remodeling and efficient 80S dissociation, yielding a 40S subunit capable of reinitiating translation and a 60S subunit capable of being primed for subsequent translation cycles. It remains to be seen whether Upf1p that copurifies with 40S subunits reflects a cause or consequence of ribosome dissociation, whether other NMD factors show a similar association with ribosomal subunits, and what other factors may be present in a Upfp-dependent manner. Upf1p has intrinsic ATPase and helicase activities (Czaplinski *et al.* 1995) and it will be of interest to test whether these activities are required for ribosome remodeling at a premature termination codon or for the stimulation of decay. An additional question that has remained unanswered is the fate of the released polypeptide upon premature

termination. Recent work in yeast has revealed that Upf1p-dependent, proteasome-mediated degradation of polypeptides arising from PTC-containing mRNAs takes place (Kuroha *et al.* 2009), and it has been suggested that Upf1p may serve as an E3 ubiquitin ligase to couple peptides arising from the translation of PTC substrates to the proteasome-mediated peptide degradation machinery (Takahashi *et al.* 2008). Thus, Upf1p (and perhaps the other NMD factors) appears to play a multifaceted role in dealing with all aspects of premature termination and its consequences in yeast.

Future directions

Despite gaining some understanding of the interplay between translation and mRNA decay factors, a more mechanistic understanding of the events underlying the roles played by NMD factors at premature termination will involve:

1.) characterizing the ribosome-binding domains of Upf1p,
2.) characterizing the phenotypes *in vitro* of other NMD factors in termination events at a PTC and subsequent initiation events,
3.) identifying what other factors are required to mediate premature termination events,
4.) determining whether Upf1p is recruited to terminating ribosomes in an eRF-dependent manner at a PTC,
5.) identifying the domains of Upf1p required to observe the *in vitro* phenotypes associated with premature termination events,

6.) characterizing the order of assembly of factors required to mediate termination at a PTC, and

7.) determining how events at a PTC trigger downstream decapping and decay of substrate mRNAs?

Further insight into closed loop dynamics and function will require us to:

1.) directly visualize interactions between the components of the Pab1p-eIF4G-eIF4E complex,

2.) identify which domains of eRFs 1 and 3 contribute to closed loop formation,

3.) determine the localization of the termination factors in the closed loop structure (proximal or distal on the 3'-UTR to the termination codon),

4.) determine whether the closed loop regulates post-termination ribosome recycling, and

5.) characterize the roles of the termination factors in closed loop function.

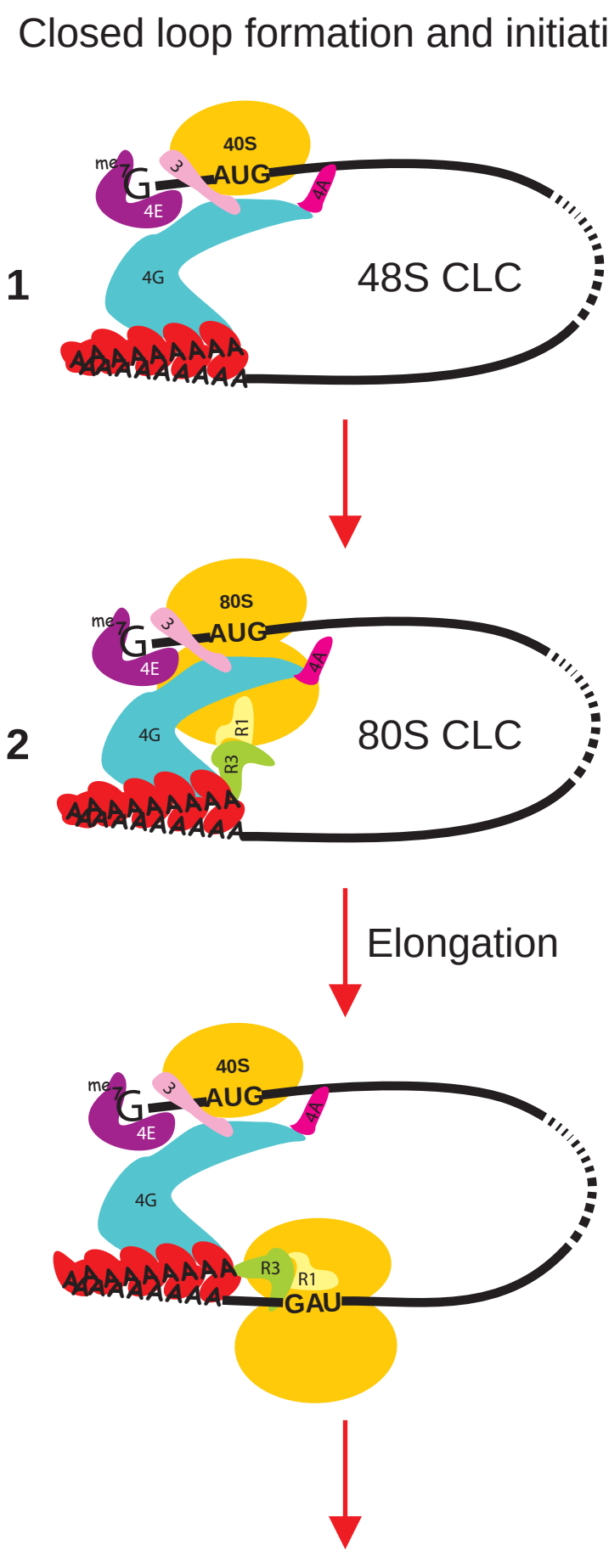

Fig. 5.1 : Two states model of the closed loop. mRNA closed loop formation takes place in two disctinct steps: (**1**) 5' cap-bound eIF4E interacts with eIF4G, which in turn associates with Pab1p to mediate 48S initiation complex formation on the mRNA, followed by (**2**) association of the translation termination factors, eRF1 and eRF3, to stabilize the closed loop complex (CLC) to allow the formation of a stable 80S translation complex on the mRNA. In addition to their roles in allowing formation of a stable 80S ribosomal complex at the initiator AUG, presence of the eRFs as part of the closed loop complex may enhance normal termination events and ribosome recycling. 4E, eIF4E; 4G, eIF4G; 3, eIF3; 4A, eIF4A; R1, eRF1; R3, eRF3; red ovals, Pab1p; yellow ovals, 40S and 60S ribosomal subunits.

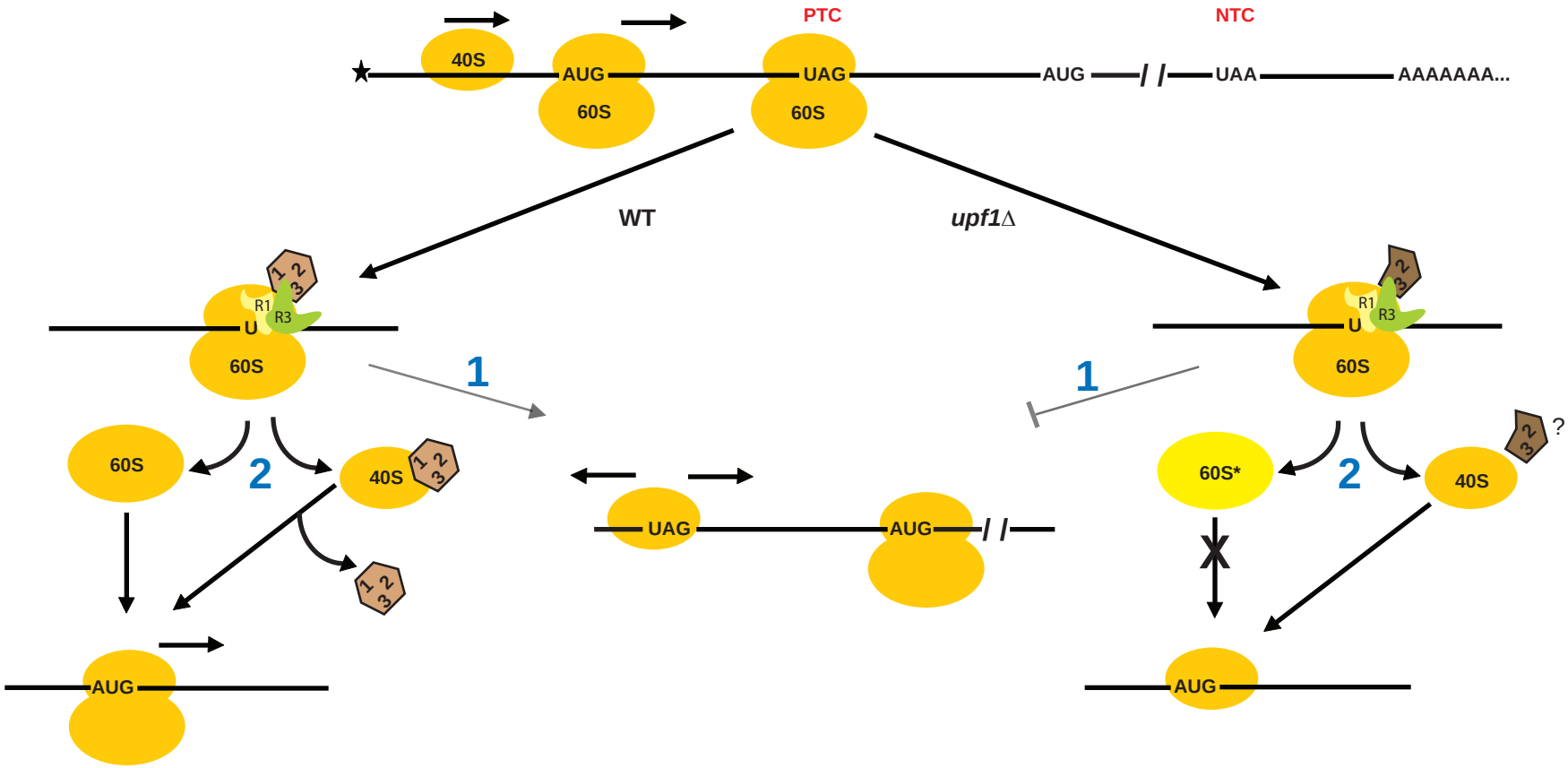

Fig. 5.2 : Upf1p enhances ribosome reutilization post-termination from a PTC. (1)Termination at a PTC is inefficient and allows **some** (gray arrows) 40S subunits to remain associated with the nonsense mRNA, where they scan for nearby AUGs (both upstream and downstream of the PTC) to reinitiate translation on the same mRNA in a *UPF*-dependent manner. (2) Ribosomes terminating at a PTC require the activity of Upf1p to allow events resulting in proper 60S dissociation in a manner that allows the dissociated 60S subunit to join a 48S initiation complex and form an 80S ribosomal complex. Dark yellow ovals, normal 40S and 60S ribosomal subunits; light yellow oval (60S*), 60S subunit defective in 80S formation; R1, eRF1; R3, eRF3; 1, Upf1p; 2, Upf2p/Nmd2p; 3, Upf3p; PTC, premature termination codon; NTC, normal termination codon; horizontal arrows, directions of subunit/ribosome movement.

APPENDICES

Appendix A – Methods used in Chapter II

Synthetic mRNAs

Synthetic, capped poly(A)-containing RNA was synthesized *in vitro* from chimeric genes cloned in a pSP65A vector that included ~65 dT residues for transcription of a poly(A) tail (Promega). The construct utilized for synthesis of *UAA* RNA contained a 5' fragment of the *S. cerevisiae can1-100* allele upstream of the firefly *LUC* open reading frame. The *can1-100* DNA fragment used for this construct contained *EcoR* I and *Sal* I sites, respectively 114 bp 5' and 147 bp 3' of the initiator ATG. This DNA fragment was generated in a one-step PCR amplification, using oligonucleotides #13 (5'-CCGGAA TTCCGGATCCAGTTTTTAATCTGTCG-3') and #12 (5'-CGTCGACTTAACTTTTCT CATCTTTC-3') and cloned into the *EcoR* I and *Sal* I restriction sites of the pSP65A vector. The remainder of the construct was derived by insertion of a *Sal* I *LUC/PGK1*-3' fragment into the *Sal* I restriction site of the same plasmid, generating pSP65A-*can1-100/LUC*. All other constructs used in this study were derived from pSP65A-*can1-100/LUC* by site-directed mutagenesis (Stratagene). The mini-DNA constructs were generated by deletion of the *LUC* ORF from a *Pst* I restriction site (created by site-directed mutagenesis) 10-15 nt downstream of the premature stop codon and a *Pst* I site immediately 3’ to the normal stop codon. All plasmid constructions were confirmed by DNA sequencing. Capped and polyadenylated RNAs were synthesized with the SP6 mMessage mMachine kit (Ambion), according to the manufacturer's protocol, from *Hind* III-linearized plasmids. RNA yields were quantified by spectrophotometry and their integrities were assessed by agarose gel electrophoresis.

Extracts and translation reactions

Saccharomyces cerevisiae strains MBS (*MATa ade2-1 his3-11,15 leu2-3,112 trp1-1 ura3-1 can1-100* [rho+] L-o, M-o)(Iizuka and Sarnow 1997), NA101 (*MATa ade2-1 his3-11,15 leu2-3,112 trp1-1 ura3-1 can1-100 upf1::HIS3* [rho+] L-o, M-o), and MT552/8a (*MATα sup45-2 ade2-1 ura3-1*)(Stansfield *et al.* 1997) were used to make extracts for *in vitro* translation by techniques described previously (Sachs *et al.* 2002). Translation assays were essentially the same as those described before (Sachs *et al.* 2002), except that 120 μg of extract was used in each assay, and the treatment with micrococcal nuclease (Pharmacia) was done at 25^{o}C for 5 min. Unless indicated otherwise, translation reactions were incubated for 4 min, with 120 ng of each RNA substrate, and terminated by incubation with CHX (0.6 mg/ml) for 3 min. Samples from the translation reactions were used for reverse transcription reactions with the oligoprimer #3029, complementary to the *LUC* sequence CGCCCTGGTTCCTGGAACAATTGC. In the CHX chase experiment [Fig. 2.3(c)], the drug was added after 4 min of translation and the reactions were incubated for 0 to 5 minutes. Translation reactions programmed with *mini* RNAs were incubated with 12 ng of the *miniUAA, miniUAA-M, miniUAA-M-W,* or *miniUGA* RNAs and toeprinting analyses of aliquots from each reaction utilized oligoprimer #55 complementary to the *PGK1* 3'-UTR sequence CCGAAAAGAAATAAATTGAATTG. Both primers #3029 and #55 hybridize to their respective RNAs at comparable positions. Translation reactions programmed with the *Inf* constructs (Fig. 2.5) were incubated with 120 ng of RNA for 45

min and luciferase activity was assayed as described previously (Tarun and Sachs 1995). All data reported are representative of at least three independent experiments.

Analysis of mRNAs with MS2 binding sites

PCR-amplified 188 nt MS2 coat protein binding sites (Coller *et al.* 1998) were inserted 73 nt 3' of PTCs in the *CAN1 UAA* and *UGA* genes (see above) and 37 (*PGK1-MS2*) or 164 (*PGK1-3'-MS2*) nt 3' of the UAG of mini-*PGK1* (Peltz *et al.* 1993). These constructs were cloned in pYX142 (*CAN1*) or pRS316 (*PGK1*) and introduced into cells harboring YCplac111-*MS2-PAB1* or pA-MP2 (Coller *et al.* 1998), YCplac111-*MS2*-dimer or pD-MS2(Coller *et al.* 1998), pMS2-Sxl (Coller *et al.* 1998), YCplac111-*MS2-SUP35,* YCplac111-*MS2-SUP45* (with *MS2* fusions under the control of the *TPI1* promoter), or no plasmid. RNA was isolated and analyzed by northern blotting as described previously (Peltz *et al.* 1993). Hybridization probes were prepared by random priming of double-stranded DNA. *PGK1-MS2* and *PGK1-3'-MS2* mRNAs were detected with a 0.5-kb *Bgl* II fragment of the MS2-binding domain; detection of the *CYH2, TCM1, and SCR1* RNAs utilized gene-specific PCR fragments; and detection of *CAN1-MS2-LUC* mRNAs utilized a fragment of the *LUC* ORF.

Immunoprecipitation (IP)

Yeast cells, grown at 30°C in minimal media to OD_{600}=1, were harvested, washed, and resuspended in IP buffer (10 mM Tris-HCl at pH 7.5, 30 mM $MgCl_2$, 100 mM NaCl, 2 mM PMSF, 2X Protease Inhibitor cocktail (Sigma), 0.01% TritonX-100, 50 µg/ml CHX, 0.1 mM DTT). Glass beads (425-600 µm) were added and cells were

broken by vortexing 15 seconds eight times, with intermittent cooling on ice. Lysates were clarified twice by centrifugation (7,700Xg, 4°C). Protein A Sepharose beads (Pierce) were preincubated for 3h at 4°C in IP buffer with rabbit polyclonal α-MS2 coat protein antibodies or normal rabbit serum (Pierce), pre-coated overnight at 4°C with 1 mg of MBS cell extract in 400 µl of IP buffer, washed 3 times with 1ml of IP buffer, mixed with 400 µg aliquots of clarified cell extract, and incubated at 4°C for 3h, under agitation. Beads were separated from unbound proteins (sup) by a 10 sec centrifugation and washed 4 times with IP buffer at 4°C. The bound fraction was eluted by boiling for 5 min in SDS gel sample buffer. Wash samples were precipitated by TCA and resuspended in sample buffer. Samples were fractionated by SDS-PAGE and characterized by western blotting. Input, sup, and wash represented 1/20, 1/10, and 1/3 of the loading of the IP samples, respectively. RNA recovery from IPs was performed as above with two changes: RNasin (80U/ml) was added to the IP buffer and the beads were washed with 250µl aliquots of this solution. RNA was recovered from the beads and IP fractions by phenol/chloroform extraction (Peltz *et al.* 1993).

Appendix B – Methods used in Chapter III

Yeast strains, vectors, and transformations

The yeast strains used in this chapter, and their genotypes, are listed in Table B1. Strain YRG467 was constructed by transforming HFY467 with plasmid pRS315-*NMD2*(C-Sal) (He *et al.* 1996). For *in vivo* studies, strains were grown in selective media (Amberg *et al.* 2005) at 30^{o}C, or at 24^{o}C for temperature-sensitive strains. Yeast transformations were performed by the rapid protocol (Soni *et al.* 1993) and yeast vectors utilized included pRIP1 (Parker and Jacobson 1990), pRS314 (Sikorski and Hieter 1989), YEplac22 (Gietz and Sugino 1988), and pRS316 (Sikorski and Hieter 1989). For *in vitro* translation experiments, MBS and strains derived from it (NA101, NA102, and NA103) were grown in YEPD at 25^{o}C for extract preparation (Amrani *et al.* 2004).

Plasmid-borne expression constructs

Constructs used for *in vivo* expression analyses are described in Table B2. Oligonucleotides used in this study are listed in Table B3. Construct 1, a chimeric *PGK1*/*LUC* gene (Fig. 1A), consists of the *PGK1* 5'-untranslated region (UTR), the first 5% of the *PGK1* open reading frame (ORF) followed by a UAG stop codon (contextually a premature termination codon), an 82 nt *PGK1* sequence element (derived from a 106 nt segment previously designated as a DSE [(Peltz *et al.* 1993)] – see Table B2) that contains two AUG codons (out of frame with the upstream *PGK1* ORF) fused in frame to the *LUC* ORF lacking its normal start codon, and the 3'-UTR of *PGK1*. All constructs

for *in vivo* luciferase expression experiments contain a 5'*Bam*HI site and a 3'*Hin*dIII site and were subcloned into vectors by excising with *Bam*HI/*Hin*dIII. PCR fragments 1 and 2 were generated using the *mini-PGK1* allele as a template. This allele contains a 58-nt tag in its 3'-UTR to allow later detection of its mRNA on a northern blot (Peltz *et al.* 1993). Fragment 1 was generated using the M13/pUC Reverse Amplification primer (BRL) and primer 3-106-82 and digested with *Bam*HI and *Pst*I restriction enzymes. Fragment 2 was generated using primer 5-PPGKH and the M13/pUC Forward Amplification primer (BRL) and digested with *Pst*I and *Hin*dIII. Fragment 3 was generated by PCR using pXP1 as a template (a kind gift from Dr. Paul Dobner), and primers 5-PSLUCP and 3-PLUCSP, and digested with *Pst*I. Fragments 1 and 2 were ligated into pGEM-3Z(f)+ (Promega) and cut with *Bam*HI/*Hin*dIII. The resulting construct was cut with *Pst*I, incubated with calf intestinal alkaline phosphatase (CIAP), and ligated with fragment 3 to generate construct 3. Construct 1 was generated by digesting construct 3 with *Sal*I to remove a 10bp fragment and religating to close. *Bam*HI/*Hin*dIII fragments containing construct 3 and construct 1 were then subcloned into the centromeric yeast vectors pRIP1 (cut with *Bam*HI/*Hin*dIII) and pRS314 (cut with *Sma*I), and the high-copy plasmid, YEplac112 (cut with *Bam*HI/*Hin*dIII). The resulting constructs were transformed into strains HFY114, YRG467, HFY115, HFY861, HFY467, HFY872, and HFY874.

Construct 2 was generated with the Chameleon site-directed mutagenesis kit (Stratagene) using the following strategy: plasmid pRIP1 containing construct 1 was digested with *Bam*HI/*Sal*I to yield an 800bp fragment containing the 5'-end of construct 1 from the *PGK1* start to the junction of the 82 nt *PGK1* sequence element and *LUC*

and an 8kb fragment containing the remainder of the construct and pRIP1. The smaller fragment was subcloned into pGEM-3Z(f)+ to yield pGEM-3Z(f)+/PGKBS. The resulting plasmid was mutagenized with primers PGKDATG and pGEM-SEL. A *Bam*HI/*Sal*I fragment containing the mutagenized construct was then ligated with the 8kb fragment described above to yield construct 2. Construct 5 was generated similarly, with primers PGKΔTAG and pGEM-SEL, followed by mutagenic primer FUSION. These constructs were also placed into pRS314 and YCplac22. Construct 4 was generated using primers PGKDELINIT and PGKΔTAG. Construct 6 was generated as follows: an approximately 560bp fragment was made by PCR using pGEM-3Z(f)+/PGKBS as a template and primers M13 reverse and PGKUAGSAL2, and cut with *Bam*HI/*Sal*I. This fragment was ligated into the 8kb fragment described above to yield construct 6. All of the above constructs were transformed into HFY114, YRG467, HFY115, HFY861, HFY467, HFY872, and HFY874.

To generate construct 7, construct 1 was subcloned into pGEM-3Z(f)+ and cut with *Nhe*I. Linkers NHELINKERA and NHELINKERB were annealed together and ligated into the *Nhe*I site. These constructs were sequenced for orientation such that NHELINKERA reads 5'→3'. The resulting construct [pGEM-(Sal)*luc*NHE] was digested with *Stu*I to cut within the NHE linker and treated with CIAP. Oligonucleotide primers HPR1A and HPR2A were annealed together and HPL1A and HPL2A were annealed together. The resulting short double-stranded fragments (designated HairpinR and HairpinL, respectively) were isolated on a 15% acrylamide gel and purified by the crush and soak method (Maxam and Gilbert 1977). Ligations were performed such that HairpinR and HairpinL were ligated together for 0 and 5 minutes before addition of the

*Stu*I-cut pGEM-(Sal)*luc*NHE. Colonies from the above ligations were screened by colony PCR for 162bp inserts containing HairpinR and HairpinL (as opposed to double HairpinR or double HairpinL inserts) and sequenced for orientation such that HairpinL was 5' of HairpinR. The resulting *Bam*HI/*Hin*dIII fragment-containing construct 7 was subcloned into YCplac22. This construct was transformed into HFY114, YRG467, HFY115, HFY861, HFY467, HFY872, and HFY874. Construct 8 was made by deleting the UAG stop codon of construct 7 using the Quick-Change site-directed mutagenesis kit (Stratagene). Mutagenic primers were DSTOP1 and DSTOP2. This construct was transformed into yeast strains HFY114, YRG467, HFY115, HFY861, HFY467, HFY872, and HFY874.

The *CAN1/LUC* ("Fusion") construct used as a template for the preparation of synthetic mRNA for *in vitro* translation experiments has been described elsewhere (Amrani *et al.* 2004). pRS316pA-*CAN1* and pRS316pA-*can1-100* templates were derived by ligating an *Eco*RI/*Hin*dIII fragment of plasmid CFE86 (containing the complete *CAN1* gene; a kind gift from Chunfang Li) or plasmid CFE87 (which contains the complete *can1-100* gene; a kind gift from Chunfang Li) into pRS316pA linearized by cleavage with *Eco*RI and *Hin*dIII. To generate pRS316pA, oligonucleotide primers Xho-pA-Asp (5'-[phos]TCGAG$(A)_{75}$G-3') and Asp-pT-Xho (5'-[phos]GTACC$(T)_{75}$C-3') were annealed, alkaline phosphatase-treated (Roche), and ligated into *Xho*I/*Asp*718-linearized pRS316.

Measurement of luciferase activity in cells, Bradford assays, and northern analyses

Yeast cultures (30ml) were grown in selective medium overnight at 24^{o}C to an OD_{600} of 0.7-1.2. Fourml of each culture were removed and the cells pelleted and frozen at -70^{o}C for later RNA extraction. An additional 20ml of each culture was pelleted and washed twice with 1X PBS (0.01M NaH_2PO_4, 0.15M NaCl). The cells were resuspended in 2ml 1X PBS and split between 2 microcentrifuge tubes. These were then pelleted and stored at -70^{o}C to await glass bead extraction. The frozen cell pellets were resuspended in 200 μL luciferase extraction buffer (LEB) (0.1M KPO_4, pH 7.8, 1mM DTT, 1mM PMSF). Acid-washed glass beads (200 mg; Sigma 425-600 μm) were added and the tubes were then vortexed for 30 sec and placed on ice for 30 sec, alternately, for 5 min. The tubes were then spun in a microcentifuge at 14,000 rpm for 5 min at 4^{o}C and the supernatant (extract) placed into a fresh tube on ice. The following components were then added to a luminometer cuvette: 100 μL LEB, 20 μL extract, and 350 μL Luciferase assay buffer (LAB), pH 7.8 (25 mM glycylglycine, pH 7.8, 15 mM KPO_4, pH 7.8, 15 mM $MgSO_4$, 4 mM EGTA, 2 mM ATP, 1 mM DTT). Assays were performed in a Monolight 2010 luminometer by injecting 100 μL of 200 μM D-luciferin, potassium salt (Analytical Luminescence Labs) in 25 mM glycylglycine, pH 7.8 and measuring light output for 10 sec. Extracts were stored at -70^{o}C following luciferase assays until Bradford assays were performed. Bradford assays were performed on a Beckman DU7400 Spectrophotometer with the Biorad Protein Assay Kit according to the microassay protocol using 10 μL extract per assay. RNA was prepared from frozen cell pellets as described previously (Herrick *et al.* 1990) and quantitated on a Beckman DU7400

Spectrophotometer. Aliquots (10 μg) of total RNA were loaded onto a 1% agarose/formaldehyde/MOPS gel and electrophoresed, blotted, and hybridized as described previously (Herrick *et al.* 1990). Transcripts derived from the different constructs were detected with an oligonucleotide (Peltz *et al.* 1993) which hybridizes to the 3'-UTR of the respective construct mRNAs, but which does not hybridize to the endogenous *PGK1* mRNA. mRNA signals were quantitated using a Betascope (Betagen) blot analyzer. mRNA levels were normalized for loading by stripping the blots and rehybridizing with a random-primed probe targeted to the *CYH2* mRNA. Final luciferase activity was expressed as relative light units (RLU) of 20 μL extract, per μg protein in 20 μL extract, per unit of construct mRNA in 10 μg total RNA, normalized for loading differences with the *CYH2* mRNA signal. Each set of assays performed on a given day included three cultures of construct 1 in strain HFY114 on a YCp plasmid, and each northern blot from each set of assays contained the RNAs from these three cultures. The average luciferase activity (expressed in RLU/μg protein/unit mRNA) of these three cultures was assigned a value of 100% to which all other luciferase activities in a set of assays were compared.

Extract preparation, synthetic mRNA, *in vitro* translation, and toeprinting assays

S.cerevisiae strains MBS, NA101, NA102, and NA103 were used to make extracts for *in vitro* translations as described (Iizuka and Sarnow 1997; Wu *et al.* 2007; He *et al.* 2008). Capped and polyadenylated *CAN1/LUC* mRNA was synthesized with the SP6 mMessage mMachine kit (Ambion) as per the manufacturer's protocol, from *Hin*dIII-linearized plasmids. Capped and polyadenylated *CAN1* and *can1-100* mRNAs

were synthesized *in vitro* from *Kpn*I-linearized pRS316pA-*CAN1* and pRS316pA-*can1-100* plasmids using the T7 mMessage mMachine kit (Ambion) as per the manufacturer's protocol. Translation assays were as described (Amrani *et al.* 2004; Wu *et al.* 2007), except that each assay was performed at 18^{o}C without prior treatment of the extract with micrococcal nuclease (MN), unless otherwise specified, and used 100 μg of extract and 100ng of the *CAN1/LUC* mRNA unless specified otherwise. When used, MN pre-treatment of extracts was performed at 25°C for 5 min (Amrani *et al.* 2004). Protein concentrations of translation extracts were measured using the BCA Protein Assay Kit (Pierce). Translation reactions were incubated as specified in the figure legends and frozen in a dry ice/ethanol bath until luciferase assays were to be performed. The latter were done with a TD20/20 luminometer (Promega), as described previously (Amrani *et al.* 2004). For translation reactions involving FLAG-Upf1p (a kind gift from Dr. Stephanie Kervestin), 270-360ng of FLAG-Upf1p or BSA was preincubated with extracts on ice for 10 min prior to adding the rest of the components of the translation reactions. For add-back of purified 40S and 60S ribosomal subunits, 5μg of purified 40S subunits, 10μg of purified 60S subunits, or BSA was added to the reaction without prior incubation with extracts. For toeprinting reactions, translations were terminated by incubation for 3 min with 2 mM cycloheximide or GMP-PNP (Sigma), aliquotted, frozen in a dry ice/ethanol bath, and stored at -70^{o}C until reverse transcription reactions were to be performed (Amrani *et al.* 2008) with oligomer #105 (5'-CGTCTGTGGTCTGTTTGTGAAGCC-3'). All *in vitro* translation experiments, except add-back experiments with ribosomal subunits, were performed at least three times with independently prepared extracts. Add-back

experiments with ribosomal subunits were done at least twice with independently prepared extracts.

Sucrose gradient analyses

For mRNA:ribosome association assays, the equivalent of six translation reactions were incubated for 30 min at 18^{o}C, stopped by the addition of 2mM CHX, and fractionated on an 11ml 7-47% sucrose gradient. The gradients were scanned at A_{254} , and the resulting absorbance profiles were used to determine the position of the polysomal and non-polysomal fractions (Mangus and Jacobson 1999; Amrani *et al.* 2008). RNA was extracted from each fraction and analysed by northern blotting as described previously (Mangus and Jacobson 1999), using random-primed probes directed against the *LUC* ORF or the 3' half of the *can1-100* ORF (Amrani *et al.* 2008). All experiments were done at least twice with independently prepared extracts.

Ribosome subunit preparation and western blot analysis

We utilized a procedure for purification of 40S and 60S ribosomal subunits that had been described previously (Algire *et al.* 2002), except that we used 9L of strain MBS grown in YPD at 25^{o}C to an OD_{600} of 1.0. Fractions enriched for 40S and 60S subunits were concentrated in Amicon Ultra-15 100K NMWL filter devices (Miilipore). Protein concentrations were measured using the BCA Protein Assay Kit (Pierce). The 40S fraction contained 18S rRNA, but no detectable 25S rRNA, and the 60S fraction contained 25S rRNA, but no detectable 18S rRNA, as visualized on a 1% formaldehyde-agarose gel stained with ethidium bromide. Upf1 association with 40S

and 60S ribosomal subunits was assessed by western blot analysis using methods and anti-Upf1p antibody described previously (Mangus and Jacobson 1999).

Table B1. Yeast strains used in this study

Strain	Genotype	Reference
HFY114	*MAT*a, *ade2-1, his3-11,15, leu2-3,112, trp1-1, ura3-1, can1-100*	(He *et al.* 2003)
HFY115	*MAT*a, *ade2-1, his3-11,15, leu2-3,112, trp1-1, ura3-1, can1-100, nmd2::HIS3*	(He *et al.* 2003)
HFY467	*MAT*a, *ade2-1, his3-11,15, leu2-3,112, trp1-1, ura3-1, can1-100, nmd2::HIS3, upf1::URA3*	(He and Jacobson 1995)
HFY861	*MAT*a, *ade2-1, his3-11,15, leu2-3,112, trp1-1, ura3-1, can1-100, upf3::HIS3*	(He *et al.* 1997)
HFY872	*MAT*a, *ade2-1, his3-11,15, leu2-3,112, trp1-1, ura3-1, can1-100, upf1::URA3, upf3::HIS3*	(He *et al.* 1997)
HFY874	*MAT*a, *ade2-1, his3-11,15, leu2-3,112, trp1-1, ura3-1, can1-100, upf3::HIS3, nmd2::URA3*	(He *et al.* 1997)
YRG467	*MAT*a, *ade2-1, his3-11,15, leu2-3,112, trp1-1, ura3-1, can1-100, nmd2::HIS3, upf1::URA3* + [pRS315-*NMD2*(C-Sal)]	This study
RY262	*MAT*α, *his4-519, ura3-52, rpb1-1*	(Herrick *et al.* 1990)
SWP154(-)	*MAT*α,*upf1-*Δ*1::URA3,ura3-52,rpb1-1,leu2-1, his4-38*	(Peltz *et al.* 1993)
MBS	*MAT*a, *ade2-1, his3-11,15, leu2-3,112, trp1-1, ura3-1, can1-100, [rho+], L-o, M-o*	(Iizuka and Sarnow 1997)
NA101	*MAT*a, *ade2-1, his3-11,15, leu2-3,112, trp1-1, ura3-1, can1-100, [rho+], L-o, M-o, upf1::HIS3*	(Amrani *et al.* 2004)
NA102	*MAT*a, *ade2-1, his3-11,15, leu2-3,112, trp1-1, ura3-1, can1-100, [rho+], L-o, M-o, nmd2::HIS3*	(Amrani *et al.* 2004)
NA103	*MAT*a, *ade2-1, his3-11,15, leu2-3,112, trp1-1, ura3-1, can1-100, [rho+], L-o, M-o, upf3::HIS3*	This study

Table B2. Pertinent features of constructs used in this study

Construct	Description
Mini-*PGK1*	Contains the 5'-UTR and first 5% of the *PGK1* ORF followed by a premature termination codon, a 106 nt *PGK1* sequence element required for NMD-sensitivity that contains two AUG codons, and the 3'-UTR of *PGK1* (Peltz *et al.* 1993). There is an *Nhe*I restriction site at the UAG stop codon that terminates the *PGK1* ORF prematurely. This *PGK1* construct and all other related constructs were subcloned into various vectors with a 5' *Bam*HI site and a 3' *Hin*dIII site.
Construct 1	Similar to the mini-*PGK1* allele (above), except that the 106 nt sequence element was truncated to 82 nt (retaining the two AUG codons) and the *LUC* coding region (minus its endogenous AUG start codon) was inserted immediately 3' to it. The *LUC* coding region is in frame with the two AUG codons of the 82 nt sequence element, generating a 1716 bp ORF in the +1 reading frame relative to the *PGK1* ORF. A *Sal*I site joins the 82 nt sequence element and the 5' end of the *LUC* coding region; a *Pst*I site joins the 3' end of the *LUC* coding region and the *PGK1* 3'-UTR. As in mini-*PGK1*, an *Nhe*I site lies at the UAG codon.
Construct 2	Identical to construct 1, except that each of the two AUGs of the 82 nt *PGK1* sequence element were deleted. The first ORF following the *PGK1* premature termination codon begins at an AUG codon 82 nt into the *LUC* coding region.
Construct 3	Similar to construct 1, except that the *LUC* coding region is in the +2 reading frame, relative to the *PGK1* ORF, and out of frame with the two AUGs of the 82 nt *PGK1* sequence element. There is a 10bp linker between the 82 nt *PGK1* sequence element and the *LUC* coding region containing the sites 5'-*Sa*lI-*Pst*I-*Sal*I-3'. Digestion with *Sal*I and religation to close yielded construct 1.
Construct 4	Identical to construct 1, except that the premature UAG codon between the *PGK1* ORF and the 82 nt *PGK1* sequence element was deleted.
Construct 5	Identical to construct 1, except that the premature UAG codon of *PGK1* plus the first nt of the 82 nt *PGK1* sequence element were deleted, generating an ORF that begins at the *PGK1* AUG initiation codon and ends at the *LUC* termination codon.

Construct 6	The *PGK1* ORF and the 82 nt *PGK1* sequence element of construct 1 were deleted between the *PGK1* AUG initiation codon and the beginning of the *LUC* coding region. A *Sal*I site lies at the junction of the *PGK1* 5'-UTR and the *LUC* coding region.
Construct 7	A stem-loop cassette consisting of a strong stem-loop preceded by a 30nt leader was inserted into construct 1 between the premature UAG codon of *PGK1* and the 82 nt *PGK1* sequence element. *Nhe*I sites are present at the UAG codon and between the stem-loop and the 82 nt *PGK1* sequence element. A *Sa*lI site lies between the 82 nt *PGK1* sequence element and the *LUC* coding region. A *Pst*I site is at the *LUC* UAA termination codon.
Construct 8	Identical to construct 8, except that the UAG termination codon of *PGK1* was deleted, generating an ORF starting at the *PGK1* initiation codon and ending at the *LUC* termination codon.

Table B3. Oligonucleotide primers used in this study

Oligonucleotide	Sequence
3-106-82	5’-AAAACTGCAGTCGACGCCAGCCAGCTGGAATACCT T-3’
5-PPGKH	5’-AAAACTGCAGGATCTCCCATGTCTCTACTGGT-3’
5-PSLUCP	5’-AAAACTGCAGTCGACGCCAAAAACATAAAGAAAG-3’
3-PLUCSP	AAAACTGCAGTTACAATTTGGACTTTCCGCC-3’
PGKDATG	5’-AGTCCTAGCTAGCTAGGACTTCATCATTGCTGCTTT CTCTGCTGCCAACACCAAGACTGTCACTGACAA-3’
pGEM-SEL	5’-CTATAGGGCGATATCGAGCTCG-3’
PGKΔTAG	5’-AGAGTTCTAGCTAGCGACTTCATCATTGCT-3’
FUSION	5’-ATTCCAGCTGGCTGGGTCGACCTGCAGGCA-3’
PGKDELINIT	5’-ACAAATATAAAAACATCTTTATCTTCAAAG-3’
106DEL83	5’-TTCCAGCTGGCTGGCTCGACGCCAAAAACA-3’
106DEL1	5’-GTTCTAGCTAGCTAGACTTCATCATTGCTG-3’
PGKUAGSAL2	5’-GTCGACCCTAGCTAGCTAGAACTCTGAT-3’
NHELINKERA	5’-CTAGCTAGAGCGCTGATATCAGGCCTCTAG-3’
NHELINKERB	5’-CTAGCTAGAGGCCTGATATCAGCGCTCTAG-3’
SALLINKERA	5’-TCGACAGCGCTGATATCAGGCCTG-3’
SALLINKERB	5’-TCGACAGGCCTGATATCAGCGCTG-3’
HPR1A	5’-TGGGCAGAAGCCTTGACAGCGGCTTC-3’
HPR2A	5’-GAAGCCGCTGTCAAGGCTTCTGCCCAAT-3’

HPL1A	5’-GTCGGTCCAGAAGTTGAAGCCGCTGTCAAGGCTTCTGCCCAAT-3’
HPL2A	5’-TGGGCAGAAGCCTTGACAGCGGCTTCAACTTCTGGACCGAC-3’
HAIRPINL1	5’-GTCGGTCCAGAAGTTGAAGCCGCTGTCAAGGCTTCTGCTTAAT-3’
HAIRPINL2	5’-TAAGCAGAAGCCTTGACAGCGGCTTCAACTTCTGGACCGAC-3’
HAIRPINR1	5’-TAAGCAGAAGCCTTGACAGCGGCTTC-3’
HAIRPINR2	5’-GAAGCCGCTGTCAAGGCTTCTGCTTAAT-3’
DSTOP1	5’-CATCAGAGTTCTAGCTAGCAGCGCTGATATCAGGGTCG-3’
DSTOP2	5’-CGACCCTGATATCAGCGCTGCTAGCTAGAACTCTGATG -3’
SAL-PST	5’-TCGATGCA-3’

Appendix C – Methods used in Chapter IV

Synthetic mRNAs

Synthetic, capped poly(A)-containing *miniUAA1*, *UAA* and *AAA* mRNAs were transcribed *in vitro* from chimeric genes cloned in a pSP65A vector that included ~65 dT residues for transcription of a poly(A) tail (Amrani *et al.* 2004). mRNAs of intermediate lengths originated from truncated DNA constructs derived from pSP65A-*CAN1/LUC* (Amrani *et al.* 2004) by deletion of the *LUC* ORF from *Pst* I restriction sites (created by site-directed mutagenesis; Stratagene). mRNAs differing in poly(A) tail length were synthesized from *miniUAA1* DNA cloned in pSP65A vectors that contain the corresponding lengths of dT residues (Munroe and Jacobson 1990). The construct utilized for synthesis of long ADE2 mRNA was generated in a one-step PCR amplification, using *EcoR* I site-containing oligonucleotide #165 (which also contains mutations of two upstream AUGs) (5'-CGGAATTCATTATAGAGCATTTCATATAT*AAA*TTGGTGCGT*AAA*ATCGTTGGATCTC TC-3') and *BamH* I site-containing oligonucleotide #164 (5'-GAGGATCC*AAA*TTCTT*AAAAAA*GGACACCTGTAAGCGTTG -3') and cloned into the *EcoR* I and *BamH* I restriction sites of the pSP65A vector. The *miniADE2* DNA construct was generated by deletion of the 1575nt fragment from a *Pst* I restriction site 260-265 nt downstream of the start of the construct and a *Pst* I site immediately 5’ to the normal stop codon (both sites were created by site-directed mutagenesis). All plasmid

constructions were confirmed by DNA sequencing. Capped and polyadenylated RNAs were synthesized with the SP6 mMessage mMachine kit (Ambion), according to the manufacturer's protocol, from *Hind* III-linearized plasmids for poly(A)-containing mRNA or from *Cla* I linearized plasmids for mRNA lacking the poly(A) tail. At least 80% of *in vitro* transcribed mRNAs were capped, as determined by immunoprecipitation using anti-2,2,7-trimethylguanosine agarose conjugate (Calbiochem). Uncapped mRNA was synthesized using the MEGAscript kit (Ambion). RNA yields were quantified by spectrophotometry and their integrities were assessed by agarose gel electrophoresis.

Extracts and translation reactions

Saccharomyces cerevisiae strains (Table C1) were used to make extracts for *in vitro* translation by techniques described previously (Wu *et al.* 2007). Wild-type strains from different genetic backgrounds gave similar results. Translation and toeprinting assays were essentially the same as those described before (Amrani *et al.* 2004). Unless indicated otherwise, translation reactions were incubated for 4 min with 0.06 pmol of each RNA substrate, and terminated by incubation for 3 min with 2mM cycloheximide or GMP-PNP. Where indicated, translation initiation was subjected to competitive inhibition by 2.7 mM cap analog (m^7GpppG), a concentration that readily distinguishes initiation complexes that are, respectively, sensitive or resistant to this compound. Toeprinting utilized two different primers that were complementary to their respective targets at comparable distances from the AUG of interest. Primer #3029 was used for mRNAs spanning 600nt (*miniUAA*2) to 2135nt (*AAA*) and primer #55 was used with *miniUAA1* mRNA. Samples from translation reactions programmed with *ADE2* and

miniADE2 mRNAs were toeprinted with primer #172, complementary to the sequence CACT*AAA*GAATCTTCAAGT*AAA*ACATCCC, and primer #3238, complementary to the sequence GGACTTCATACATAG*AAA*TCAACG, respectively. For mRNA:ribosome association assays, the equivalent of four translation reactions were fractionated in an 11ml sucrose gradient (7-47%). The gradients were fractionated and scanned at 254 nm, and the resulting absorbance profiles were used to determine the position of the polysomal and non-polysomal fractions (Mangus and Jacobson 1999). RNA was extracted from each fraction and analyzed by northern blotting as described previously (Mangus and Jacobson 1999).

Table C1. Yeast strains used in this study

Strain	Genotype
MBS (Iizuka and Sarnow 1997)	*MAT*a *ade2-1 his3-11,15 leu2-3,112 trp1-1 ura3-1 can1-100* [rho+] L-o, M-o
yDM206 (Mangus *et al.* 1998)	*MAT*a *ade2-1 his3-11,15 leu2-3,112 trp1-1 ura3-1 can1-100 pab1::HIS3 pbp1::LEU2*
yDM146 (Mangus *et al.* 1998)	*MAT*a *ade2-1 his3-11,15 leu2-3,112 trp1-1 ura3-1 can1-100 pbp1::LEU2*
yJP62	*MAT*α *ade2-1 his3-11,15 leu2-3,112 trp1-1 ura3-1 pab1::HIS3* [pYCplac111*PAB1 LEU2 CEN4*]
yJP103	*MAT*α *ade2-1 his3-11,15 leu2-3,112 trp1-1 ura3-1 pab1::HIS3* [pYCplac111*pab1-134 LEU2 CEN4*]
yJP104	*MAT*α *ade2-1 his3-11,15 leu2-3,112 trp1-1 ura3-1 pab1::HIS3* [pYCplac111*pab1-184 LEU2 CEN4*]
yJP78	*MAT*α *ade2-1 his3-11,15 leu2-3,112 trp1-1 ura3-1 pab1::HIS3* [pYCplac11*pab1-*Δ*RRM1 LEU2 CEN4*]
yJP68	*MAT*α *ade2-1 his3-11,15 leu2-3,112 trp1-1 ura3-1 pab1::HIS3* [pYCplac111*pab1-*Δ*C-term* (deletion of aa 406-577) *LEU2 CEN4*]
yAS2069 (Tarun *et al.* 1997)	*MAT*a *ade2-1 his3-11,15 leu2-3,112 trp1-1 ura3-1 pep4::HIS3 tif4631::LEU2 tif4632::ura3* [*pTIF4631 TRP1 CEN*]
yAS2071 (Tarun *et al.* 1997)	*MAT*a *ade2-1 his3-11,15 leu2-3,112 trp1-1 ura3-1 pep4::HIS3 tif4631::LEU2 tif4632::ura3* [*pTIF4631-*Δ*N300 TRP1 CEN*]
NA200	*MAT*α *ade2-1 ura3-1*
NA207	*MAT*α *ade2-1 ura3-1 sup35::ADE2* [pRS316, *sup35-R419G*, *URA3*,*CEN*]
MT552/8a (Stansfield *et al.* 1997)	*MAT*α *sup45-2 ade2-1 ura3-1*
TP11B-4-1 (Barnes *et al.* 1993)	*MAT*a *ade1 leu2-3,112 ura3-52 prt1-1*
21R (Barnes *et al.* 1993)	*MAT*a *ade1 leu2-3,112 ura3-52*
H3016 (Nielsen *et al.* 2004)	*MAT*α *ade8 leu1 trp1 ura3 cdc33* [p3351 *CDC33 URA3 2*μ]
H3015 (Nielsen *et al.* 2004)	*MAT*α *ade8 leu1 trp1 ura3 cdc33* [p1992 *URA3 2*μ]

Appendix D – Toeprinting overview

We have used the toeprinting technique to study ribosomal positioning on synthetic mRNAs. This assay is based on primer extension inhibition by reverse transcriptase (RT) encountering a physical block, such as a ribosome on an mRNA molecule. In our assays, translation reactions containing synthetic RNAs are terminated by the addition of a drug that blocks ribosomal movement. The elongation inhibitor cycloheximide (CHX) is used to visualize 80S ribosomes positioned at AUG codons (Fig. D1). Use of the non-hydrolyzable GTP analog, GMP-PNP, allows visualization of 40S ribosomal subunits at an AUG codon (Fig. D2). Alternatively, these drugs can be omitted to visualize ribosomes whose movement/dissociation is markedly slower, thus allowing inhibition of RT activity. Translation reaction termination is followed by the addition of a radiolabeled oligonucleotide complementary to a sequence on the mRNA downstream of a region of interest. Addition of the RT allows extension of this oligonucleotide until the enzyme encounters the stalled ribosome or ribosomal subunit on the mRNA. The cDNA products are resolved on a sequencing gel and the leading edge of the ribosome is inferred by comparison of the position of the cDNA product to the sequence of the same region of the exogenously added RNA. The position of the cDNA band is usually 16/17 nucleotides downstream of the codon situated in the ribosomal P site (designated +16/17 toeprint) and 12-14 nucleotides downstream of the codon situated in the A site (designated +12 or +14 toeprint). Bonafide toeprint bands are distinguished from background bands by performing the analysis in parallel

reactions supplemented with the translation initiation inhibitor, cap analog, which results in a cDNA product with a highly diminished signal at positions which are occupied by ribosomes in reactions lacking the cap analog.

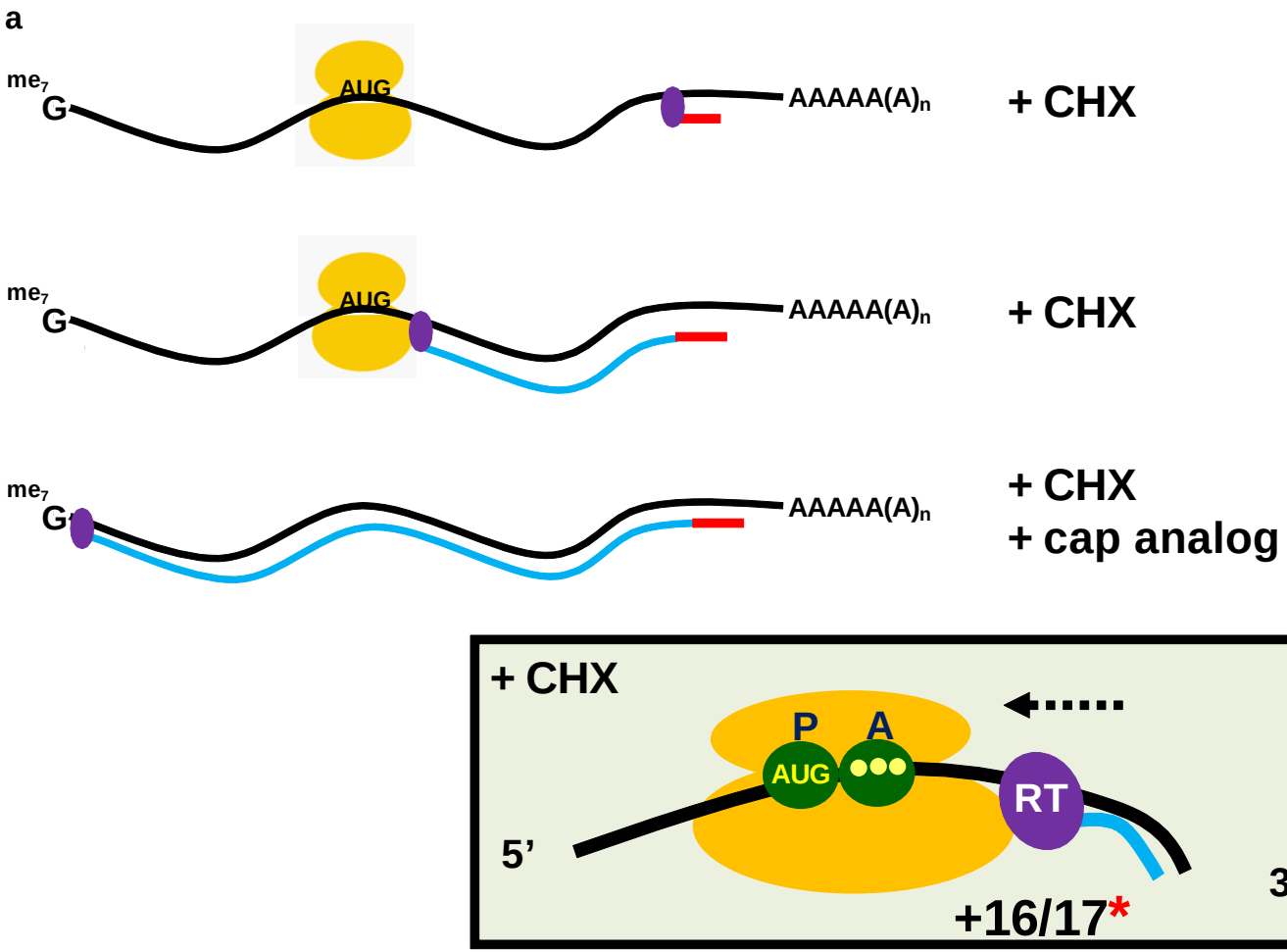

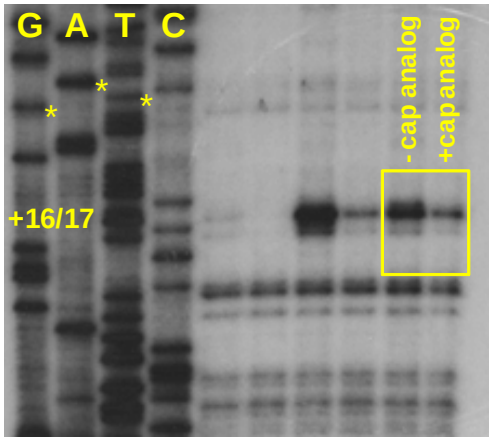

*** A +16/17 toeprint band reflects the distance between the first nucleotide of the initiation codon in the P site ('A' of the 'AUG') to the 3' end of the primer extension product. The yellow highlighted lanes on the gel show toeprint bands in the absence or presence of cap analog.**

Fig. D1 : Toeprinting 80S ribosomes. (a) Schematic outlining formation of the cDNA products visualized as toeprint bands. In the presence of CHX, 80S ribosomes (yellow circles) are stalled with an AUG codon in their P sites. A radiolabeled oligonucleotide (red bar) is annealed to a complementary sequence on the mRNA. Reverse transcriptase (RT; purple oval) extends the oligonucleotide until it is blocked by the stalled ribosome. The cDNA product (blue bar) can then be visualized on a polyacrylamide sequencing gel. Addition of cap analog reduces formation of 80S complexes on the mRNA and leads to dimished 80S-dependent cDNA products. **(b)** Polyacrylamide sequencing gel showing the presence of CHX-dependent +16/17 toeprint bands (yellow box) in the absence and presence of cap analog. A sequencing reaction of plasmid template DNA corresponding to the mRNA of interest is shown on the left with the position of the AUG codon highlighted (yellow stars).

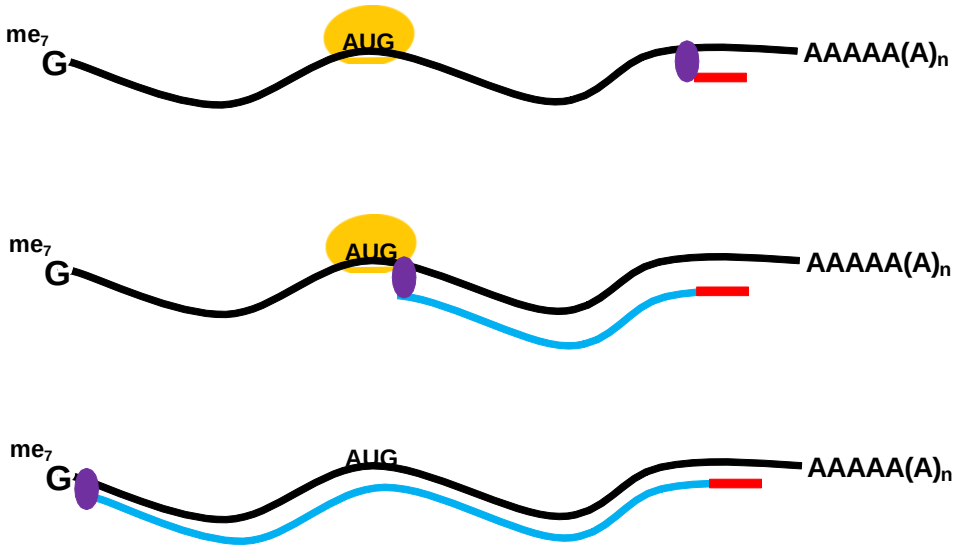

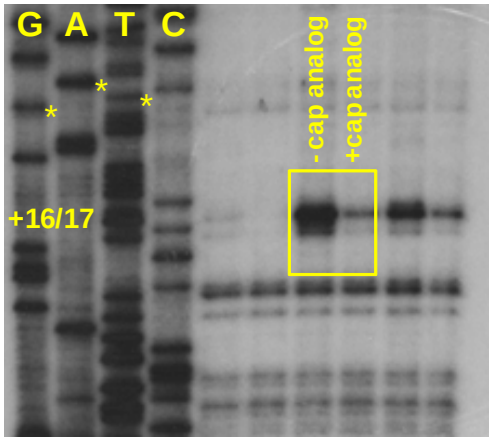

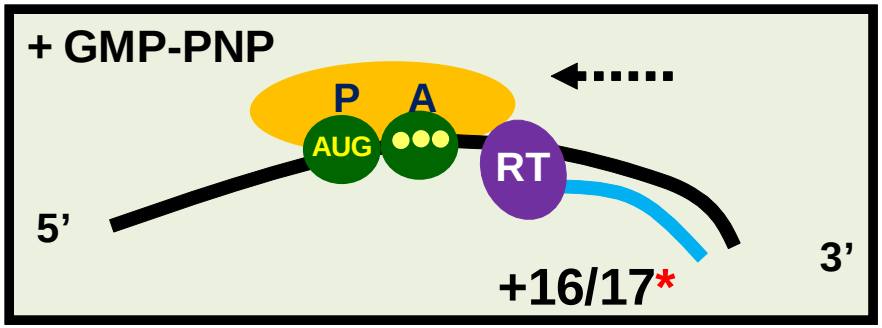

*** A +16/17 toeprint band reflects the distance between the first nucleotide of the initiation codon in the P site ('A' of the 'AUG') to the 3' end of the primer extension product. The yellow highlighted lanes on the gel show toeprint bands in the absence or presence of cap analog.**

Fig. D2 : Toeprinting 40S ribosomal subunits. (a) Schematic outlining formation of the cDNA products visualized as toeprint bands. In the presence of GMP-PNP, 40S ribosomes (yellow circles) are stalled with an AUG codon in their P sites. A radiolabeled oligonucleotide (red bar) is added which anneals to a complementary sequence on the mRNA. Reverse transcriptase (RT; purple oval) extends the oligonucleotide until it is blocked by the stalled ribosomal subunit. The cDNA product (blue bar) can then be visualized on a polyacrylamide sequencing gel. Addition of cap analog reduces formation of 40S complexes on the mRNA and leads to dimished 40S-dependent cDNA products. **(b)** Polyacrylamide sequencing gel showing the presence of GMP-PNP-dependent +16/17 toeprint bands (yellow box) in the absence and presence of cap analog. A sequencing reaction of plasmid template DNA corresponding to the mRNA of interest is shown on the left with the position of the AUG codon

References

Algire, M. A., D. Maag*, et al.* (2002). Development and characterization of a reconstituted yeast translation initiation system. RNA **8**(3): 382-397.

Alkalaeva, E. Z., A. V. Pisarev*, et al.* (2006). In vitro reconstitution of eukaryotic translation reveals cooperativity between release factors eRF1 and eRF3. Cell **125**(6): 1125-1136.

Allmang, C., E. Petfalski*, et al.* (1999). The yeast exosome and human PM-Scl are related complexes of 3' --> 5' exonucleases. Genes Dev **13**(16): 2148-58.

Altamura, N., O. Groudinsky*, et al.* (1992). *NAM7* nuclear gene encodes a novel member of a family of helicases with a Zn-ligand motif and is involved in mitochondrial functions in *Saccharomyces cerevisiae*. J. Mol. Biol. **224**(3): 575-587.

Amberg, D. C., D. J. Burke*, et al.* (2005). Methods in Yeast Genetics. Cold Spring Harbor, NY, Cold Spring Harbor Laboratory Press.

Amrani, N., R. Ganesan*, et al.* (2004). A *faux* 3'-UTR promotes aberrant termination and triggers nonsense-mediated mRNA decay. Nature **432**(7013): 112-118.

Amrani, N., S. Ghosh*, et al.* (2008). Translation factors promote the formation of two states of the closed-loop mRNP. Nature **453**(7199): 1276-1280.

Anders, K. R., A. Grimson*, et al.* (2003). SMG-5, required for *C.elegans* nonsense-mediated mRNA decay, associates with SMG-2 and protein phosphatase 2A. EMBO J. **22**: 641-650.

Applequist, S. E., M. Selg*, et al.* (1997). Cloning and characterization of HUPF1, a human homolog of the *Saccharomyces cerevisiae* nonsense mRNA-reducing UPF1 protein. Nucleic Acids Res. **25**(4): 814--21.

Aravind, L. and E. V. Koonin (2000). Eukaryote-specific domains in translation initiation factors: implications for translation regulation and evolution of the translation system. Genome Res. **10**(8): 1172-84.

Atkin, A. L., N. Altamura*, et al.* (1995). The majority of yeast UPF1 co-localizes with polyribosomes in the cytoplasm. Mol. Biol. Cell **6**(5): 611-625.

Atkin, A. L., L. R. Schenkman*, et al.* (1997). Relationship between yeast polyribosomes and Upf proteins required for nonsense mRNA decay. J. Biol. Chem. **272**(35): 22163-22172.

Aziz, N. and H. N. Munro (1987). Iron regulates ferritin mRNA translation through a segment of its 5' untranslated region. Proc. Natl. Acad. Sci. U. S. A. **84**(23): 8478-8482.

Badis, G., C. Saveanu*, et al.* (2004). Targeted mRNA degradation by deadenylation-independent decapping. Mol Cell **15**(1): 5-15.

Baer, B. W. and R. D. Kornberg (1983). The protein responsible for the repeating structure of cytoplasmic poly(A)-ribonucleoprotein. J. Cell. Biol. **96**(3): 717-721.

Barnes, C. A., R. A. Singer*, et al.* (1993). Yeast *prt1* mutations alter heat-shock gene expression through transcript fragmentation. EMBO J. **12**(8): 3323-32.

Beelman, C. A. and R. Parker (1995). Degradation of mRNA in eukaryotes. Cell **81**(2): 179-183.

Behm-Ansmant, I., D. Gatfield*, et al.* (2007). A conserved role for cytoplasmic poly(A)-binding protein 1 (PABPC1) in nonsense-mediated mRNA decay. EMBO J. **26**(6): 1591-1601.

Behm-Ansmant, I. and E. Izaurralde (2006). Quality control of gene expression: a stepwise assembly pathway for the surveillance complex that triggers nonsense-mediated mRNA decay. Genes Dev. **20**(4): 391-398.

Bloemendal, H., W. S. Bont*, et al.* (1967). Isolation and properties of polyribosomes and fragments of the endoplasmic reticulum from rat liver. Biochem J **103**(1): 177-82.

Bonetti, B., L. Fu*, et al.* (1995). The efficiency of translation termination is determined by a synergistic interplay between upstream and downstream sequences in *Saccharomyces cerevisiae*. J. Mol. Biol. **251**(3): 334-345.

Brogna, S. and J. Wen (2009). Nonsense-mediated mRNA decay (NMD) mechanisms. Nat. Struct. Mol. Biol. **16**(2): 107-113.

Buhler, M., S. Steiner*, et al.* (2006). EJC-independent degradation of nonsense immunoglobulin-mu mRNA depends on 3' UTR length. Nat. Struct. Mol. Biol. **13**(5): 462-464.

Casey, J. L., M. W. Hentze*, et al.* (1988). Iron-responsive elements: regulatory RNA sequences that control mRNA levels and translation. Science **240**(4854): 924-928.

Chagnovich, D. and R. Lehmann (2001). Poly(A)-independent regulation of maternal hunchback translation in the Drosophila embryo. Proc. Natl. Acad. Sci. U. S. A. **98**(20): 11359-11364.

Chamieh, H., L. Ballut*, et al.* (2008). NMD factors UPF2 and UPF3 bridge UPF1 to the exon junction complex and stimulate its RNA helicase activity. Nat. Struct. Mol. Biol. **15**(1): 85-93.

Chan, W. K., L. Huang*, et al.* (2007). An alternative branch of the nonsense-mediated decay pathway. EMBO J. **26**(7): 1820-1830.

Chen, C. Y., R. Gherzi*, et al.* (2001). AU binding proteins recruit the exosome to degrade ARE-containing mRNAs. Cell **107**(4): 451-64.

Chen, C. Y. and A. B. Shyu (1995). AU-rich elements: characterization and importance in mRNA degradation. Trends Biochem. Sci. **20**(11): 465-70.

Chen, C. Y., D. Zheng*, et al.* (2009). Ago-TNRC6 triggers microRNA-mediated decay by promoting two deadenylation steps. Nat. Struct. Mol. Biol. **16**(11): 1160-1166.

Cheng, Z., D. Muhlrad*, et al.* (2007). Structural and functional insights into the human Upf1 helicase core. EMBO J. **26**(1): 253-264.

Chiu, S. Y., G. Serin*, et al.* (2003). Characterization of human Smg5/7a: a protein with similarities to Caenorhabditis elegans SMG5 and SMG7 that functions in the dephosphorylation of Upf1. RNA **9**(1): 77-87.

Christensen, A. K., L. E. Kahn*, et al.* (1987). Circular polysomes predominate on the rough endoplasmic reticulum of somatotropes and mammotropes in the rat anterior pituitary. Am. J. Anat. **178**(1): 1-10.

Clerici, M., A. Mourao*, et al.* (2009). Unusual bipartite mode of interaction between the nonsense-mediated decay factors, UPF1 and UPF2. EMBO J. **28**(15): 2293-2306.

Cole, S. E., F. J. LaRiviere*, et al.* (2009). A convergence of rRNA and mRNA quality control pathways revealed by mechanistic analysis of nonfunctional rRNA decay. Mol. Cell **34**(4): 440-450.

Coller, J. and R. Parker (2004). Eukaryotic mRNA decapping. Annu. Rev. Biochem. **73**: 861-890.

Coller, J. and R. Parker (2005). General translational repression by activators of mRNA decapping. Cell **122**(6): 875-886.

Coller, J. M., N. K. Gray*, et al.* (1998). mRNA stabilization by poly(A) binding protein is independent of poly(A) and requires translation. Genes Dev. **12**(20): 3226-3235.

Cosson, B., A. Couturier*, et al.* (2002). Poly(A)-binding protein acts in translation termination via eukaryotic release factor 3 interaction and does not influence *PSI*(+) propagation. Mol. Cell. Biol. **22**(10): 3301-3315.

Cui, Y., K. W. Hagan*, et al.* (1995). Identification and characterization of genes that are required for the accelerated degradation of mRNAs containing a premature translational termination codon. Genes Dev. **9**(4): 423-436.

Culbertson, M. R., K. M. Underbrink*, et al.* (1980). Frameshift suppression *Saccharomyces cerevisiae*. Genetic properties of group II suppressors. Genetics **95**(4): 833-853.

Czaplinski, K., M. J. Ruiz-Echevarria*, et al.* (1998). The surveillance complex interacts with the translation release factors to enhance termination and degrade aberrant mRNAs. Genes Dev. **12**(11): 1665-1677.

Czaplinski, K., Y. Weng*, et al.* (1995). Purification and characterization of the Upf1 protein: a factor involved in translation and mRNA degradation. RNA **1**(6): 610-623.

Daar, I. O. and L. E. Maquat (1988). Premature translation termination mediates triosephosphate isomerase mRNA degradation. Mol. Cell. Biol. **8**(2): 802-13.

De Gregorio, E., T. Preiss*, et al.* (1998). Translational activation of uncapped mRNAs by the central part of human eIF4G is 5' end-dependent. RNA **4**(7): 828-36.

Denning, G., L. Jamieson*, et al.* (2001). Cloning of a novel phosphatidylinositol kinase-related kinase: characterization of the human SMG-1 RNA surveillance protein. J. Biol. Chem. **276**(25): 22709-22714.

Dmitriev, S. E., A. V. Pisarev*, et al.* (2003). Conversion of 48S translation preinitiation complexes into 80S initiation complexes as revealed by toeprinting. FEBS Lett. **533**(1-3): 99-104.

Doma, M. K. and R. Parker (2006). Endonucleolytic cleavage of eukaryotic mRNAs with stalls in translation elongation. Nature **440**(7083): 561-4.

Doma, M. K. and R. Parker (2007). RNA quality control in eukaryotes. Cell **131**(4): 660-8.

Dong, S., C. Li*, et al.* (2007). YRA1 autoregulation requires nuclear export and cytoplasmic Edc3p-mediated degradation of its pre-mRNA. Mol Cell **25**(4): 559-73.

Drinnenberg, I. A., D. E. Weinberg*, et al.* (2009). RNAi in budding yeast. Science **326**(5952): 544-550.

Dunckley, T., M. Tucker*, et al.* (2001). Two related proteins, Edc1p and Edc2p, stimulate mRNA decapping in *Saccharomyces cerevisiae*. Genetics **157**(1): 27-37.

Eberle, A. B., S. Lykke-Andersen*, et al.* (2009). SMG6 promotes endonucleolytic cleavage of nonsense mRNA in human cells. Nat. Struct. Mol. Biol. **16**(1): 49-55.

Eberle, A. B., L. Stalder*, et al.* (2008). Posttranscriptional gene regulation by spatial rearrangement of the 3' untranslated region. PLoS Biol. **6**(4): e92.

Fabian, M. R., G. Mathonnet*, et al.* (2009). Mammalian miRNA RISC recruits CAF1 and PABP to affect PABP-dependent deadenylation. Mol Cell **35**(6): 868-80.

Faghihi, M. A. and C. Wahlestedt (2009). Regulatory roles of natural antisense transcripts. Nat. Rev. Mol. Cell. Biol. **10**(9): 637-643.

Fischer, N. and K. Weis (2002). The DEAD box protein Dhh1 stimulates the decapping enzyme Dcp1. EMBO J. **21**(11): 2788-2797.

Frischmeyer, P. A., A. van Hoof*, et al.* (2002). An mRNA surveillance mechanism that eliminates transcripts lacking termination codons. Science **295**(5563): 2258-2261.

Funakoshi, Y., Y. Doi*, et al.* (2007). Mechanism of mRNA deadenylation: evidence for a molecular interplay between translation termination factor eRF3 and mRNA deadenylases. Genes Dev. **21**(23): 3135-3148.

Gaba, A., A. Jacobson*, et al.* (2005). Ribosome occupancy of the yeast *CPA1* upstream open reading frame termination codon modulates nonsense-mediated mRNA decay. Mol. Cell **20**: 449-460.

Gallie, D. R. (1991). The cap and poly(A) tail function synergistically to regulate mRNA translational efficiency. Genes Dev. **5**(11): 2108-2116.

Garneau, N. L., J. Wilusz*, et al.* (2007). The highways and byways of mRNA decay. Nat. Rev. Mol. Cell. Biol. **8**(2): 113-126.

Gatfield, D. and E. Izaurralde (2004). Nonsense-mediated messenger RNA decay is initiated by endonucleolytic cleavage in *Drosophila*. Nature **429**(6991): 575-578.

Gatfield, D., L. Unterholzner*, et al.* (2003). Nonsense-mediated mRNA decay in *Drosophila*: at the intersection of the yeast and mammalian pathways. EMBO J. **22**(15): 3960-3970.

Gebauer, F., D. F. Corona*, et al.* (1999). Translational control of dosage compensation in *Drosophila* by Sex-lethal: cooperative silencing via the 5' and 3' UTRs of msl-2 mRNA is independent of the poly(A) tail. EMBO J. **18**(21): 6146-54.

Gehring, N. H., J. B. Kunz*, et al.* (2005). Exon-junction complex components specify distinct routes of nonsense-mediated mRNA decay with differential cofactor requirements. Mol. Cell **20**(1): 65-75.

Gehring, N. H., G. Neu-Yilik*, et al.* (2003). Y14 and hUpf3b form an NMD-activating complex. Mol. Cell **11**(4): 939-949.

Gietz, R. D. and A. Sugino (1988). New yeast-*Escherichia coli* shuttle vectors constructed with in vitro mutagenized yeast genes lacking six-base pair restriction sites. Gene **74**(2): 527-34.

Gitlin, L. and R. Andino (2003). Nucleic acid-based immune system: the antiviral potential of mammalian RNA silencing. J. Virol. **77**(13): 7159-7165.

Gitlin, L., S. Karelsky*, et al.* (2002). Short interfering RNA confers intracellular antiviral immunity in human cells. Nature **418**(6896): 430-4.

Gonzalez, C. I., A. Bhattacharya*, et al.* (2001). Nonsense-mediated mRNA decay in *Saccharomyces cerevisiae*. Gene **274**(1-2): 15-25.

Goyer, C., M. Altmann*, et al.* (1993). TIF4631 and TIF4632: two yeast genes encoding the high-molecular-weight subunits of the cap-binding protein complex (eukaryotic initiation factor 4F) contain an RNA recognition motif-like sequence and carry out an essential function. Mol Cell Biol **13**(8): 4860-4874.

Gozalbo, D. and S. Hohmann (1990). Nonsense suppressors partially revert the decrease of the mRNA level of a nonsense mutant allele in yeast. Curr. Genet. **17**(1): 77-79.

Grimson, A., S. O'Connor*, et al.* (2004). SMG-1 is a phosphatidylinositol kinase-related protein kinase required for nonsense-mediated mRNA Decay in Caenorhabditis elegans. Mol. Cell. Biol. **24**(17): 7483-7490.

Hagan, K. W., M. J. Ruiz-Echevarria*, et al.* (1995). Characterization of *cis*-acting sequences and decay intermediates involved in nonsense-mediated mRNA turnover. Mol. Cell. Biol. **15**(2): 809-823.

Harger, J. W. and J. D. Dinman (2004). Evidence against a direct role for the Upf proteins in frameshifting or nonsense codon readthrough. RNA **10**(11): 1721-1729.

He, F., N. Amrani*, et al.* (2008). Qualitative and quantitative assessment of the activity of the yeast nonsense-mediated mRNA decay pathway. Methods Enzymol. **449**: 127-147.

He, F., A. H. Brown*, et al.* (1996). Interaction between Nmd2p and Upf1p is required for activity but not for dominant-negative inhibition of the nonsense-mediated mRNA decay pathway in yeast. RNA **2**(2): 153-170.

He, F., A. H. Brown*, et al.* (1997). Upf1p, Nmd2p, and Upf3p are interacting components of the yeast nonsense-mediated mRNA decay pathway. Mol. Cell. Biol. **17**(3): 1580-1594.

He, F. and A. Jacobson (1995). Identification of a novel component of the nonsense-mediated mRNA decay pathway by use of an interacting protein screen. Genes Dev. **9**(4): 437-454.

He, F., X. Li*, et al.* (2003). Genome-wide analysis of mRNAs regulated by the nonsense-mediated and 5' to 3' mRNA decay pathways in yeast. Mol. Cell **12**(6): 1439-1452.

He, F., S. W. Peltz*, et al.* (1993). Stabilization and ribosome association of unspliced pre-mRNAs in a yeast *upf1*- mutant. Proc. Natl. Acad. Sci. USA **90**(15): 7034-7038.

Heaton, B., C. Decker*, et al.* (1992). Analysis of chimeric mRNAs derived from the STE3 mRNA identifies multiple regions within yeast mRNAs that modulate mRNA decay. Nucleic Acids Res. **20**(20): 5365-5373.

Heindell, H. C., A. Liu*, et al.* (1978). The primary sequence of rabbit alpha-globin mRNA. Cell **15**(1): 43-54.

Hentze, M. W., S. W. Caughman*, et al.* (1987). Identification of the iron-responsive element for the translational regulation of human ferritin mRNA. Science **238**(4833): 1570-1573.

Herrick, D. and A. Jacobson (1992). A coding region segment is necessary, but not sufficient for rapid decay of the HIS3 mRNA in yeast. Gene **114**(1): 35-41.

Herrick, D., R. Parker*, et al.* (1990). Identification and comparison of stable and unstable mRNAs in Saccharomyces cerevisiae. Mol. Cell. Biol. **10**(5): 2269-2284.

Hilleren, P. and R. Parker (1999). mRNA surveillance in eukaryotes: kinetic proofreading of proper translation termination as assessed by mRNP domain organization? RNA **5**(6): 711-719.

Hinnebusch, A. G. (2005). Translational regulation of GCN4 and the general amino acid control of yeast. Annu. Rev. Microbiol. **59**: 407-450.

Hoshino, S., M. Imai*, et al.* (1999). The eukaryotic polypeptide chain releasing factor (eRF3/GSPT) carrying the translation termination signal to the 3'-poly(A) tail of mRNA. Direct association of erf3/GSPT with polyadenylate-binding protein. J. Biol. Chem. **274**(24): 16677-16680.

Hosoda, N., T. Kobayashi*, et al.* (2003). Translation termination factor eRF3 mediates mRNA decay through the regulation of deadenylation. J. Biol. Chem. **278**(40): 38287-38291.

Hsu, C. L. and A. Stevens (1993). Yeast cells lacking 5'-->3' exoribonuclease 1 contain mRNA species that are poly(A) deficient and partially lack the 5' cap structure. Mol. Cell. Biol. **13**(8): 4826-4835.

Hsu, M. T. and M. Coca-Prados (1979). Electron microscopic evidence for the circular form of RNA in the cytoplasm of eukaryotic cells. Nature **280**(5720): 339-40.

Hu, W., T. J. Sweet*, et al.* (2009). Co-translational mRNA decay in Saccharomyces cerevisiae. Nature **461**(7261): 225-229.

Huez, G., G. Marbaix*, et al.* (1978). Functional stabilisation of HeLa cell histone messenger RNAs injected into *Xenopus* oocytes by 3'-OH polyadenylation. Nature **271**(5645): 572-3.

Huntzinger, E., I. Kashima*, et al.* (2008). SMG6 is the catalytic endonuclease that cleaves mRNAs containing nonsense codons in metazoan. RNA **14**(12): 2609-2617.

Iizuka, N. and P. Sarnow (1997). Translation-competent extracts from *Saccharomyces cerevisiae*: effects of L-A RNA, 5' cap, and 3' poly(A) tail on translational efficiency of mRNAs. Methods **11**(4): 353-60.

Imataka, H. and N. Sonenberg (1997). Human eukaryotic translation initiation factor 4G (eIF4G) possesses two separate and independent binding sites for eIF4A. Mol. Cell. Biol. **17**(12): 6940-7.

Ishigaki, Y., X. Li*, et al.* (2001). Evidence for a pioneer round of mRNA translation: mRNAs subject to nonsense-mediated decay in mammalian cells are bound by CBP80 and CBP20. Cell **106**(5): 607-17.

Isken, O., Y. K. Kim*, et al.* (2008). Upf1 phosphorylation triggers translational repression during nonsense-mediated mRNA decay. Cell **133**(2): 314-327.

Ito-Harashima, S., K. Kuroha*, et al.* (2007). Translation of the poly(A) tail plays crucial roles in nonstop mRNA surveillance via translation repression and protein destabilization by proteasome in yeast. Genes Dev. **21**(5): 519-524.

Ivanov, P. V., N. H. Gehring*, et al.* (2008). Interactions between UPF1, eRFs, PABP and the exon junction complex suggest an integrated model for mammalian NMD pathways. EMBO J. **27**(5): 736-747.

Jacobson, A. (1996). Poly(A) metabolism and translation: the closed loop model. Translational Control. J. W. Hershey, M. B. Mathews and N. Sonenberg. Cold Spring Harbor, N.Y., Cold Spring Harbor Laboratory Press**:** 451-480.

Jacobson, A. and M. Favreau (1983). Possible involvement of poly(A) in protein synthesis. Nucleic Acids Res. **11**(18): 6353-6368.

Jacobson, A. and E. Izaurralde (2007). Nonsense-mediated mRNA decay: from yeast to metazoans. Translational Control in Biology and Medicine. M. B. Mathews, N. Sonenberg and J. W. B. Hershey. Cold Spring Harbor, NY, Cold Spring Harbor Laboratory Press**:** 655-687.

Jacobson, A. and S. W. Peltz (1996). Interrelationships of the pathways of mRNA decay and translation in eukaryotic cells. Annu. Rev. Biochem. **65**: 693-739.

Jacobson, A. and S. W. Peltz (2000). Destabilization of nonsense-containing transcripts in *Saccharomyces cerevisiae*. Translational Control of Gene Expression. N. Sonenberg, J. W. B. Hershey and M. B. Mathews. Cold Spring Harbor, N.Y., Cold Spring Harbor Laboratory Press**:** 827-847.

Johansson, M. J., F. He*, et al.* (2007). Association of yeast Upf1p with direct substrates of the NMD pathway. Proc. Natl. Acad. Sci. U S A **104**(52): 20872-20877.

Johns, L., A. Grimson*, et al.* (2007). Caenorhabditis elegans SMG-2 selectively marks mRNAs containing premature translation termination codons. Mol. Cell. Biol. **27**(16): 5630-5638.

Kadlec, J., D. Guilligay*, et al.* (2006). Crystal structure of the UPF2-interacting domain of nonsense-mediated mRNA decay factor UPF1. RNA **12**(10): 1817-1824.

Kadlec, J., E. Izaurralde*, et al.* (2004). The structural basis for the interaction between nonsense-mediated mRNA decay factors UPF2 and UPF3. Nature Struct. Mol. Biol. **11**(4): 330-337.

Karim, M. M., Y. V. Svitkin*, et al.* (2006). A mechanism of translational repression by competition of Paip2 with eIF4G for poly(A) binding protein (PABP) binding. Proc Natl Acad Sci U S A **103**(25): 9494-9499.

Kashima, I., A. Yamashita*, et al.* (2006). Binding of a novel SMG-1-Upf1-eRF1-eRF3 complex (SURF) to the exon junction complex triggers Upf1 phosphorylation and nonsense-mediated mRNA decay. Genes Dev. **20**(3): 355-367.

Kawashima, T., M. Pellegrini*, et al.* (2009). Nonsense-mediated mRNA decay mutes the splicing defects of spliceosome component mutations. RNA **15**(12): 2236-2247.

Kedersha, N., G. Stoecklin*, et al.* (2005). Stress granules and processing bodies are dynamically linked sites of mRNP remodeling. J. Cell Biol. **169**(6): 871-884.

Keeling, K. M., J. Lanier*, et al.* (2004). Leaky termination at premature stop codons antagonizes nonsense-mediated mRNA decay in S. cerevisiae. RNA **10**(4): 691-703.

Kessler, S. H. and A. B. Sachs (1998). RNA recognition motif 2 of yeast Pab1p is required for its functional interaction with eukaryotic translation initiation factor 4G. Mol. Cell. Biol. **18**(1): 51-57.

Khabar, K. S. (2005). The AU-rich transcriptome: more than interferons and cytokines, and its role in disease. J. Interferon Cytokine Res. **25**(1): 1-10.

Kim, V. N., N. Kataoka*, et al.* (2001). Role of the nonsense-mediated decay factor hUpf3 in the splicing- dependent exon-exon junction complex. Science **293**(5536): 1832-1836.

Kim, Y. K., L. Furic*, et al.* (2005). Mammalian Staufen1 recruits Upf1 to specific mRNA 3'UTRs so as to elicit mRNA decay. Cell **120**(2): 195-208.

Kinniburgh, A. J., L. E. Maquat*, et al.* (1982). mRNA-deficient beta o-thalassemia results from a single nucleotide deletion. Nucleic Acids Res. **10**(18): 5421-7.

Kopeina, G. S., Z. A. Afonina*, et al.* (2008). Step-wise formation of eukaryotic double-row polyribosomes and circular translation of polysomal mRNA. Nucleic Acids Res. **36**(8): 2476-2488.

Korner, C. G. and E. Wahle (1997). Poly(A) tail shortening by a mammalian poly(A)-specific 3'-exoribonuclease. J Biol Chem **272**(16): 10448-56.

Kozak, M. (1998). Primer extension analysis of eukaryotic ribosome-mRNA complexes. Nucleic. Acids. Res. **26**(21): 4853-4859.

Kuroha, K., T. Tatematsu*, et al.* (2009). Upf1 stimulates degradation of the product derived from aberrant messenger RNA containing a specific nonsense mutation by the proteasome. EMBO Rep. **10**(11): 1265-1271.

Lamphear, B. J., R. Kirchweger*, et al.* (1995). Mapping of functional domains in eukaryotic protein synthesis initiation factor 4G (eIF4G) with picornaviral proteases. Implications for cap-dependent and cap-independent translational initiation. J. Biol. Chem. **270**(37): 21975-21983.

LaRiviere, F. J., S. E. Cole*, et al.* (2006). A late-acting quality control process for mature eukaryotic rRNAs. Mol. Cell **24**(4): 619-626.

Le Hir, H., D. Gatfield*, et al.* (2001). The exon-exon junction complex provides a binding platform for factors involved in mRNA export and nonsense-mediated mRNA decay. EMBO J. **20**(17): 4987-4997.

Le Hir, H., E. Izaurralde*, et al.* (2000). The spliceosome deposits multiple proteins 20-24 nucleotides upstream of mRNA exon-exon junctions. EMBO J. **19**(24): 6860-6869.

LeBlanc, J. J. and K. L. Beemon (2004). Unspliced Rous sarcoma virus genomic RNAs are translated and subjected to nonsense-mediated mRNA decay before packaging. J. Virol. **78**(10): 5139-5146.

Lebreton, A., R. Tomecki*, et al.* (2008). Endonucleolytic RNA cleavage by a eukaryotic exosome. Nature **456**(7224): 993-6.

Lee, B. S. and M. R. Culbertson (1995). Identification of an additional gene required for eukaryotic nonsense mRNA turnover. Proc. Natl. Acad. Sci. USA **92**(22): 10354-10358.

Leeds, P., S. W. Peltz*, et al.* (1991). The product of the yeast *UPF1* gene is required for rapid turnover of mRNAs containing a premature translational termination codon. Genes Dev. **5**(12A): 2303-2314.

Leeds, P., J. M. Wood*, et al.* (1992). Gene products that promote mRNA turnover in *Saccharomyces cerevisiae*. Mol. Cell. Biol. **12**(5): 2165-2177.

Leipuviene, R. and E. C. Theil (2007). The family of iron responsive RNA structures regulated by changes in cellular iron and oxygen. Cell. Mol. Life Sci. **64**(22): 2945-2955.

Lejeune, F., Y. Ishigaki*, et al.* (2002). The exon junction complex is detected on CBP80-bound but not eIF4E-bound mRNA in mammalian cells: dynamics of mRNP remodeling. Embo J **21**(13): 3536-3545.

Liu, Q., J. C. Greimann*, et al.* (2006). Reconstitution, activities, and structure of the eukaryotic RNA exosome. Cell **127**(6): 1223-37.

Lockard, R. E., K. Currey*, et al.* (1986). Secondary structure model for mouse beta Maj globin mRNA derived from enzymatic digestion data, comparative sequence and computer analysis. Nucleic Acids Res. **14**(14): 5827-5841.

Losson, R. and F. Lacroute (1979). Interference of nonsense mutations with eukaryotic messenger RNA stability. Proc. Natl. Acad. Sci. USA **76**(10): 5134-5137.

Maderazo, A. B., J. P. Belk*, et al.* (2003). Nonsense-containing mRNAs that accumulate in the absence of a functional nonsense-mediated mRNA decay pathway are destabilized rapidly upon its restitution. Mol. Cell. Biol. **23**(3): 842-851.

Maderazo, A. B., F. He*, et al.* (2000). Upf1p control of nonsense mRNA translation is regulated by Nmd2p and Upf3p. Mol. Cell. Biol. **20**(13): 4591-4603.

Madin, K., T. Sawasaki*, et al.* (2004). Formation of circular polyribosomes in wheat germ cell-free protein synthesis system. FEBS Lett **562**(1-3): 155-9.

Mangus, D. A., N. Amrani*, et al.* (1998). Pbp1p, a factor interacting with *Saccharomyces cerevisiae* poly(A)-binding protein, regulates polyadenylation. Mol. Cell. Biol. **18**(12): 7383-7396.

Mangus, D. A., M. C. Evans*, et al.* (2003). Poly(A)-binding proteins: multifunctional scaffolds for the post-transcriptional control of gene expression. Genome Biol. **4**(7): 223.1-223.14.

Mangus, D. A. and A. Jacobson (1999). Linking mRNA turnover and translation: assessing the polyribosomal association of mRNA decay factors and degradative intermediates. Methods **17**(1): 28-37.

Maquat, L. E. (1995). When cells stop making sense: effects of nonsense codons on RNA metabolism in vertebrate cells. RNA **1**(5): 453-465.

Marzluff, W. F., E. J. Wagner*, et al.* (2008). Metabolism and regulation of canonical histone mRNAs: life without a poly(A) tail. Nat. Rev. Genet. **9**(11): 843-854.

Mata, J., S. Marguerat*, et al.* (2005). Post-transcriptional control of gene expression: a genome-wide perspective. Trends Biochem Sci **30**(9): 506-14.

Matsui, K., M. Nishizawa*, et al.* (2008). Natural antisense transcript stabilizes inducible nitric oxide synthase messenger RNA in rat hepatocytes. Hepatology **47**(2): 686-97.

Maxam, A. M. and W. Gilbert (1977). A new method for sequencing DNA. Proc. Natl. Acad. Sci. USA **74**(2): 560-564.

Medghalchi, S. M., P. A. Frischmeyer*, et al.* (2001). Rent1, a trans-effector of nonsense-mediated mRNA decay, is essential for mammalian embryonic viability. Hum. Mol. Genet. **10**(2): 99-105.

Meister, G. and T. Tuschl (2004). Mechanisms of gene silencing by double-stranded RNA. Nature **431**(7006): 343-9.

Mendell, J. T., S. M. Medghalchi*, et al.* (2000). Novel Upf2p orthologues suggest a functional link between translation initiation and nonsense surveillance complexes. Mol. Cell. Biol. **20**(23): 8944-8957.

Metzstein, M. M. and M. A. Krasnow (2006). Functions of the nonsense-mediated mRNA decay pathway in Drosophila development. PLoS Genet. **2**(12): e180.

Mitchell, P., E. Petfalski*, et al.* (1997). The exosome: a conserved eukaryotic RNA processing complex containing multiple 3'-->5' exoribonucleases. Cell **91**(4): 457-66.

Muhlemann, O., A. B. Eberle*, et al.* (2008). Recognition and elimination of nonsense mRNA. Biochim. Biophys. Acta **1779**(9): 538-549.

Muhlrad, D., C. J. Decker*, et al.* (1994). Deadenylation of the unstable mRNA encoded by the yeast *MFA2* gene leads to decapping followed by 5'-->3' digestion of the transcript. Genes Dev. **8**(7): 855-866.

Muhlrad, D. and R. Parker (1992). Mutations affecting stability and deadenylation of the yeast *MFA2* transcript. Genes Dev. **6**(11): 2100-2111.

Muhlrad, D. and R. Parker (1999). Aberrant mRNAs with extended 3' UTRs are substrates for rapid degradation by mRNA surveillance. RNA **5**(10): 1299-1307.

Muhlrad, D. and R. Parker (1999). Recognition of yeast mRNAs as "nonsense containing" leads to both inhibition of mRNA translation and mRNA degradation: implications for the control of mRNA decapping. Mol. Biol. Cell. **10**(11): 3971-3978.

Mullen, T. E. and W. F. Marzluff (2008). Degradation of histone mRNA requires oligouridylation followed by decapping and simultaneous degradation of the mRNA both 5' to 3' and 3' to 5'. Genes Dev. **22**(1): 50-65.

Mullner, E. W., B. Neupert*, et al.* (1989). A specific mRNA binding factor regulates the iron-dependent stability of cytoplasmic transferrin receptor mRNA. Cell **58**(2): 373-382.

Munroe, D. and A. Jacobson (1990). mRNA poly(A) tail, a 3' enhancer of translational initiation. Mol. Cell. Biol. **10**(7): 3441-3455.

Nielsen, K. H., B. Szamecz*, et al.* (2004). Functions of eIF3 downstream of 48S assembly impact AUG recognition and GCN4 translational control. EMBO J. **23**(5): 1166-1177.

Nott, A., H. Le Hir*, et al.* (2004). Splicing enhances translation in mammalian cells: an additional function of the exon junction complex. Genes Dev. **18**(2): 210-222.

Ohnishi, T., A. Yamashita*, et al.* (2003). Phosphorylation of hUPF1 induces formation of mRNA surveillance complexes containing hSMG-5 and hSMG-7. Mol. Cell **12**(5): 1187-1200.

Olivas, W. and R. Parker (2000). The Puf3 protein is a transcript-specific regulator of mRNA degradation in yeast. EMBO J. **19**(23): 6602-11.

Otero, L. J., M. P. Ashe*, et al.* (1999). The yeast poly(A)-binding protein Pab1p stimulates *in vitro* poly(A)-dependent and cap-dependent translation by distinct mechanisms. EMBO J. **18**(11): 3153-3163.

Page, M. F., B. Carr*, et al.* (1999). *SMG-2* is a phosphorylated protein required for mRNA surveillance in *Caenorhabditis elegans* and related to Upf1p of yeast. Mol. Cell. Biol. **19**(9): 5943-5951.

Parker, R. and A. Jacobson (1990). Translation and a 42-nucleotide segment within the coding region of the mRNA encoded by the *MAT*α1 gene are involved in

promoting rapid mRNA decay in yeast. Proc. Natl. Acad. Sci. USA **87**(7): 2780-2784.

Parker, R. and U. Sheth (2007). P bodies and the control of mRNA translation and degradation. Mol. Cell **25**(5): 635-646.

Peabody, D. S. and P. Berg (1986). Termination-reinitiation occurs in the translation of mammalian cell mRNAs. Mol. Cell. Biol. **6**(7): 2695-703.

Peltz, S. W., G. Brewer*, et al.* (1991). Regulation of mRNA turnover in eukaryotic cells. Crit. Rev. Eukaryot. Gene Expr. **1**(2): 99-126.

Peltz, S. W., G. Brewer*, et al.* (1987). Substrate specificity of the exonuclease activity that degrades H4 histone mRNA. J. Biol. Chem. **262**(19): 9382-8.

Peltz, S. W., A. H. Brown*, et al.* (1993). mRNA destabilization triggered by premature translational termination depends on at least three *cis*-acting sequence elements and one *trans*-acting factor. Genes Dev. **7**(9): 1737-1754.

Peltz, S. W., F. He*, et al.* (1994). Nonsense-mediated mRNA decay in yeast. Prog. Nucleic Acid Res. Mol. Biol. **47**: 271-298.

Peltz, S. W. and J. Ross (1987). Autogenous regulation of histone mRNA decay by histone proteins in a cell-free system. Mol. Cell. Biol. **7**(12): 4345-56.

Peltz, S. W., C. Trotta*, et al.* (1993). Identification of the *cis*-acting sequences and *trans*-acting factors involved in nonsense-mediated mRNA decay. Protein Synthesis and Targetting in Yeast. J. M. M. Tuite, A., and F. Sherman, Springer-Verlag. **H71:** 1-10.

Perlick, H. A., S. M. Medghalchi*, et al.* (1996). Mammalian orthologues of a yeast regulator of nonsense transcript stability. Proc. Natl. Acad. Sci. USA **93**(20): 10928-32.

Pestova, T. V., I. N. Shatsky*, et al.* (1996). Functional dissection of eukaryotic initiation factor 4F: the 4A subunit and the central domain of the 4G subunit are sufficient to mediate internal entry of 43S preinitiation complexes. Mol. Cell. Biol. **16**(12): 6870-6878.

Pisarev, A. V., C. U. Hellen*, et al.* (2007). Recycling of eukaryotic posttermination ribosomal complexes. Cell **131**(2): 286-299.

Ponting, C. P. (2000). Novel eIF4G domain homologues linking mRNA translation with nonsense-mediated mRNA decay. Trends Biochem. Sci. **25**(9): 423-6.

Pulak, R. and P. Anderson (1993). mRNA surveillance by the *Caenorhabditis elegans smg* genes. Genes Dev. **7**(10): 1885-1897.

Rehwinkel, J., J. Raes*, et al.* (2006). Nonsense-mediated mRNA decay: Target genes and functional diversification of effectors. Trends Biochem. Sci. **31**(11): 639-646.

Rissland, O. S. and C. J. Norbury (2009). Decapping is preceded by 3' uridylation in a novel pathway of bulk mRNA turnover. Nat. Struct. Mol. Biol. **16**(6): 616-623.

Ruiz-Echevarria, M. J., C. I. Gonzalez*, et al.* (1998). Identifying the right stop: determining how the surveillance complex recognizes and degrades an aberrant mRNA. EMBO J. **17**(2): 575-589.

Sachs, A. (2000). Physical and functional interactions between the mRNA cap structure and the poly(A) tail. Translational Control of Gene Expression. N. Sonenberg, J.

W. Hershey and M. B. Mathews. Cold Spring Harbor, Cold Spring Harbor Laboratory Press**:** 447-465.

Sachs, A. B., M. W. Bond*, et al.* (1986). A single gene from yeast for both nuclear and cytoplasmic polyadenylate-binding proteins: domain structure and expression. Cell **45**(6): 827-835.

Sachs, A. B. and R. W. Davis (1990). Translation initiation and ribosomal biogenesis: involvement of a putative rRNA helicase and *RPL46*. Science **247**(4946): 1077-1079.

Sachs, A. B., R. W. Davis*, et al.* (1987). A single domain of yeast poly(A)-binding protein is necessary and sufficient for RNA binding and cell viability. Mol. Cell. Biol. **7**(9): 3268-3276.

Sachs, M. S., Z. Wang*, et al.* (2002). Toeprint analysis of the positioning of translation apparatus components at initiation and termination codons of fungal mRNAs. Methods **26**(2): 105-114.

Saini, P., D. E. Eyler*, et al.* (2009). Hypusine-containing protein eIF5A promotes translation elongation. Nature **459**(7243): 118-21.

Salas-Marco, J. and D. M. Bedwell (2004). GTP hydrolysis by eRF3 facilitates stop codon decoding during eukaryotic translation termination. Mol. Cell. Biol. **24**: 7769-7778.

Schilders, G., R. Raijmakers*, et al.* (2005). MPP6 is an exosome-associated RNA-binding protein involved in 5.8S rRNA maturation. Nucleic Acids Res **33**(21): 6795-804.

Schmid, M. and T. H. Jensen (2008). The exosome: a multipurpose RNA-decay machine. Trends in Biochemical Sciences **33**(10): 501-510.

Schneuwly, S., R. D. Shortridge*, et al.* (1989). Drosophila ninaA gene encodes an eye-specific cyclophilin (cyclosporine A binding protein). Proc Natl Acad Sci U S A **86**(14): 5390-4.

Schwartz, D., C. J. Decker*, et al.* (2003). The enhancer of decapping proteins, Edc1p and Edc2p, bind RNA and stimulate the activity of the decapping enzyme. Rna **9**(2): 239-51.

Serin, G., A. Gersappe*, et al.* (2001). Identification and characterization of human orthologues to *Saccharomyces cerevisiae* Upf2 protein and Upf3 protein (*Caenorhabditis elegans SMG-4*). Mol. Cell. Biol. **21**(1): 209-23.

Sheth, U. and R. Parker (2003). Decapping and decay of messenger RNA occur in cytoplasmic processing bodies. Science **300**(5620): 805-808.

Sheth, U. and R. Parker (2006). Targeting of aberrant mRNAs to cytoplasmic processing bodies. Cell **125**(6): 1095-1109.

Shirley, R. L., A. S. Ford*, et al.* (2002). Nuclear import of Upf3p is mediated by importin-alpha/-beta and export to the cytoplasm is required for a functional nonsense-mediated mRNA decay pathway in yeast. Genetics **161**(4): 1465-1482.

Shirley, R. L., M. J. Lelivelt*, et al.* (1998). A factor required for nonsense-mediated mRNA decay in yeast is exported from the nucleus to the cytoplasm by a nuclear export signal sequence. J. Cell Sci. **111**(Pt 21): 3129-3143.

Shyu, A. B., J. G. Belasco*, et al.* (1991). Two distinct destabilizing elements in the c-fos message trigger deadenylation as a first step in rapid mRNA decay. Genes Dev. **5**(2): 221-231.

Sikorski, R. S. and P. Hieter (1989). A system of shuttle vectors and yeast host strains designed for efficient manipulation of DNA in *Saccharomyces cerevisiae*. Genetics **122**(1): 19-27.

Silva, A. L., P. Ribeiro*, et al.* (2008). Proximity of the poly(A)-binding protein to a premature termination codon inhibits mammalian nonsense-mediated mRNA decay. RNA **14**(3): 563-576.

Singh, G., I. Rebbapragada*, et al.* (2008). A competition between stimulators and antagonists of Upf complex recruitment governs human nonsense-mediated mRNA decay. PLoS Biol. **6**(4): e111.

Song, H., P. Mugnier*, et al.* (2000). The crystal structure of human eukaryotic release factor eRF1-mechanism of stop codon recognition and peptidyl-tRNA hydrolysis. Cell **100**(3): 311-321.

Soni, R., J. P. Carmichael*, et al.* (1993). Parameters affecting lithium acetate-mediated transformation of *Saccharomyces cerevisiae* and development of a rapid and simplified procedure. Curr. Genet. **24**(5): 455-459.

Stalder, L. and O. Muhlemann (2008). The meaning of nonsense. Trends Cell Biol. **18**(7): 315-321.

Stalder, L. and O. Muhlemann (2009). Processing bodies are not required for mammalian nonsense-mediated mRNA decay. RNA **15**: 1265-1273.

Stansfield, I., V. V. Kushnirov*, et al.* (1997). A conditional-lethal translation termination defect in a *sup45* mutant of the yeast *Saccharomyces cerevisiae*. Eur. J. Biochem. **245**(3): 557-563.

Taft, R. J., K. C. Pang*, et al.* (2009). Non-coding RNAs: regulators of disease. J. Pathol.

Takahashi, S., Y. Araki*, et al.* (2008). Upf1 potentially serves as a RING-related E3 ubiquitin ligase via its association with Upf3 in yeast. RNA **14**(9): 1950-1958.

Tarun, S. Z., Jr. and A. B. Sachs (1995). A common function for mRNA 5' and 3' ends in translation initiation in yeast. Genes Dev. **9**(23): 2997-3007.

Tarun, S. Z., Jr. and A. B. Sachs (1996). Association of the yeast poly(A) tail binding protein with translation initiation factor eIF-4G. EMBO J. **15**(24): 7168-7177.

Tarun, S. Z., Jr., S. E. Wells*, et al.* (1997). Translation initiation factor eIF4G mediates *in vitro* poly(A) tail-dependent translation. Proc. Natl. Acad. Sci. USA **94**(17): 9046-9051.

Teixeira, D., U. Sheth*, et al.* (2005). Processing bodies require RNA for assembly and contain nontranslating mRNAs. RNA **11**(4): 371-382.

Thomas, K. R. and M. R. Capecchi (1986). Introduction of homologous DNA sequences into mammalian cells induces mutations in the cognate gene. Nature **324**(6): 34-38.

Tucker, M. and R. Parker (2000). Mechanisms and control of mRNA decapping in Saccharomyces cerevisiae. Annu Rev Biochem **69**: 571-95.

Tucker, M., M. A. Valencia-Sanchez*, et al.* (2001). The transcription factor associated Ccr4 and Caf1 proteins are components of the major cytoplasmic mRNA deadenylase in S*accharomyces cerevisiae*. Cell **104**(3): 377-386.

Uchida, N., S. Hoshino*, et al.* (2002). A novel role of the mammalian GSPT/eRF3 associating with poly(A)-binding protein in cap/poly(A)-dependent translation. J. Biol. Chem. **277**(52): 50286-50292.

van Dijk, E. L., G. Schilders*, et al.* (2007). Human cell growth requires a functional cytoplasmic exosome, which is involved in various mRNA decay pathways. Rna **13**(7): 1027-35.

van Hoof, A., P. A. Frischmeyer*, et al.* (2002). Exosome-mediated recognition and degradation of mRNAs lacking a termination codon. Science **295**(5563): 2262-2264.

Wang, L., M. S. Lewis*, et al.* (2005). Domain interactions within the Ski2/3/8 complex and between the Ski complex and Ski7p. Rna **11**(8): 1291-302.

Wang, W., I. J. Cajigas*, et al.* (2006). A role for Upf2p phosphorylation in *Saccharomyces cerevisiae* nonsense-mediated mRNA decay. Mol. Cell. Biol. **26**: 3390-4000.

Wang, W., K. Czaplinski*, et al.* (2001). The role of Upf proteins in modulating the translation read-through of nonsense-containing transcripts. EMBO J. **20**(4): 880-890.

Welch, E. M., E. R. Barton*, et al.* (2007). PTC124 targets genetic disorders caused by nonsense mutations. Nature **447**(7140): 87-91.

Welch, E. M. and A. Jacobson (1999). An internal open reading frame triggers nonsense-mediated decay of the yeast SPT10 mRNA. EMBO J. **18**(21): 6134-6145.

Wells, S. E., P. E. Hillner*, et al.* (1998). Circularization of mRNA by eukaryotic translation initiation factors. Mol. Cell **2**(1): 135-140.

Wickens, M., D. S. Bernstein*, et al.* (2002). A PUF family portrait: 3'UTR regulation as a way of life. Trends Genet. **18**(3): 150-157.

Wilkinson, M. F. (2003). The cycle of nonsense. Mol. Cell **12**(5): 1059-1061.

Wittkopp, N., E. Huntzinger*, et al.* (2009). Nonsense-mediated mRNA decay effectors are essential for zebrafish embryonic development and survival. Mol. Cell. Biol. **29**: 3517-3528.

Wu, C., N. Amrani*, et al.* (2007). The use of fungal in vitro systems for studying translational regulation. Methods Enzymol **429**: 203-25.

Yamashita, A., N. Izumi*, et al.* (2009). SMG-8 and SMG-9, two novel subunits of the SMG-1 complex, regulate remodeling of the mRNA surveillance complex during nonsense-mediated mRNA decay. Genes Dev. **23**(9): 1091-1105.

Yamashita, A., T. Ohnishi*, et al.* (2001). Human SMG-1, a novel phosphatidylinositol 3-kinase-related protein kinase, associates with components of the mRNA surveillance complex and is involved in the regulation of nonsense-mediated mRNA decay. Genes Dev. **15**(17): 2215-2228.

Yazaki, K., T. Yoshida*, et al.* (2000). Polysomes of eukaryotic cells observed by electron microscopy. J Electron Microsc (Tokyo) **49**(5): 663-8.

Yun, D. F. and F. Sherman (1995). Initiation of translation can occur only in a restricted region of the CYC1 mRNA of *Saccharomyces cerevisiae*. Mol. Cell. Biol. **15**(2): 1021-1033.

Zhang, J. and L. E. Maquat (1997). Evidence that translation reinitiation abrogates nonsense-mediated mRNA decay in mammalian cells. EMBO J. **16**(4): 826-33.

Zhang, J., X. Sun*, et al.* (1998). Intron function in the nonsense-mediated decay of beta-globin mRNA: indications that pre-mRNA splicing in the nucleus can influence mRNA translation in the cytoplasm. RNA **4**(7): 801-15.

Zhang, S., M. J. Ruiz-Echevarria*, et al.* (1995). Identification and characterization of a sequence motif involved in nonsense-mediated mRNA decay. Mol. Cell. Biol. **15**(4): 2231-2244.

Zhang, S., E. M. Welch*, et al.* (1997). Polysome-associated mRNAs are substrates for the nonsense-mediated mRNA decay pathway in *Saccharomyces cerevisiae*. RNA **3**(3): 234-244.

Zhouravleva, G., L. Frolova*, et al.* (1995). Termination of translation in eukaryotes is governed by two interacting polypeptide chain release factors, eRF1 and eRF3. EMBO J. **14**(16): 4065-4072.

Zuk, D., J. P. Belk*, et al.* (1999). Temperature-sensitive mutations in the *Saccharomyces cerevisiae MRT4*, *GRC5*, *SLA2* and *THS1* genes result in defects in mRNA turnover. Genetics **153**(1): 35-47.

Zuk, D. and A. Jacobson (1998). A single amino acid substitution in yeast eIF-5A results in mRNA stabilization. EMBO J. **17**(10): 2914-2925.